DYNAMIC OUTPUT FEEDBACK CONTROLLER SYNTHESIS FOR NEGATIVE IMAGINARY SYSTEMS AND APPLICATION TO VIBRATION ATTENUATION

A thesis submitted to the University of Manchester
for the degree of Doctor of Philosophy
in the Faculty of Faculty of Science and Engineering

2022

Suleiman Sabo Kurawa
Department of Electrical and Electronic Engineering

Contents

Word count 20,370

List of Tables

List of Figures

The University of Manchester

Suleiman Sabo Kurawa
Doctor of Philosophy
DYNAMIC OUTPUT FEEDBACK CONTROLLER SYNTHESIS FOR NEGATIVE IMAGINARY SYSTEMS AND APPLICATION TO VIBRATION ATTENUATION
May 2, 2022

Abstract

In the Single-Input-Single-Output (SISO) setting, Negative Imaginary (NI) systems refer to systems with negative frequency response for all positive frequencies. The NI theory was motivated by the study of inertial systems with collocated position sensor and force actuator. This type of systems can have nonminimum phase zero, be improper and have up to a relative degree of two. Thus, stability analysis and controller synthesis using passivity theorem may not be applicable. Moreover, using traditional design techniques such as $\mathcal{H}_\infty$ and $\mathcal{H}_2$ to control this kind of systems may lead to conservative results and poor performance due to the oscillatory nature of the systems and the effect of the unmodelled dynamics on the closed-loop system performance.

The NI property can be observed in a number of physical systems such as cantilever beams, large space structures, robotic manipulators, gantry crane systems, vibration shock absorbers, series elastic actuators and mechatronic systems. This, in addition to the simple internal stability result of interconnected NI systems, which depends only on the DC loop gain, has made the theory appealing for practical engineering applications. Example of some of these applications include vibration control of lightly-damped flexible structure, motion control of robotic arm, the control of a DC servo motor, nano-positioning control of an atomic force microscope, consensus control of multi-agent systems, to mention but a few.

Due to the vast areas of application of the NI theory, controller synthesis techniques that achieve some transient performance level, such as prescribed decay rate, becomes imperative. This thesis therefore focuses on the synthesis technique of such controllers. A set of Linear Matrix Inequalities (LMIs) conditions are proposed for the synthesis of a dynamic output feedback controller. These LMIs render the closed-loop system to be NI and ensure that the DC gain condition for closed-loop internal stability is satisfied. The proposed conditions also ensures that the closed-loop system has prescribed decay rate via the $\alpha-$ pole placement technique.

The thesis then introduces a new class of NI systems called the Linear Time-Varying (LTV) NI systems. First, a time domain definition is provided, before a state-space characterization is proposed using Linear Differential Matrix Inequalities (LDMIs). Furthermore, a specialized case of the LTV NI systems called the Linear Parameter-Varying (LPV) NI systems are introduced. The state-space characterization of the LPV NI systems is provided using LMIs. Finally, a set of sufficient conditions for the stability of two asymptotically stable LTV NI systems is proposed and the result is shown to specialise to the LPV NI systems case.

Also, this thesis introduces a robust controller synthesis technique using the principles of Internal Model Control (IMC) and NI theory. In the proposed technique,

the design of the Youla parameter is cast as an NI controller synthesis problem. Two different synthesis methods are provided, both of which are sufficient conditions. One is an LMI-based approach and the other is a frequency domain approach.

Finally, the thesis deals with hardware validation of the proposed LMI-based IMC NI controller synthesis technique. The efficacy of the technique is demonstrated on a flexible cantilever beam with collocated position sensor and force actuator. The controller is designed to attenuate the vibration of the flexible structure caused by external disturbances.

Declaration

No portion of the work referred to in the thesis has been submitted in support of an application for another degree or qualification of this or any other university or other institute of learning.

Copyright Statement

Dedication

This thesis is dedicated to my parents, late Dr. Sabo Suleiman Kurawa and Professor Dije Muhammad Suleiman.

Acknowledgements

I would like to use this opportunity to thank everyone that helped me throughout my PhD programme.

Foremost, I would like to thank my parents, Dr. Sabo Suleiman Kurawa (late) and Professor Dije Muhammad Suleiman, my sister and brothers: Nafisa, Najeeb, Nasir, Muhammad and Sadiq for their magnanimous and unflinching support during my graduate studies.

I would like to express my sincere gratitude to my supervisor, Professor Alexander Lanzon, for his insightful and judicious contributions to my work. His guidance and enlightening advices have helped me throughout my studies to become a good independent researcher and a better person in general. I would like to thank him for always being there for me.

Beside my supervisor, I would like to thank Dr. Parijat Bhowmick for his help and contribution. I will always cherish those thought-provoking academic discussions and friendly chats (before COVID-19 cut them short) we had.

My sincere thanks go to the members of our control team: Dr. Somasundar Kannan, Dr. Gabriela Reyes, Dr. Ola Skeik, Dr. Junyan Hu, Daniel Abara, Peter Hilborne and Yu-Hsiang Su, for all the academic discussions and fun time we had together. I would also like to appreciate Dr. Gwadabe Kurawa and Mrs. Farida Sadauki for making Manchester a second home for me.

Finally, I would like to acknowledge my sponsors: Petroleum Technology Development Fund (PTDF).

Publications

The materials in Chapters 4, 5, 6 and 7 have been published or submitted for publication in the following

- S. Kurawa, P. Bhowmick and A. Lanzon, "Dynamic output feedback controller synthesis using an LMI-based $\alpha-$strictly negative imaginary framework," In *Proceedings of 27th Mediterranean Conference on Control and Automation,* pp. 81-86, July 2019. See reference [59] for more information.

- S. Kurawa, P. Bhowmick and A. Lanzon, "Negative imaginary theory for a class of linear time-varying systems," *Systems & Control Letters,* vol. 5, no. 3, pp. 1001-1006, July 2021. See reference [60] for more information.

- S. Kurawa, P. Bhowmick and A. Lanzon, "A dynamic controller synthesis methodology for negative imaginary systems using th internal model control principle," submitted to *Automatica,* July 2021. See reference [61] for more information.

Nomenclature

Miscellaneous

$\blacksquare$	end of proof
$\Im\{s\}$	imaginary part of s
$\mathcal{RH}_\infty$	set of aysmptotically stable, rational, real, proper transfer function matrices
$\Re\{s\}$	real part of s

Acronyms and notations

AC	Absolute Continuity
ARE	Algebraic Riccati Equation
BR	Bounded Real
CT	Continuous Time
DLMI	Differential Linear Matrix Inequality
DT	Discrete Time
FFNI	Finite Frequency Negative Imaginary
FFPR	Finite Frequency Positive Real
IMC	Internal Model Control

IQC	Integral Quadratic Constraint
IRC	Integral Resonant Control
LFT	Linear Fractional Transformation
LMI	Linear Matrix Inequality
LPV	Linear Parameter-Varying
LTI	Linear Time Invariant
LTV	Linear Time Variant
LTV	Linear Time-Varying
MFC	Macro Fibre Composite
MIMO	Multi Input Multi Output
NI	Negative Imaginary
OSNI	Output Strictly Negative Imaginary
PDE	Partial Differential Equation
PR	Positive Real
PZT	Lead Zirconate Titanate
SBR	Strictly Bounded Real
SDP	Semi Definite Programming
SISO	Single Input Single Output
SNI	Strictly Negative Imaginary
SSNI	Strongly Strict Negative Imaginary
SSPR	Strongly Strict Positive Real
UAV	Unmanned Aerial Vehicle

WSNI	Weakly Strict Negative Imaginary
WSPR	Weakly Strict Positive Real
ZSD	Zero State Detectable

Matrix and system operations

$\mathcal{F}_l(\bullet,\bullet)$	lower linear fractional transformation
$\mathcal{F}_u(\bullet,\bullet)$	upper linear fractional transformation
$\det(A)$	determinant of matrix A
$\dim(A)$	dimension of matrix A
$\mathrm{Ker}(A)$	kernel of matrix A
$\mathrm{rank}(A)$	rank of matrix A
$\sigma(A)$	spectrum of matrix A
$A > (\geq) 0$	positive (semi)definite matrix A
A^*	complex conjugate transform of matrix A
A^T	transpose of matrix A
A^{-1}	inverse of matrix A
$G(s)^{-1}$	inverse of the transfer function matrix $G(s)$
$G^T(s)$	transpose of the transfer function matrix $G(s)$
$\bar{\lambda}_{\max}(A)$	the maximum eigenvalue of matrix A that has only real eigenvalues
$\lambda_i(A)$	the ith eigenvalue of matrix A
$\mathbf{I}_n$	$n \times n$ identity matrix
$\underline{\lambda}_{\min}(A)$	the minimum eigenvalue of matrix A that has only real eigenvalues

Number sets

$\mathbb{C}$	field of complex numbers
$\mathbb{C}^n$	field of complex vectors with n elements
$\mathbb{C}^{n\times m}$	field of complex matrices with n rows and m columns
$\mathbb{F}^{n\times m}$	field of complex or real matrices with n rows and m columns
$\mathbb{R}$	field of real numbers
$\mathbb{R}^n$	field of real vectors with n elements
$\mathbb{R}^{n\times m}$	field of real matrices with n rows and m columns
$\mathbb{R}_{\geq 0}$	non-negative real numbers

Symbols

$<$	less than
$=$	equal to
$>$	greater than
$\cup$	union
$\equiv$	equivalent to
$\exists$	there exist
$\forall$	for all
$\geq$	greater than or equal to
$\iff$	equivalent to
$\implies$	implies
$\in$	belongs to
$\leq$	less than or equal to

$\neq$	not equal to
$\not\equiv$	not equivalent to
$\subset$	subset of
$\rightarrow$	tends to

Chapter 1

Introduction

1.1 Background

The study of Negative Imaginary (NI) systems was motivated by the study of lightly damped inertial systems with collocated force actuator and position sensor [15,16].These kind of systems are modelled by Partial Differential Equation (PDEs). However, they can also be expressed as the sum of an infinite number of lightly damped second order linear system with highly resonant modes. For all positive frequencies, the linear system exhibit a negative frequency response with a phase that lies between 0^o and -180^o. Due to the negative frequency response of the systems, those kind of systems were termed as Negative Imaginary Systems.

One of the main advantage of modelling flexible systems as NI systems (i.e. using collocated force actuator and position sensor) is that even when higher order system will be considered, it will still have the NI property. Moreover, if on the other hand, we consider a reduced order model for control purpose, the reduced order model still retains the NI property together with the spillover or unmodelled dynamics. Hence, the NI theory can be used to control the reduced order model whilst being robust to the unmodelled dynamics by satisfying a simple DC gain condition. Furthermore, the closed-loop system synthesized using the NI theory will also be robust to any other mechanical perturbation, in addition to the unmodelled dynamics, having the NI property and also satisfying the DC gain condition.

The NI theory was developed for positive feedback interconnection of linear systems having the NI systems property. Consider the positive feedback interconnection of

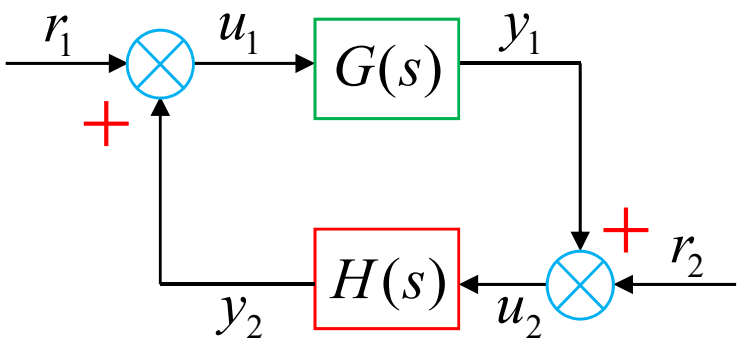

Figure 1.1: A positive feedback interconnection of NI systems.

an NI system $G(s)$, with a Strictly Negative Imaginary (SNI) system $H(s)$ show in Figure 1.1. For simplicity, we consider the case where the two systems are Single-Input-Single-Output (SISO) systems so that we can make reference to the Nyquist plots of the systems. The stability of the positive feedback interconnection follows using the Nyquist stability criterion. First, since we have a positive feedback interconnection, then the critical Nyquist point of interest is the $+1 + j0$ point.

Since $G(s)$ is NI and $H(s)$ is SNI, then $\angle G(j\omega) \in [-180^o, 0^o]$, $\angle H(j\omega) \in (-180^o, 0^o)$ and $\angle G(j\omega)H(j\omega) \in (-360^o, 0^o)$, $\forall\ \omega > 0$. Also, since $H(s)$ and $G(s)$ are real and rational, then $G(j\omega)H(j\omega)$ will have real frequency response at $\omega = 0$ and $\omega = \infty$. Hence, when $G(\infty)H(\infty) = 0$ and $G(0)H(0) < 1$, the critical Nyquist point will not be encircled and thus, closed-loop stability is guaranteed. Therefore, a necessary and sufficient condition for the stability of two NI system is the DC gain being less than unity if one of the systems is strictly proper.

A good control system is characterized by good performance and robust stability. It therefore comes as no surprise that these two main aspects of the control system keep on getting quite a lot of attention.

For robust stability, when the designer has as much information on the feedback interconnected systems as possible, then the Nyquist stability theorem can provide the necessary and sufficient tool for ensuring internal stability [15–17].

If however, the designer has limited information on the feedback interconnected systems, it may still be possible to design a closed-loop control system with guaranteed internal stability if the systems have certain properties. For example, the robust stability of a feedback interconnection of Bounded Real (BR) systems with contractive gain can be established using the small-gain theorem [18, 88]. While for the feedback

interconnection of Positive Real (PR) systems, passivity theorem can be used to establish robust stability [15, 16, 19, 45].

Such theorems (i.e. passivity and small-gain) serve as important tools in stability analysis as they allow for the establishment of necessary and sufficient conditions for the robust stability even when the designer has limited information on the interconnected systems.

Therefore, the NI stability result is similar to some of the well known robust stability result in the literature, such as passivity and small-gain theorem. However, the NI stability result has some fundamental differences to these results. For example, in the position control of lightly damped structure having collocated force actuator and position sensor, such systems exhibit the NI properties and not the PR systems properties. As such, passivity theorem cannot be used for the analysis of such systems.

Also, the NI stability result is not an absolute value type of result. For example, a negative DC gain such as $G(0)H(0) < -50I$ will guarantee stability of the positive feedback interconnection of $G(s)$ and $H(s)$ using the NI theory but not via the small-gain theorem. Hence, NI stability theory is not a one-sided type of stability result as is the small-gain theorem. Furthermore, the small-gain theorem is a result that needs to hold for all frequencies while NI stability result is only a DC gain condition.

Due to these nuances and appealing stability result, the NI theory has been applied in a number of practical engineering application. These include vibration attenuation of flexible structures [55], control of DC machine with parametric uncertainty [27], control of flexible robotic arm [39], Consensus control of networked systems [48, 49, 53], position control of nanopositioning systems such as Atomic Force Microscope [40, 41], damping control of guitar string [38], control of large bridge structures [36], to mention but a few.

1.2 Motivation

Since the introduction of NI systems by [15, 16], NI theory has proven to be quite popular due to its simple stability result and the wide range of possible areas of application. As such, the NI synthesis problem has attracted a lot of attention in recent times.

The NI synthesis problem is broadly classified into two categories viz: the first being that of designing a controller to render the closed-loop NI (wihtout the controller itself being NI) while the second entails designing the controller itself to be NI. In the first case, an NI or SNI uncertainty is first extracted from the nominal plant and the NI synthesis problem becomes that of synthesizing either an NI or SNI closed-loop system depending on the uncertainty. Most of the NI synthesis solutions in the literature addressed this type of problem. Some of the solutions include the work in [32, 41, 66, 79, 81].

However, non of the above stated work addressed the issue of performance of the closed-loop system. Some of the recent works that address the issue of performance of the closed-loop systems do have other shortcomings. For example, [64] relied on the transformation from PR to NI systems. However, using that transformation, an Strictly Positive Real (SPR) system is transformed into an NI (not SNI) system. This is due to the introduction of a blocking zero at the origin which makes the system NI. So, if the uncertainty is NI, the closed-loop system will also be NI which will not satisfy the conditions for robust stability as one of the systems is required to be SNI.

The work in [82] addressed the NI synthesis problem with $\mathcal{H}_\infty$ closed-loop performance. This was done by first designing an NI controller and then minimizing its distance from another synthesized $\mathcal{H}_\infty$ controller. But there is no guarantee that the NI controller will retain any of the property of the $\mathcal{H}_\infty$ controller just by minimizing the distance between the two controller.

Other solution such as the one offered in [70] used full state feedback for synthesis. But some of the states might not be available for measurement and even if they are, it might not be cost-effective to measure all of them.

For the second type of synthesis problem, where the controller is synthesized itself to be NI, only a handful of work addressed such kind of problem. In [20], it was shown that the Integral Resonant Control (IRC) was a form of SNI system. Hence, IRC controllers were designed for vibration attenuation in [36, 55]. However, in [55], the controller parameters were obtained via a nonlinear optimization which is difficult to solve while [36] did not provide a synthesis technique.

The work in this thesis is therefore motivated by providing a solutions to some of the shortcomings of the NI synthesis problem. The first solution addresses the issue

of designing a dynamic output feedback controller that renders the closed-loop system SNI and is robust to all class of NI uncertainties satisfying a certain DC gain condition. The synthesized closed-loop system also has some time domain performance in the form of prescribed decay rate.

However, sometimes separating the uncertainty from the nominal plant can be difficult. Hence, applying the solutions using the first synthesis approach may not always be possible. The second solution involves the use of the principles of Internal Model Control (IMC) to synthesize an NI(or SNI) controller for an uncertain SNI (or NI) plant (respectively). This approach also provides a tuning parameter that is used to improve the performance of the closed-loop system and also facilitates perfect nominal set-point tracking for a constant reference signal.

Finally, most of the work in the NI literature are theoretical, with handful practical validation. Thus, the work in this thesis is also motivated to bridge this gap between theory and practice. Therefore, we built a test rig to validate one of the synthesis techniques proposed in this thesis.

1.3 Aims and Objectives

The main aim of this thesis is to address the issue of the NI synthesis problem, which include synthesizing a controller that renders the closed-loop system NI or synthesizing the controller itself to be NI. Here, we aim to provide an Linear Matrix Inequality (LMI)-based synthesis technique for NI systems. This is due to the fact that LMIs can readily be solved using Semi Definite Programming (SDP) solvers, hence making the the synthesis technique appealing for industrial applications.

Another main aim of the thesis to ensure that the synthesized controllers improve the time domain performance of the closed-loop system. However, unlike the traditional performance measures used in robust control, such as $\mathcal{H}_\infty$ and $\mathcal{H}_2$ performance measures, we use measures such as output tracking, decay rate, settling time, damping of the closed-loop system e.t.c. This is done so that the tuning becomes more intuitive.

Among the objectives of this thesis include building a test rig that will be used to validate some of the synthesis technique developed in the thesis. The test rig will be in the form of a flexible structure system will collocated force actuator and position sensor.

The designed controller should be able to attenuate the vibration of the structure and at the same time be robust to the unmodelled dynamics of the flexible structure system.

Although the NI literature has been rich with contributions, there are still some practical systems that are yet to be captured by the current literature. For example, if we consider the rectilinear motion of a time-varying point mass, then the relationship between the position and the thrust has a time-varying NI property. Therefore, this thesis aims to extend NI literature to account for those kind of systems.

1.4 Contributions

In line with the aforementioned aims and objectives of the thesis, together with the shortcomings highlighted in the background of this thesis, the major contributions of this thesis are in the areas of solution to the NI synthesis problem and analysis of linear time-varying (LTV) NI systems.

In our first contribution, we provided a definition of $\alpha-$ SNI systems. We showed that these are asymptotically stable NI systems with a prescribed decay rate dictated by the variable α. We also showed the difference between these kind of systems with the Strongly Strictly Negative Imaginary (SSNI) systems existing in the literature. Furthermore, we used the α- SNI property for the synthesis of a dynamic output feedback controller that renders the closed-loop system $\alpha-$ SNI. This ensures that the poles of the closed-loop system are atleast on or to the left of $-\alpha$ in the left half of the complex plane. As such, the variable α was used as a measure of improving the performance of the closed-loop system, which in this case is the decay rate of the closed-loop system.

Another major contribution of this thesis is in extending the NI literature to account for a new class of systems called the LTV and Linear Parameter-Varying (LPV) NI systems. We first provided an input-output time domain definition of LTV NI and Output Strictly Negative Imaginary (OSNI) systems. We showed that both systems are dissipative with respect to a supply rate which is dependent on the input and derivative of the output of the system. This essentially is the power supplied to the system as the input the force and the derivative of the output is velocity. We also

provided a state-space characterization of both LTV NI and OSNI systems. The state-space characterization helps to facilitate easy analysis and synthesis of this kind of systems. We concluded the work on LTV NI systems by providing a stability result for the positive feedback interconnection of an LTV NI system with and LTV OSNI system.

In a similar flavour, we provided a state-space characterization LPV NI and LPV OSNI systems. We also studied the conditions necessary to ensure the stability of an unforced positive feedback interconnection of an LPV NI system with an LPV OSNI system.

One of the main aim of this thesis is provide controller synthesis techniques that are easy and intuitive. It is common knowledge that IMC are popular in the industry due to their ease of design and robustness property. For any nominal stable, minimum phase plant, designing a stable Youla parameter guarantees robust stability using the IMC design technique. However, almost all systems have some level of uncertainty and this nice property of robustness of the IMC controller does not extend to uncertain plants.

Hence, in this thesis, we combined the IMC design principle with the NI theory to extend the robustness property to account for uncertain NI systems. We provide a DC gain condition that ensures that the Youla parameter is always stable for a certain NI controller, thus robustly stabilizing a given NI system with a known DC gain. We provide two methods of synthesizing a controller using the IMC-NI principles; one via a frequency domain approach and the other using LMIs. We show that both methods can facilitate nominal set-pointing tracking of a constant reference signal with only knowledge of the DC gain of the system. Moreover, we also show that the different synthesis techniques can be used to improve some other performance of the closed-loop system such as damping.

The final contribution of the thesis is in the application of the NI-IMC based controller to a hardware system for a vibration attenuation problem. First, we built a test rig of a flexible structure system, which consisted of a cantilever beam with collocated force actuator and position sensor. We also provided a model of the plant via Matlab system identification toolbox. We considered the first two resonant modes and consider the rest of the modes as unmodelled dynamics. We used the model to

design a controller using LMI based technique of the NI-IMC synthesis procedure. We successfully applied the designed controller on the flexible structure system to robustly attenuate the vibration as the cantilever beam is subjected to external disturbances and also remain robustly stable against the unmodelled dynamics.

1.5 Outline of the Thesis

The rest of the report will be organized as follows: Chapter 2 provides a comprehensive literature review of the NI system theory. Chapter 3 provides the background information required for a better understanding of the NI theory. In Chapter 4, $\alpha-$ SNI systems are introduced. An LMI-based dynamic output feedback controller synthesis technique using the $\alpha-$ SNI framework is also provided in this chapter. Chapter 5 introduces a new class of NI systems termed as LTV NI systems. The time domain definition of the systems is provided and a state-space characterisation of the LTV NI systems is developed. Stability result for the positive feedback interconnection of two LTV NI systems is also established in this Chapter. The results are then specialised to the LPV NI systems. In Chapter 6, an NI controller synthesis technique is introduced using the IMC framework. Two different techniques are presented: one based on a frequency domain approach and the other is an LMI-based approach. Chapter 7 deals with the experimental validation of the IMC based controller synthesis introduced in Chapter 6. Finally, the conclusions and future work are provided in Chapter 8.

Chapter 2

Literature Review

This chapter provides a comprehensive literature review of the NI theory. It introduces the different definitions of NI systems, the different flavours of NI state-space characterizations and robust stability results of the positive feedback interconnection of the two NI systems.

We also provide a comprehensive explanation of the various solution of the NI synthesis problem proposed in the literature thus far. This is due to the fact that the NI synthesis problem is central to this thesis and hence, it is important to bring the reader up to date with recent contributions to the solution of that problem and also highlight the shortcomings that we try to address.

In the study of inertial systems, [15,16] realized that by considering lightly damped structures with collocated position (and not velocity) sensor and force actuator, systems with a different characteristics to those used in passivity and small-gain theorem were obtained. Such systems were termed as NI systems. These are systems that have negative imaginary frequency response for all positive frequency $\omega \in (0, \infty)$ [15]. In the SISO case, this can be interpreted as the Nyquist plot lying on or below the real axis of the complex plane. A typical plot of a system with the NI property is shown in Fig. 2.1, where the Nyquist plot will lie in the red region. The characteristics exhibited by the NI systems was similar to that observed in the SISO positive postion feedback control systems in [1,2]. The NI systems may be nonminimum phase, improper and can have relative degree of up to two and as such passivity theorem could not be applied to them. Moreover, using small-gain theorem will lead to a conservative result [16, 31].

Due to the aforementioned reasons, [16,31] set out to provide a complete state-space

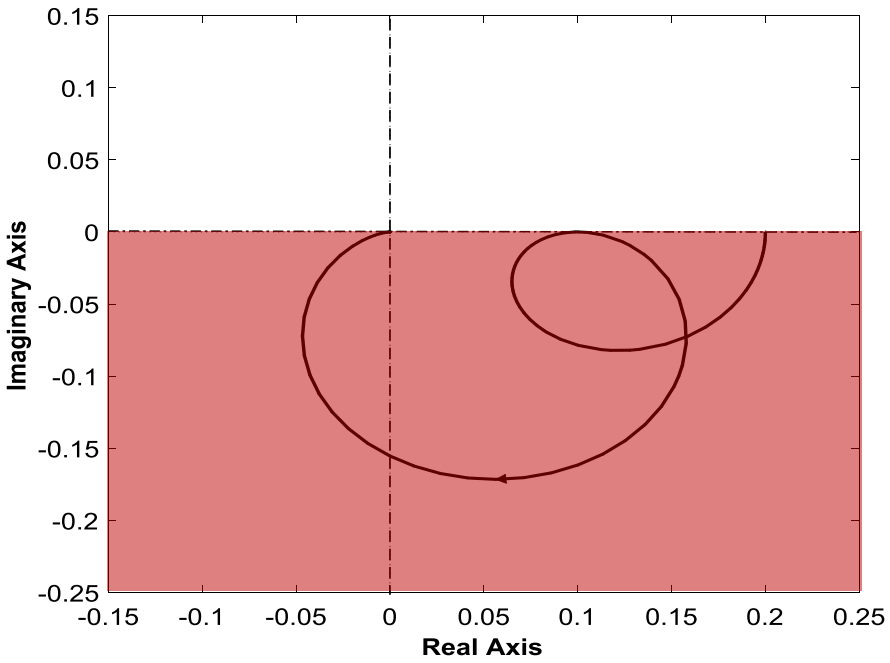

Figure 2.1: Red region shows where the Nyquist plot of a SISO NI system lies.

representation of the NI systems and the conditions for the robust stability of such systems. In a similar vein to the passivity and small-gain theorem, necessary and sufficient conditions for the robust stability of a positive feedback interconnection of NI systems was established. For robust stability of a positive feedback interconnection of an NI system with a SNI system, under certain assumptions, a DC gain of less than unity was required [16, 31]. The SNI systems are the class of NI systems that touch the real axis only at zero and infinite frequencies.

Unlike passivity theorem, this was a conditional stability result. The robust stability result of NI systems was obtained by exploiting the relationship between NI systems and PR systems. Also, an NI lemma which was used as a litmus test to check whether a transfer function matrix was NI was proposed [15, 16]. However, the stability results in [15, 16] were established based on the assumption that the NI systems had no poles either at the origin or on the imaginary axis. Also, a minimal state-space realization was assumed.

[20] also proposed an NI lemma similar that of [15, 16] and an SNI lemma. A pertubation technique was used for proposing the SNI lemma. Using the pertubation technique, two different SNI lemmas were proposed. The pertubation technique was

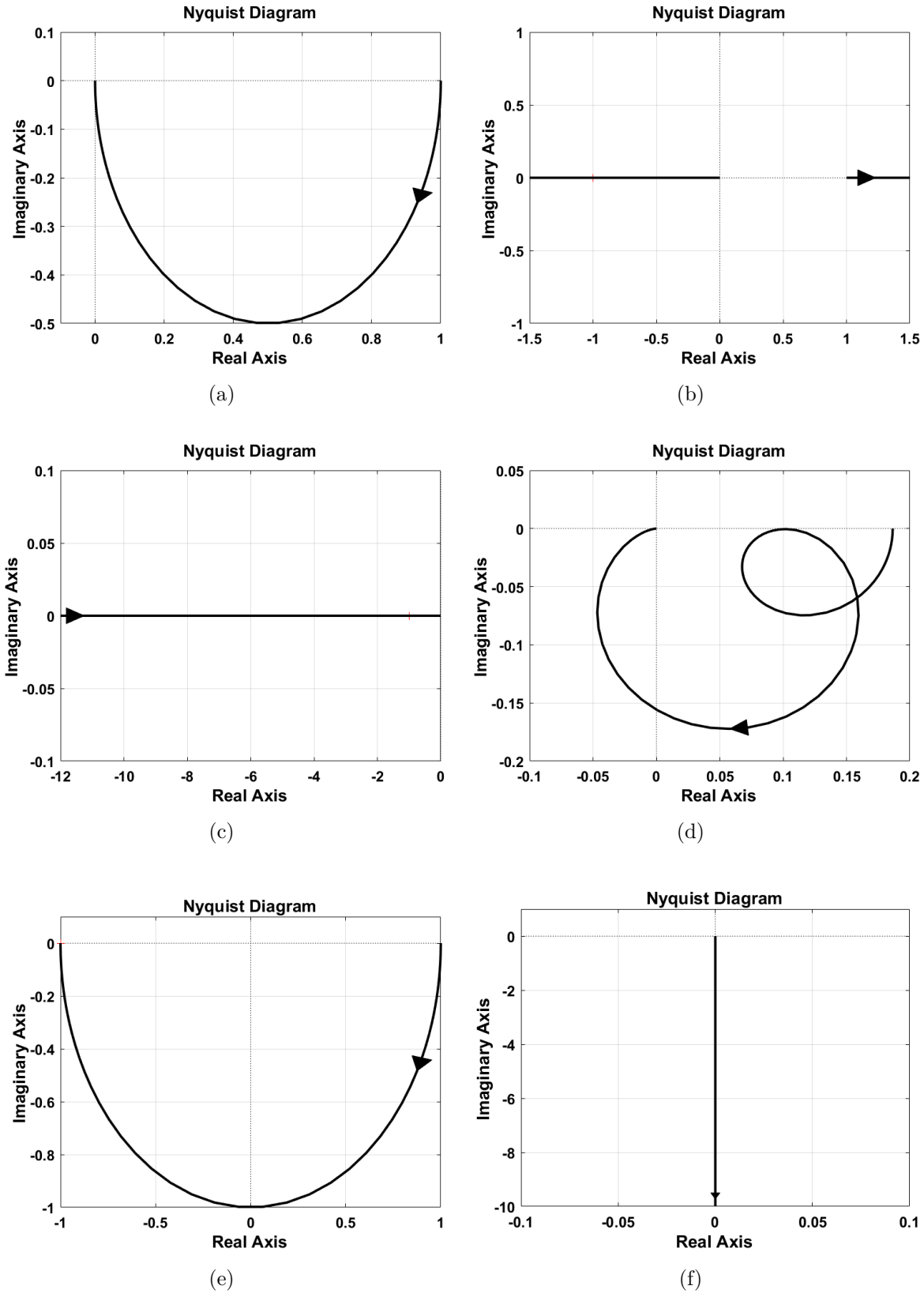

Figure 2.2: Examples of Nyquist plot of SISO NI systems (a) Simple first order system $\frac{1}{s+1}$; (b) Loseless system $\frac{1}{s^2+1}$; (c) Double integrator $\frac{1}{s^2}$; (d) Higher order system $\frac{2s^2+s+1.1}{2s^4+7s^3+17s^2+17s+5.9}$; (e) Nonminimum phase system $\frac{1-s}{s+1}$; (f) Improper system $-s$.

also utilized in showing that an Integral Resonant Controller (IRC) was an SNI system. Moreover, the various proposed lemmas all invoked minimality of the state-space representation.

In [25], the definition of NI systems was extended to include poles on the imaginary axis but not at the origin. Necessary and sufficient conditions for systems to be NI and SNI were also provided via an NI and SNI lemma. The SNI lemma was termed as the Weakly Strict NI (WSNI) lemma as it was analogous to the Weakly Strict PR (WSPR) lemma. The requirement for the DC gain to be less than unity for internal stability was also shown to be valid for NI systems with poles on the imaginary axis. Similar to [15, 16], [25] also assumed a minimal state-space realization for the system.

An SSNI lemma was proposed in [21]. The lemma was termed as the SSNI lemma because it was analogous to the Strongly Strict PR (SSPR) lemma. The minimality assumption in [16, 31] and [25] was relaxed in [21]. The property of reciprocal system was exploited in the establishment of the SSNI lemma.Two SSNI lemmas were proposed. The first lemma gave necessary and sufficient condition for a system to be SSNI under the assumption that the system is observable. The other lemma was given under the assumption that the system had no observable uncontrollable modes.

The definition of NI systems was extended in [74] to cover systems expressed in descriptor form. This was due to the fact that many important systems were expressed in descriptor form rather than the regular state-space representation. Using the relationship between NI and PR systems and the notion of Weierstrass form transformation, necessary and sufficient conditions for the descriptor systems to be NI were established in [74].

[22, 34] further extended the class of NI systems to cover the lossless systems. Necessary and sufficient conditions under which a system can be termed as lossless NI were provided. They also established the fact that a DC gain of less than unity was required for internal stability of a positive feedback interconnection of a lossless NI and an SNI system.

Finite Frequency NI (FFNI) systems were introduced in [23, 24]. These are systems which have NI properties over certain frequency range in addition to being Lyapunov stable. Using the relationship between Finite Frequency PR (FFPR) and FFNI systems, an FFNI lemma was proposed. Moreover, necessary and sufficient conditions were

established for a system to be FFNI under the proposed lemma. It was also shown that as the limit frequency approached infinity, the FFNI lemma was equivalent to the NI lemma that already existed in the literature.

A time domain interpretation of the FFNI lemma was also provided [23, 24]. The interpretation was given in terms of input, output and state of the system rather than the state-space realization. The representation was given with a view of making it easier to extend the lemma to nonlinear systems since nonlinear systems cannot be represented in transfer function form.

In a similar approach to [21], [32] relaxed the minimality assumption and proposed an NI lemma. This lemma also used the relationship between NI and PR systems. Under the assumption that the feedthrough matrix is symmetric, the lemma stated that a system was NI if a positive semidefinite matrix solution of a particular LMI exist.

A method for identifying NI and SNI SISO and Multi Input Multi Output (MIMO) systems was proposed by [40]. This method was based on the Hamiltonian matrix of the transfer function matrix. For a SISO system, a minimal state-space realization was adjudged to be NI if the Hamiltonian matrix had no eigenvalues of odd multiplicity on the open negative real axis and the imaginary axis poles of the PR counterpart are positive. For SISO SNI systems, it was established that the Hamiltonian matrix is required to have all its eigenvalues in the open real axis and the state matrix should be Hurwitz.

While for MIMO systems, a minimal state-space realization was deemed to be NI if no pure imaginary eigenvalue of the Hamiltonian matrix is of odd multiplicity. However, the MIMO system is SNI if the Hamiltonian matrix has no pure imaginary axis eigenvalue except at the origin.

The first attempt in proposing stability results that apply to distributed-parameter NI systems was addressed in [46, 83]. In [46], sufficient conditions were provided for the internal stability of a positive feedback interconnection of NI systems with poles on the imaginary axis (but not the origin) and an SNI systems using Integral Quadratic Constraint (IQC) approach. While in [83], necessary and sufficient conditions for internal stability of an NI system with poles on the imaginary axis but not the origin and an SNI system was established. The sufficiency part was proved by developing

multiplier at zero and infinite frequency such that the IQC at those frequencies hold.

Unlike the previous results in the literature, the stability conditions established in [46, 83] do not rely on the state-space matrices of the system. The result could be applied to NI systems with non-rational transfer function such as time delay NI systems.

A major extension to the definition of NI systems was given in [29, 39] to include systems with free body dynamics (i.e. systems with poles at the origin). It was shown that NI systems could have up to two poles at the origin. Necessary and sufficient conditions for the internal stability of a positive feedback interconnection of an SNI system and an NI system with pole(s) at the origin were also provided. These conditions were mainly matrix sign definite conditions.

The focal point of establishing the stability conditions in [29, 39] in addition to mathematical tools such as singular value decomposition and Schurs' complement, was the Laurent series expansion. The expansion made it possible to obtain the coefficients that contain the information of the free body dynamics of interest.

With the work of [29,39] that allows for NI systems with poles at the origin, [41,75] proposed a new generalized NI lemma. This lemma was based on the existence of a positive semidefinite matrix solution to a given LMI condition. [41, 75] also proposed new NI and SNI lemmas in terms of Algebraic Riccati Equations (AREs).

A more general NI property for descriptor systems was addressed in [71]. An LMI based approach with equality constraint was used to derive necessary and sufficient conditions for descriptor systems to be NI via a state-space formulation. The LMI conditions thus provided a more numerically efficient method for determining the NI property of the descriptor systems compared to the work in [74]. Under some technical assumptions, [71] proposed an NI, SNI and lossless NI lemmas. These lemmas were shown to coincide with the NI, SNI and lossless NI lemmas that existed in the literature when the descriptor system is reduced to standard state-space representation.

The first attempt to define NI systems to include systems with non rational transfer function matrices was made in [35]. The authors considered symmetric transfer function matrices. Using the concept of skew imaginary matrix, NI systems were defined in terms of sign conditions in the domain of analyticity.

Using the definition presented in [35], NI systems were extended to cover a wide

range of systems which included systems with pole at infinity, systems with negative relative degree, systems with non-rational transfer function matrix and nonminimum phase systems. All these systems were not captured by earlier definition of NI systems. This new definition also included NI systems that already existed in the literature.

The dissipativity of the states of NI systems with respect to a particular supply function was also established by [35]. Furthermore, a relationship between NI and PR systems was also given based on the new definition.

Sequel to the result presented in [35], [47] used similar approach to provide a definition of symmetric SNI systems also via a sign condition in the domain of analyticity. The definition captured a new class of SNI systems (i.e. SNI systems with non rational transfer function) that were otherwise not captured by the existing definition in the literature. [47] also provided a new definition for SSNI and WSNI systems.

Another important contribution by [47] was the introduction of a transformation that transformed SSNI systems to SSPR systems. Subsequent to this work, it had been widely believed that SSNI systems could only be transformed to PR systems as reported in the NI literature. Finally, conditions under which NI, SNI or WSNI properties are preserved for a feedback interconnection were also presented.

Since some NI transfer functions may not be symmetric, the definitions provided in [35] and [47] may not be applicable to some NI systems. Therefore, [76] considered a new class of NI systems that may also be non proper, non symmetric but rational. However, [76] only gave sufficient conditions for the transfer function matrix to be NI. The work was also restricted to NI systems and SNI systems were not addressed.

In view of the increasing importance of digital control in present day systems, [37] provided a Discrete Time (DT) equivalence of the work in [35, 47]. A DT definition for non necessarily rational NI, SSNI and WSNI symmetric systems was provided. The relationship between DT NI and DT PR systems was also presented.

Necessary and sufficient conditions for a DT symmetric, real, rational and proper transfer function matrix to be NI were also given in [37]. Moreover, conditions under which DT NI, SSNI and WSNI systems preserve their properties in a feedback interconnection were also established. Furthermore, necessary and sufficient conditions for a positive feedback interconnection of a DT NI system and a DT WSNI to be internally stable was provided.

[77] also provided a DT counter part of the work in [76]. However, unlike in the Continuous Time (CT) framework, [77] focused on proper (and not non-proper) transfer function matrix. A simple bilinear transformation was presented for transforming CT NI systems to DT NI systems. A relationship between DT PR and DT NI systems was also established. A DT NI lemma which provided necessary and sufficient conditions to allow for the algebraic characterization of a linear DT system as NI was given. Finally, stability condition for a positive feedback interconnection of DT NI and DT SNI system was proposed.

With the extension of the definition of NI systems to include poles at the imaginary axis and the origin, [57] revisited the conditions required for internal stability. [57] sought to improve the necessary and sufficient condition established in [29, 39] which were deemed to be complicated and difficult to ascertain while at the same time relaxing some gain assumptions imposed in [15, 16].

Necessary and sufficient conditions for internal stability of NI systems with poles on the imaginary axis but not at the origin were first derived. The assumptions of the NI and SNI system gain at infinity imposed in [16, 31] were relaxed in deriving the conditions. Two different necessary and sufficient conditions were established. These conditions were shown to reduce to the stability results established in [16, 31] when the same assumptions were imposed. The result was also specialized to SISO systems resulting in a more simpler necessary and sufficient conditions.

In the second part of the work by [57], the internal stability of NI systems with poles at the origin was addressed. Robust stability conditions were derived using a linear shift transformation and the existence of a certain negative definite matrix. The conditions derived in [57] were shown to be the same as those established in [29, 39] when the NI system is considered to be strictly proper as assumed in the latter. The stability conditions were also shown to correspond to the conditions established in the first part of the work when the NI system does not have a pole at the origin.

Finally, since the necessary and sufficient conditions established in [57] depended on the existence of a particular negative definite matrix, a definitive method of obtaining such a matrix was established and it was also shown that such a matrix need not to be unique.

As earlier stated, in addition to robust stability, control systems should also have

good performance. For this reason, [30] addressed the issue of robust performance of NI systems. This was done by transforming the NI systems to BR systems via PR systems. In the robust performance analysis, a fictional BR uncertainty was introduced. The fictional uncertainty transformed the robust performance problem to a robust stability problem. Hence, the problem became that of ensuring the internal stability of a closed-loop system in the presence of a mixed SNI and Strictly BR (SBR) uncertainty. With the problem being in the standard structured singular value framework, a quantifiable value for the performance could be obtained.

[30] also established necessary and sufficient condition for a system with mixed NI and BR uncertainty to be internally stable under the assumption that the nominal system was stabilizable and detectable.

In some cases, practical systems may not have pure NI or SNI property but rather a mixture of properties. For example, the same system may have NI property at certain frequency range and PR or BR property at other frequency range.Thus, [28] addressed the issue of systems with mixed NI and small-gain property.

This was done by exploiting the dissipative property of the system with respect to three frequency dependent triplets. Three different frequency regions were identified viz: NI frequency region, BR frequency region and NI plus BR frequency region. A frequency dependent flag was used in identifying the region which the system was in at any particular time. Using the frequency dependent triplets and the frequency flag, [28] established necessary and sufficient conditions for the internal stability of a positive feedback interconnection of a system with mixed NI and BR property and an SNI system. It was shown in [28] that the established internal stability conditions captured a larger class of NI systems as compared to the class in [15, 16].

As with other similar robust stability theorems (such as passivity and small-gain), efforts have also been made in controller synthesis for NI systems due to the importance of these systems in practical applications. The first effort in controller synthesis for NI systems was presented in [31, 33].

Owing to the fact that robust $\mathcal{H}_\infty$ controller synthesis methods for BR systems was well documented in the literature, [31, 33] transformed NI systems to BR systems such that $\mathcal{H}_\infty$ techniques could be applied to the transformed system. The transformation of the NI systems to BR systems was via PR systems. Hence, [31, 33] showed that for

a generalized plant that is both stabilizable and detectable, the problem of obtaining a controller that internally stabilizes the plant and makes the closed-loop system NI is akin to the problem of obtaining a controller that internally stabilizes another generalized plant (obtained via transforming the original generalized plant) while at the same time making its' input-output map contractive.

But since the transformation used in [31, 33] from NI to BR systems was via PR systems, a blocking zero at zero was introduced to the transformed system. For this reason, SNI systems could not be transformed to SPR or SBR systems. Therefore, a definitive controller synthesis technique was not given in [31, 33].

Having established that IRC was an SNI system, [20] synthesized an IRC controller to robustly stabilize an NI plant which was a flexible structure with collocated force actuator and position sensor. A static state feedback controller was also synthesized in [20]. The static feedback controller was designed such that the closed-loop system was NI and had a DC gain of less than unity. The uncertainty of the system was assumed to be SNI which ensured the satisfaction of the DC loop gain condition thereby resulting in a robustly stable closed-loop system.

A static state feedback controller based on LMI formulation was developed in [32]. It was assumed that all the states of the system were available for the controller design and that the uncertainty of the system was SNI. The controller was also synthesized to ensure that the DC gain of the system was less than unity which was a necessary and sufficient condition for robust internal stability.

Another static state feedback controller was synthesized in [41]. A Riccati-based approach was employed for the synthesis. Schur decomposition was used to transform the original plant and the controller synthesis reduced to solving two Lyapunov equations. However, this synthesis method always results in a Lyapunov stable closed-loop system.

On the other hand, [66] tackled the problem of both output and state feedback controller synthesis. Three different NI controller synthesis methods were presented. The first two methods were output feedback, where a static and a dynamic output feedback controllers were designed which rendered the closed-loop system NI. The third method was an observer based state feedback controller.

In the obsever based controller synthesis method, the seperation principle was

shown to still hold when the plant input is available for the observer design. This led to a more easier controller design process. Furthermore, an algorithm for calculating the gain (for static output feedback controller) or the controller matrices (for dynamic output feedback controller) was also developed. Also, [66] showed that it was possible to impose a structural constraint on the developed controllers by taking advantage of the structures of these controllers.

Sufficient conditions for the solution of SNI synthesis problem was proposed in [79, 81]. Both static state and dynamic output feedback synthesis problems were addressed. The synthesis was based on the solution of ARE. For the static state feedback, it was shown that a gain which renders the closed-loop system NI exist if the solution of an ARE exist. This gain can further ensure that the closed-loop system is SNI and asymptotically stable if some eigenvalue and singularity conditions are fulfilled. A similar approach to the static state synthesis was utilized for the synthesis of the dynamic output feedback controller but under some more restrictive assumptions. Here, also, the closed-loop system is strengthened from NI to SNI if certain conditions are fulfilled.

An SNI full state static feedback control synthesis technique was proposed by [70]. Necessary and sufficient conditions were provided for the SNI synthesis problem using a Lyapunov based design approach as opposed to ARE used in [79, 81]. Under certain assumptions, [70] was able to prove that the synthesized closed-loop system was SNI and had a prescribed degree of stability dictated by a certain pertubation constant.

The problem of dynamic output feedback synthesis that transforms the closed-loop system to an SSNI system was addressed in [58]. The synthesis technique was based on the LMI framework introduced in [73]. The synthesized controller achieves robust stability against NI/SNI uncertainty via the DC gain condition of the NI theory. It was also shown that other performance objectives such as $\mathcal{H}_2$ and $\mathcal{H}_\infty$ performance could be readily incorporated into the design via the multi-objective LMI formulation. Finally, [58] showed that the synthesized controller can still maintain some level of robust $\mathcal{H}_\infty$ performance in the presence of NI/SNI uncertainty.

In [82], an SNI controller synthesis technique with $\mathcal{H}_\infty$ performance was proposed. This was achieved by first synthesizing an $\mathcal{H}_\infty$ controller before subsequently designing the SNI controller by minimizing the distance between the $\mathcal{H}_\infty$ controller and the SNI

controller, with the SNI conditions being imposed as LMI constraints. Robust stability to NI uncertainties was achieved by imposing an LMI DC gain constraint that satisfies the DC gain condition of the NI theory for internal stability of an NI-SNI positive feedback interconnection.

The work in [31,33] did not provide a systematic approach to design the NI controller while synthesis methods such as those proposed in [20, 32, 41, 66, 70, 79, 81] use static state feedback design which may not be feasible when all the states are not available for measurement. Moreover, even in cases where the states are available for measurement, the sensors used for measuring that states might be very expensive.

The dynamic output feedback synthesis proposed in [79, 81] uses ARE which is difficult to solve. Both the static and dynamic output feedback synthesis technique in [66] do not address the issue of output performance of the closed-loop system. Although [64] addressed the issue of performance, the dynamic output feedback synthesis technique proposed uses a transformation from PR to NI which does not hold for the strict case.

Due to these shortcomings, the work in Chapter 4 aims to provide a dynamic output feedback synthesis via an LMI-based technique with a method of improving the time domain performance of the closed-loop system using a particular constant to define the minimum decay rate of the closed-loop system.

There are some systems such as a flexible structure system with time-varying mass and a collocated force actuator and position sensor, which give rise to a class of NI system referred to as LTV NI systems. This class of systems has not been addressed in the literature so far and are studied in Chapter 5.

Recent work in [58] that proposed a multi-objective dynamic output feedback synthesis may result in difficulties when fitting the framework to practical systems. On the other hand, for the synthesis technique proposed in [82], there is no guarantee that the NI controller synthesized using that approach will retain the properties of the corresponding $\mathcal{H}_\infty$ controller by just minimising the distance between the two controllers. Hence, Chapter 6 provides a controller synthesis method using LMI, that can easily be fitted to practical systems and provides guidelines on how to design the controller and tune it for a better output performance of the closed-loop system.

Since its' inception, the NI system theory has received quite a lot of attention and

within few years, substantial amount of literature can be found on the topic. However, it has also been shown to have quite a lot of practical applications.

An IRC was designed to damp the first five mode of a guitar string in [38]. The process involved stretching and fixing the string at both ends before placing it in a magnetic field. An electric current was then supplied to the string which caused it to vibrate. By using a collocated force actuator and displacement sensor, the dynamics of the system was found to satisfy the NI property. Hence, IRC was designed to damp the resonant modes while ensuring robust stability. Experimental setup was used to confirm the validity of the control system.

NI theory has also been used in consensus control of networked systems. The work in [49] explored the conditions under which consensus of networked NI systems is achieved in the presence of NI uncertainty and $\mathcal{L}_2$ disturbance. The work focused on output feedback consensus as opposed to state feedback which was usually considered in the literature. The authors in [49] were also able to show that a single agent system has more robustness compared to networked systems. Finally, the convergence of some commonly occuring NI systems was shown to depend on the initial pattern for zero initial conditions of the controller.

The work in [48] also focused on consensus control but of heterogeneous NI systems. However in this approach, unlike in [49], the incidence matrix and not the laplacian matrix was used in deriving the feedback control law. This was done to preserve the NI property of the networked systems. Both $\mathcal{L}_2$ external disturbance and NI uncertainty were also considered. Necessary and sufficient conditions for robust output feedback consensus were first derived for networked NI systems without poles at the origin. Afterwards, the robust output feedback consensus problem for strictly proper networked NI systems with poles at the origin was addressed.

The underlying dynamics of a 3-mirror optical cavity system was found to be NI. The authors in [42] therefore designed an IRC to improve the damping of the piezo-electric transducer. Internal stability was ensured by making the DC gain of the optical cavity system and the controller to be less than unity.

Nanopositioning systems [40, 41] are another area where NI theory was applied. In [40], the developed spectral methods for checking the NI and SNI property of a system was applied to two different nanopositioning systems. The first was the

cantilever beam while the second was an atomic force microscope. In [41], a state feedback controller was designed for an atomic force microscope to make the closed-loop system with respect to the lateral position NI.

The control of a DC machine with parametric uncertainty was addressed in [27]. Robust stability conditions for SISO NI systems with parametric uncertainty was first developed. Robust stability conditions via structured singular value were also established. Finally, a static proportional controller was designed for the DC machine with zero order parametric uncertainty that ensured the robust stability conditions developed were satisfied.

As stated already, the synthesis technique developed in Chapter 6 was with a view to ease application on practical systems, in addition to achieving robust stability and improved performance. In terms of vibration attenuation problem using NI theory, most of the work designed an IRC to achieve damping of the resonant modes [36,38,55]. However, in cases like [36,38], there was no explanation on how to design the parameters of the IRC controller. Also, in [55], the parameters of the IRC controller were obtained using a nonlinear optimisation technique and the controller performance was dependent on the initial guess of the parameters. But it is common knowledge that nonlinear optimisation is difficult to solve and does not have a closed-form solution. Thus, the controller synthesis technique introduced in Chapter 6, which is based on the solutions of LMIs [that can easily be solved by SDP solvers], is used to design an NI controller for a cantilever beam hardware to attenuate the vibration of the flexible structure in Chapter 7.

Chapter 3

Preliminaries

This section gives a primer on all the technical tools needed to understand the subsequent chapters in this thesis. This is essential as it provides the reader with the background knowledge needed to have a clear understanding of the technical contributions of the thesis.

This chapter starts by introducing basic linear algebra information used in such as different properties types and characteristics of matrices. It also provides some matrix manipulation tools such as Schur complement. The knowledge of linear algebra is extensively used in the thesis for both analysis of stability and synthesis of NI systems.

The chapter also provides information on linear dynamical systems. This include information such as the various representation of state-space LTI NI systems, the transpose and inverse of a dynamic system, internal stability of a positive feedback interconnection of linear LTI systems and some tools used for the analysis of LTV systems such as Barbalat's lemma. The knowledge of linear dynamical systems and that of linear algebra is used extensively in proving the main results of this thesis.

Finally, the chapter provides some of the major results in the field of NI systems theory. This include the definition of NI systems and it's subsets, the NI lemmas and their different flavours, together with the NI stability theory. This information provides the cornerstone on which the thesis is built upon on. As such a clear understanding of it is imperative to have a clear picture of the thesis.

3.1 Linear Algebra

3.1.1 Eigenvalue and Eigenvector of a Matrix

Eigenvalues and eigenvectors are very important in linear algebra as they give a lot of information of a particular matrix. They are used in a number of application such as linear transformations, stability analysis, matrix diagonalization, vibration analysis to mention but a few.

Definition 1. *[89] A nonzero vector $x \in \mathbb{C}^n$ is referred to the right eigenvector of $M \in \mathbb{C}^{n\times n}$ if there exist a scalar $\lambda \in \mathbb{C}$, called an eigenvalue, such that $Mx = \lambda x$. The pair λ and x are called the eigenpair of M.*

Similarly, a nonzero vector $y \in \mathbb{C}^n$ is a left eigenvector corresponding to an eigenvalue β if $y^*M = \beta y^*$.

3.1.2 Positive Definite and Semidefinite Matrix

The concept of positive definite and semidefinite matrix is widely used in control theory most especially in stability analysis. It also plays an important role in NI system theory for state-space characterization and stability analysis.

Definition 2. *[85] A matrix $A \in \mathbb{C}^{n\times n}$ is Hermitian if it is equal to its complex conjugate transpose, that is $A = A^*$; it is skew Hermitian if $A = -A^*$. If A is a real matrix satisfying the Hermitian property, it is called a symmetric matrix ($A = A^T$).*

Definition 3. *[88] A square Hermitian matrix $X = X^*$ is said to be positive (semi)definite, denoted by $X(\geq 0) > 0$, if $x^*Xx(\geq 0) > 0$ $\forall x \neq 0$.*

3.1.3 Singular Value and Singular Value Decomposition of a Matrix

The singular value of any matrix always exist as oppose to the eigenvalues which only exist for square matrices. The singular value of a matrix A can simply be defined as the squre root of A^*A or AA^*.

The singular value decomposition is an important tool in matrix analysis. This helps to give an intuitive insight into the size of a matrix via the singular values and

the strength of the input or ouput direction via the singular vectors [88].

Theorem 1. *[88] Let $X \in \mathbb{F}^{m\times n}$. There exist unitary matrices*

$$U = [u_1, u_2, ..., u_m] \in \mathbb{F}^{m\times m}$$
$$V = [v_1, v_2, ...v_n] \in \mathbb{F}^{n\times n}$$

such that

$$X = U\Sigma V^*,\ \Sigma = \begin{pmatrix} \Sigma_1 & 0 \\ 0 & 0 \end{pmatrix}$$

where

$$\Sigma_1 = \begin{bmatrix} \sigma_1 & 0 & \cdots & 0 \\ 0 & \sigma_2 & \cdots & 0 \\ \vdots & \vdots & \ddots & \vdots \\ 0 & 0 & \cdots & \sigma_i \end{bmatrix}$$

and

$\sigma_1 \geq \sigma_2 \geq \cdots \geq \sigma_i, i = \min\{m, n\}$.

3.1.4 Absolute Continuity

Absolute continuity (AC) helps in establishing the relationship between differentiation and integration. It is a more stringent condition than continuity and ensures that the derivative of a function is defined almost everywhere and the derivative is Lebesgue integrable.

Definition 4. *[4] Let f be a real-valued function defined on $[\alpha, \beta]$. Then f is absolutely continuous on $[\alpha, \beta]$ if for a given $\epsilon > 0$, $\exists\ \delta > 0$ such that*

$$\sum_{i=1}^{n} |f(x_i') - f(x_i)| < \epsilon$$

for every finite collection $\{(x_i, x_i')\}$ of non-overlapping intervals with

$$\sum_{i=1}^{n} |x_i' - x_i| < \delta.$$

3.1.5 Schur Complement

The Schur complement provides an important tool for matrix inversion as well as for the determining the positive definiteness of a symmetric matrix. These important features of the Schur complement are highlighted by the following lemma

Lemma 1. *[91] For any symmetric matrix X of the form*

$$X = \begin{pmatrix} A & B \\ B^T & C \end{pmatrix},$$

if A is invertible then the following properties hold:

1. *$X > 0$ if and only if $A > 0$ and $C - B^T A^{-1} B > 0$*
2. *If $A > 0$, then $X \geq 0$ if and only if $C - B^T A^{-1} B \geq 0$*

3.1.6 Kernel, Image and Rank of a Matrix

Definition 5. *[88] Let $M \in \mathbb{F}^{n \times n}$ be a linear transformation from $\mathbb{F}^n$ to $\mathbb{F}^m$, i.e.,*

$$M\colon \mathbb{F}^n \longrightarrow \mathbb{F}^m.$$

Then

- *The kernel or null space of M is defined by*

$$\mathrm{Ker}\,(M) = \mathcal{N}(M) := \{x \in \mathbb{F}^n : Mx = 0\}$$

- *The image or range of M is given by*

$$\mathrm{Im}\,(M) = \mathrm{R}\,(M) := \{y \in \mathbb{F}^m : y = Mx, x \in \mathbb{F}^n\}$$

- *The rank of the matrix is the defined as the maximum number of the independent row or columns of the matrix. The rank is given by*

$$\mathrm{rank}\,(M) = \dim(\mathrm{Im}(M))$$

3.1.7 Class $\mathcal{K}$ Function

We introduce the class $\mathcal{K}$ comparison function which helps in the stability analysis of nonautonomous systems.

Definition 6. *[45] Let $\sigma : [\,0, r\,) \to [\,0, \infty\,)$ be a continuous function with $r > 0$. Then σ is of class $\mathcal{K}$ if it is strictly increasing and $\sigma(0) = 0$. If $r = \infty$, then the function belongs to class $\mathcal{K}_\infty$.*

3.2 Linear Dynamical Systems

This section will give a brief overview of some basic but important theory of Linear Time-Invariant (LTI) systems. This theoretical background will be paramount in having a clear and good understanding of NI systems theory and analysis presented in subsequent chapters.

3.2.1 Linear Dynamical Systems Representation

Consider the LTI system given by the equations:

$$\dot{x}(t) = Ax(t) + Bu(t)$$
$$y(t) = Cx(t) + Du(t)$$

where $x(t) \in \mathbb{R}^n$ is called the state of the system, $u(t) \in \mathbb{R}^m$ is referred to as the system input and $y(t) \in \mathbb{R}^p$ is called the system output. The matrix $A \in \mathbb{R}^{n\times n}$ is called the state matrix. Its eigenvalues represent the poles of the system. $B \in \mathbb{R}^{n\times m}$ is referred to as input to state matrix, $C \in \mathbb{R}^{m\times n}$ is the state to output matrix while $D \in \mathbb{R}^{m\times m}$ represent the feedthrough matrix. The matrices A,B,C,D are real constant matrices.

A system is referred to as a SISO system if $m = 1$ and $p = 1$. On the other hand, a system which has multiple input ($m > 1$) and multiple output ($p > 1$) is called MIMO system.

The state-space representation of the LTI system can also be expressed as:

$$\left[\begin{array}{c|c} A & B \\ \hline C & D \end{array}\right] = C(sI - A)^{-1}B + D = G(s)$$

Some important operations on the transfer matrix $G(s)$ are given by the following definitions

Definition 7. *[88] The transpose of a transfer function matrix $G(s)$ is given by*

$$G^T(s) = B^*(sI - A)^{-*}C^* + D^* = \left[\begin{array}{c|c} A^* & C^* \\ \hline B^* & D^* \end{array}\right]$$

Definition 8. *[88] The inverse of a transfer function matrix $G(s)$ is defined by*

$$G^{-1}(s) = \left[\begin{array}{c|c} A - BD^{-1}C & -BD^{-1} \\ \hline D^{-1}C & D^{-1} \end{array}\right]$$

Definition 9. *[97]*

A state-space realization $\left[\begin{array}{c|c} A & B \\ \hline C & D \end{array}\right]$ is said to be minimal if and only if it is controllable and observable.

3.2.2 Internal Stability

Consider the positive feedback interconnection shown in Fig. 3.1 below. The system is said to be internally stable if for any energy bounded input signals (w_1, w_2), the output signals (e_1, e_2) are also energy bounded.

Lemma 2. *[88] The system in Fig.3.1 is internally stable if and only if the transfer function matrix*

$$\begin{bmatrix} I & -M(s) \\ -\Delta(s) & I \end{bmatrix}^{-1} = \begin{bmatrix} M(s)(I - \Delta(s)M(s))^{-1}\Delta(s) & M(s)(I - \Delta(s)M(s))^{-1} \\ (I - \Delta(s)M(s))^{-1}\Delta(s) & (I - \Delta(s)M(s))^{-1} \end{bmatrix}$$

from (w_1, w_2) to (e_1, e_2) belongs to $\mathcal{RH}_\infty$.

It should be noted that this internal stability result is a necessary and sufficient stability result i.e. it is an "if and only if" condition.

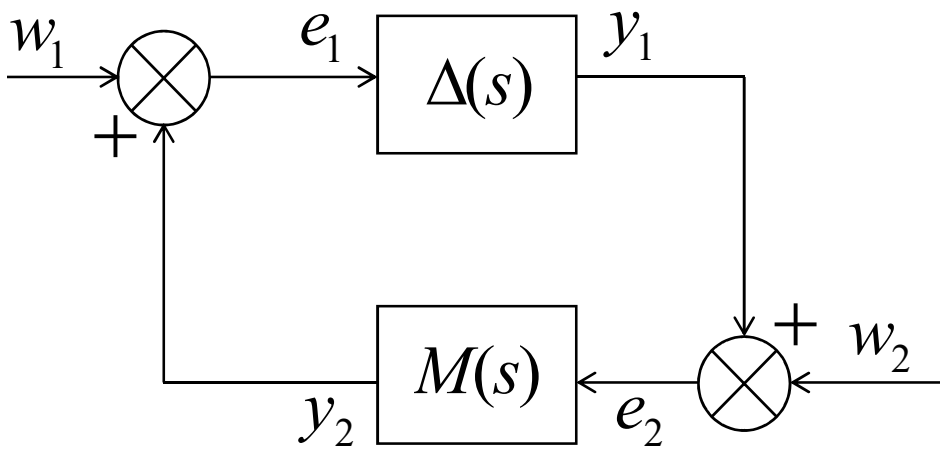

Figure 3.1: Positive Feedback Interconnection

3.2.3 Linear Fractional Transformation

Linear Fractional Transformation (LFT) play an important role in control theory by providing a unifying framework for many concepts and also helps in generalizing transfer functions and their corresponding state-space formulation to include uncertainty [84].

Definition 10. *[84, 88] Given a complex matrix M partitioned as $M = \left(\begin{smallmatrix} M_{11} & M_{12} \\ M_{21} & M_{22} \end{smallmatrix}\right) \in \mathbb{C}^{(p_1+p_2)+(q_1+q_2)}$, and let $\Delta_l \in \mathbb{C}^{q_2 \times p_2}$ and $\Delta_u \in \mathbb{C}^{q_1 \times p_1}$ be two other complex matrices. Then we can formally define a lower LFT with respect to Δ_l as the map*

$$\mathcal{F}_l(M, \bullet) : \mathbb{C}^{q_2 \times p_2} \mapsto \mathbb{C}^{p_1 \times q_1}$$

with

$$\mathcal{F}_l(M, \bullet) = M_{11} + M_{12}\Delta_l(I - M_{22}\Delta_l)^{-1}M_{21}$$

provided that the inverse $(I - M_{22}\Delta_l)^{-1}$ exists.

In a similar way, the upper LFT with respect to Δ_u is defined as

$$\mathcal{F}_u(M, \bullet) : \mathbb{C}^{q_1 \times p_1} \mapsto \mathbb{C}^{p_2 \times q_2}$$

with

$$\mathcal{F}_u(M, \Delta_u) = M_{22} + M_{21}\Delta_u(I - M_{11}\Delta_u)^{-1}M_{12}$$

provided that the inverse of $(I - M_{11}\Delta_u)^{-1}$ exists.

3.2.4 Nonlinear Systems Analysis

An important lemma in the analysis of the stability of nonlinear and time-varying systems is the Barbalat's lemma. The lemma helps in proving the smoothness of the derivative of a function when the function is bounded.

Lemma 3. *[86] Let $f(t)$ be a differentiable function with a finite limit as $t \to \infty$. Then $\dot{f}(t) \to 0$ as $t \to \infty$ if $\dot{f}$ is uniformly continuous.*

Barbalat's lemma provides a Lyapunov-like tool that can be used in the analysis of nonautonomous dynamic systems. This is shown in the following lemma

Lemma 4. *[86] If a scalar function $V(x,t)$ satisfies the following conditions*

- *$V(x,t)$ is lower bounded*
- *$\dot{V}(x,t)$ is negative semi-definite*
- *$\dot{V}(x,t)$ is uniformly continuous in time*

then $\dot{V}(x,t) \to 0$ as $t \to \infty$.

The next theorem is used to establish the boundedness of the trajectories of a nonautonomous systems.

Theorem 2. *[45] Let $\dot{x} = f(t,x)$ with $f : [0,\infty) \times \mathbb{D} \to \mathbb{R}^n$, where $\mathbb{D} \subset \mathbb{R}^n$ is a domain containing $x = 0$. Suppose*

- *$f(x,t)$ is piecewise continuous in t and locally Lipschitz x on $[0,\infty) \times \mathbb{D}$.*
- *$f(t,0)$ is uniformly bounded for all $t \geq 0$*

Let $V : [0,\infty) \times \mathbb{D} \to \mathbb{R}$ be a continuously differentiable function such that

$$\Gamma_1(x) \leq V(t,x) \leq \Gamma_2(x)$$
$$\dot{V}(t,x) = \frac{\partial V}{\partial t} + \frac{\partial V}{\partial x} \leq -\Gamma(x)$$

$\forall\, t \geq 0$, $\forall\, x \in \mathbb{D}$, where $\Gamma_1(x)$ and $\Gamma_2(x)$ are continuous positive definite functions and $\Gamma(x)$ is a continuous positive semidefinite function on $\mathbb{D}$. Let $r > 0$ be such

that $B_r \subset \mathbb{D}$ *and let* $\rho < \min_{\|x\|=r} \Gamma_1(x)$. *Then, all solutions of* $\dot{x} = f(t,x)$ *with* $x(t_0) \in \{x \in B_r \,|\, \Gamma_2(x) \leq \rho\}$ *are bounded and satisfy*

$$\Gamma(x(t)) \to 0 \quad as\, t \to \infty.$$

Furthermore, if all the assumptions hold globally and $\Gamma_1(x)$ *is radially unbounded, the statement is true for all* $x(t_0) \in \mathbb{R}^n$.

The definition of Zero State Detectability (ZSD) is used in establishing the asymptotic stability of nonlinear systems

Definition 11. *[10] Consider a nonlinear system given by*

$$\Sigma : \begin{cases} \dot{x}(t) = f(x) + G(x)u, & x(0) = x_0; \\ y(t) = h(x) + J(x)u, \end{cases} \tag{3.1}$$

with $x \in \mathbb{R}^n$, $y \in \mathbb{R}^m$ *and* $u \in \mathbb{R}^m$, *where the input is assumed to be locally square integrable. Let* $f : \mathbb{R}^n \to \mathbb{R}^n$, $G : \mathbb{R}^n \to \mathbb{R}^{n\times m}$, $h : \mathbb{R}^n \to \mathbb{R}^m$ *and* $J : \mathbb{R}^n \to \mathbb{R}^{m\times m}$ *be smooth functions with* $f(0) = 0$ *and* $h(0) = 0$.

The nonlinear system (3.1) *is said to be locally ZSD if for any trajectory* $x(t) \in \mathcal{D}$ *such that* $u(t) = 0$, $h(x(t)) = 0$ *implies* $\lim_{t\to+\infty} x(t) \to 0$, *where* $\mathcal{D}$ *is the neighbourhood of* 0. *If* $\mathcal{D} = \mathbb{R}^n$, *then the system is ZSD.*

3.2.5 Minimality of Linear Time-Varying Systems

Here, we define the controllability and observability of a LTV systems.

Definition 12. *[87] Let* $(A(t), B(t), C(t))$ *be the state-space realization of a time-varying system with* $\dim(A) = n \times n$. *The realization is said to be uniformly controllable if the controllability matrix*

$$C = [p_0, p_1, \cdots, p_{n-1}];$$
$$p_{k+1} = -A(t)p_k + \dot{p}_k; \quad p_0 = B(t),$$

is non-singular $\forall\, t$.

Similarly, via duality, the state-space realization is said to be uniformly observable if the observability matrix

$$O = [q_0, q_1, \cdots, q_{n-1}];$$
$$q_{k+1} = -A^T(t)q_k + \dot{q}_k; \quad q_0 = C^T(t),$$

is non-singular $\forall\, t$.

3.2.6 Affine Quadratic Stability

We first present the condition of a multiconvex function to be negative in a hyper-rectangular box and then use that result to provide conditions for Affine Quadratic Stability (AQS) of a linear parameter dependent system.

Consider a class of finite-dimensional, square, LPV dynamical systems described by

$$\Sigma_{LPV} : \begin{cases} \dot{x}(t) = A(\rho)x(t) + B(\rho)u(t) & x(0) = x_0, \\ y(t) = Cx(t) \end{cases} \tag{3.2}$$

where $A(\rho)$, $B(\rho)$ depend affinely on the uncertain (possibly time-varying) parameter vector $\rho = [\rho_1, \rho_2, \cdots, \rho_K] \in \mathbb{R}^K$, that is, $A(\rho) = A_0 + \rho_1 A_1 + \cdots + \rho_K A_K$ and $B(\rho) = B_0 + \rho_1 B_1 + \cdots + \rho_K B_K$. Below, we mention two technical assumptions that must be satisfied by the LPV NI systems studied here:

A1. Each parameter ρ_i varies in the known interval $[\rho_{i,\min}, \rho_{i,\max}]$ for all $i \in \{1, 2, \cdots, K\}$. This implies that the parameter vector $\rho \in \mathbb{R}^K$ is valued in a hyper-rectangle with the set of vertices $\mathcal{V} = \{(v_1, \cdots, v_K) : v_i \in \{\rho_{i,\min}, \rho_{i,\max}\}\ \forall i\}$.

A2. The rate of variation $\dot{\rho}_i$ is well defined for all $t \in \mathbb{R}_{\geq 0}$ and $\dot{\rho}_i \in [\gamma_{i,\min}, \gamma_{i,\max}]$ where the range $\gamma_{i,\min} \leq 0 \leq \gamma_{i,\max}$ is known for all $i \in \{1, \cdots, K\}$. This implies that the vector $\dot{\rho} \in \mathbb{R}^K$ varies within a hyper-rectangle having the set of vertices $\mathcal{C} = \{(e_1, \cdots, e_k) : e_i \in \{\gamma_{i,\min}, \gamma_{i,\max}\}\ \forall i\}$.

Lemma 5. *[11] Let* $f(\rho_1, \cdots, \rho_K) = \sigma_0 + \sum_i \sigma_i \rho_i + \sum_{i<j} \theta_{ij}\rho_i\rho_j + \sum_i \alpha_i \rho_i^2$ *be a scalar quadratic, multiconvex function of* $\rho \in \mathbb{R}^K$ *such that*

$$2\alpha_i = \frac{\partial^2 f}{\partial \rho_i^2}(\rho) \geq 0 \quad \forall i = 1, \cdots, K.$$

Then $f(\cdot)$ *will be negative in the parameter box of Assumption A1 if and only if it has negative values at the vertices of the parameter box.*

Next, we use Lemma 5 to provide a definition of AQS. AQS is a less conservative result than the quadratic stability because AQS uses the variation in the rate of change of the parameter to reduce conservatism [11].

Theorem 3. *[11] Consider the LPV dynamical system given by 3.2 and satisfying assumptions A1 and A2. Also, let* $\rho_{mean} = \left(\frac{\underline{\rho}_1+\overline{\rho}_1}{2}, \cdots, \frac{\underline{\rho}_K+\overline{\rho}_K}{2}\right)$ *be the average value of the parameter vector. Then the system is said to be AQS if* $A(\rho_{mean})$ *is stable and there exist* $K+1$ *symmetric matrices* $P_0, \cdots, P_K$ *with* $P(\rho) = P_0 + \rho_1 P_1 + \cdots + \rho_K P_K$ *satisfying*

$$\Gamma(v,e) = P(v)A(v) + A(v)^T P(v) + P(e) - P_0 < 0 \quad \forall (v,e) \in \mathcal{V} \times \mathcal{C} \tag{3.3a}$$

$$P_i A_i + A_i^T P_i \geq 0 \quad for i = 1, \cdots, K. \tag{3.3b}$$

If 3.3a-3.3b are satisfied, then a Lyapunov function for the system given in 3.2 with trajectories $\rho(t)$*satisfying Assumptions A1 and A2 is given by* $V(x,\rho) = x^T P(\rho) x$.

3.3 Negative Imaginary Systems

Here, we provide a background knowledge of NI and SNI systems and the internal stability results that exist in the literature. The background knowledge is imperative in understanding the theoretical developments reported in this thesis. Moreover, these technical results will be extensively used in proving the main results presented in this thesis.

Definition 13. *[76] A square real rational transfer function matrix* $G(s)$ *is NI if*

1. $G(s)$ *has no poles in* $\Re[s] > 0$
2. $j[G(j\omega) - G(j\omega)^*] \geq 0$ *for all* $\omega \in (0, \infty)$ *such that* $j\omega$ *is not a pole of* $G(s)$
3. *If* $j\omega_0$, $\omega_0 \in (0, \infty)$, *is a pole of* $G(s)$, *it is at most a simple pole, and the residue matrix* $K_0 = \lim_{s \to j\omega_0} jG(s)$ *is positive semidefinite and Hermitian*
4. *If* $s = 0$ *is a pole of* $G(s)$, *then* $\lim_{s\to 0} s^k G(s) = 0$ *for all* $k \geq 3$ *and* $\lim_{s\to 0} s^k G(s)$ *is positive semidefinite and Hermitian*
5. *If* $s = j\infty$ *is a pole of* $G(s)$, *then* $\lim_{\omega\to\infty} \frac{G(j\omega)}{(j\omega)^2}$ *is negative semidefinite Hermitian, and* $\lim_{\omega\to\infty} \frac{G(j\omega)}{(j\omega)^k} = 0$ *for all* $k \geq 3$

Condition 1 of Definition 13 means that NI systems cannot be unstable systems as they do not have poles on the open right half of the complex plane. Hence, NI systems

are at least Lyapunov stable. The restriction of the Nyquist plot of NI systems to lie on or below the real axis of the complex plane is imposed by the second condition of Definition 13.

The following lemma, referred to as the NI lemma, provides a state-space characterisation for NI systems without poles at the origin.

Lemma 6. *(**NI Lemma**) [25] Let $G(s)$ be the real, rational and proper transfer function matrix of a finite-dimensional, square and causal system G having a minimal state-space realization* $\left[\begin{array}{c|c} A & B \\ \hline C & D \end{array}\right]$. *Then, $G(s)$ is NI without poles at the origin if and only if* $\det(A) \neq 0$, $D = D^\top$ *and there exists a real matrix $Y = Y^\top > 0$ such that*

$$AY + YA^\top \leq 0 \qquad \text{and} \qquad B + AYC^\top = 0. \tag{3.4}$$

From Lemma 6, it is clear that the NI systems we consider in this thesis are allowed to have poles on the imaginary axis, but not at the origin. Hence, that is why $AY + YA^\top \leq 0$ has a non-strict inequality condition. In general, there are systems with poles on the origin that do satisfy the NI property. For example, both a single and double integrator are NI systems. The next lemma is also an NI lemma but allows for NI systems to have poles on origin whilst imposing minimality assumption.

Lemma 7. *[41, 75] Let* $\left[\begin{array}{c|c} A & B \\ \hline C & D \end{array}\right]$ *be the minimal state-space realization of the transfer funtion matrix $G(s)$ with $A \in \mathbb{R}^{n\times n}$, $B \in \mathbb{R}^{n\times m}$, $C \in \mathbb{R}^{m\times n}$ and $D \in \mathbb{R}^{m\times m}$. Then $G(s)$ is NI if and only if $D = D^T$ and there exist matrices $P = P^T \geq 0$, $W \in \mathbb{R}^{m\times m}$, and $L \in \mathbb{R}^{m\times n}$ such that the following LMI is satisfied:*

$$\begin{bmatrix} PA + A^TP & PB - A^TC^T \\ B^TP - CA & -(CB + B^TC^T) \end{bmatrix} = \begin{bmatrix} -L^TL & -L^TW \\ -W^TL & -W^TW \end{bmatrix} \leq 0.$$

We also define a subset of the NI systems, called the SNI systems as follows.

Definition 14. *(**SNI system**) [15] A square, real, rational, proper transfer function matrix $N(s)$ is said to be SNI if*

1. *$N(s)$ has no poles in $\Re\{s\} \geq 0$;*

2. $j[N(j\omega) - N(j\omega)^*] > 0$ *for all* $\omega \in (0, \infty)$.

SSNI systems form a strict subset within the SNI class that satisfy two additional frequency-domain criteria in the neighbourhood of $\omega = 0$ and $\omega = \infty$.

Definition 15. *(**SSNI System**) [21] Let* $G(s)$ *be the real, rational and proper transfer function matrix of a finite-dimensional, square, causal system* G*. Then,* $G(s)$ *is said to be SSNI if*

- $G(s)$ *is SNI;*
- $\lim\limits_{\omega\to\infty} j\omega\,[G(j\omega) - G(j\omega)^*] > 0$*;*
- $\lim\limits_{\omega\to 0} j\dfrac{1}{\omega}\,[G(j\omega) - G(j\omega)^*] > 0$.

Below, we present a slightly modified version of the SSNI lemma [21] by exploiting [59, Lemma 2].

Lemma 8. *(**SSNI Lemma**) [21, 59] Let* $G(s) \in \mathcal{RH}_\infty^{m\times m}$ *be the real, rational and proper transfer function matrix of a finite-dimensional, square and causal system* G*, having a state-space realization* $\left[\begin{array}{c|c} A & B \\ \hline C & D \end{array}\right]$*. Suppose* $\text{rank}[B] = \text{rank}[C] = m$ *and the pair* (A, C) *is observable. Then,* $G(s)$ *is SSNI if and only if* $D = D^\top$ *and there exists a real matrix* $Y = Y^\top > 0$ *such that* $AY + YA^\top < 0$ *and* $B + AYC^\top = 0$.

It is also worth pointing out here that since $AY + YA^\top < 0$, with $Y > 0$, SSNI systems are asymptotically stable systems without any poles on the imaginary axis.

We now recall the internal stability condition for a stable NI system interconnected with an SNI system via positive feedback.

Theorem 4. *[15, 57] Let* $G(s)$ *be a stable NI system and* $H(s)$ *be an SNI system. Let either* $G(\infty) = 0$*, or else* $G(\infty)H(\infty) = 0$ *and* $H(\infty) \geq 0$*. Then, the positive feedback interconnection of* $G(s)$ *and* $H(s)$*, shown in Fig. 3.2, is internally stable if and only if* $\lambda_{\max}[H(0)G(0)] < 1$.

Thus, the stability result is a necessary and sufficient type of result. Theorem 4 forms the cornerstone of the whole NI theory. Therefore, it is the theorem upon which most of the work in this thesis is centred around. The robust stability achieved by the

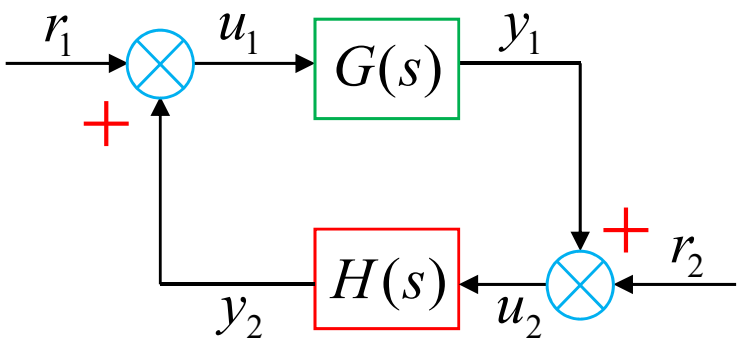

Figure 3.2: A positive feedback interconnection of NI systems.

different synthesis methods presented in this thesis is achieved by satisfying the DC gain condition of the NI stability result.

As discussed already in Section 1.1, the NI stability theory is conditional stability result, unlike the passivity theorem. However, it does include some important systems which are not covered by passivity theorem. For example, nonlinear systems can be feedback linearized to double integrator, which is NI but not passive.

Also, the NI stability result is not an absolute value type of result and impose restriction on only one frequency unlike the small-gain theorem.

The NI stability result was extended in [57, Theorem 9] to remove the restrictions on the gain at infinity.

3.4 Summary

The chapter started by introducing some matrix properties such as eigenvalues and eigenvector, (semi)positive and (semi)negative definiteness, together with some matrix manipulation tools such as Schur's complement. These will enable the reader to have a good grasp of the technical chapters in this thesis as they are used in both analysis and synthesis of NI systems.

The chapter also presented some key information on LTI systems. We introduced state-space representation of LTI systems, together with some of its common operations such as the transpose, inverse and conjugate of a state-space representation. Also, we presented the necessary and sufficient condition required for the internal stability of an LTI system.

Furthermore, we introduced some nonlinear system analysis tools such as Barbalat's

lemma, ZSD and the result required for the asymptotic stability non-autonomous nonlinear systems. The chapter also presented the minimality conditions for LTV systems, results that ensure the negativeness of a multiconvex function and AQS conditions. All these play an important role in our analysis of LTV and LPV NI systems reported in this thesis.

Finally, we highlighted some of the main results in the NI system theory. First, we provided a definition for NI, SNI and SSNI systems. We also provided the state-space characterization of NI and SSNI systems which are termed as the NI and SSNI Lemma respectively. In the final part of the chapter, we introduced the internal stability result for the positive feedback interconnection of two NI systems. This stability result is the cornerstone of the whole NI systems theory and hence, forms an essential part of the results presented in this thesis.

Chapter 4

$\alpha-$ SNI and Output Feedback Controller Synthesis

All the materials presented in this chapter were published in [59].

4.1 Introduction

In this chapter, we address the NI synthesis problem in which the aim is to synthesis a dynamic output feedback controller that renders the closed-loop system NI. In this case, the plant or the controller itself need not be NI, but the closed-loop system and the uncertainty should both possess the NI property.

Therefore, the problem we address in this chapter is: how do we synthesize a dynamic output feedback controller which renders the closed-loop system $\alpha-$ SNI and at the same time is robustly stable to all class of NI uncertainties satisfying a particular DC gain condition. The variable α dictates the decay rate of the closed-loop NI system and is used as a measure of the performance of the closed-loop system.

Hence, unless otherwise stated, NI synthesis in this chapter refers to the problem of synthesizing a controller which renders the closed-loop system NI.

There are a number of research work dedicated towards the problem of NI controller synthesis which renders the closed-loop system to be NI. For example, an LMI-based state feedback synthesis imposing closed-loop NI property is explored in [20,32]. While in [41], the state feedback synthesis has been done to enforce closed-loop NI/SNI property using an ARE-based approach. In [66], the authors introduce a static state

feedback and a dynamic output feedback controller synthesis schemes imposing closed-loop NI property. In [64], a dynamic output feedback control framework which renders the closed-loop system NI is proposed for systems with stable NI uncertainty by transforming the NI uncertainty into PR framework. Of recent, in [79] and [81], the problem of synthesizing both a state and dynamic output feedback controller that renders the closed-loop system SNI was addressed via an ARE-based approach.

However, in terms of NI synthesis that improves the time domain transient performance, [65] synthesized a state feedback NI controller by using the notion of $\alpha-$ and $\mathcal{D}-$ pole placement introduced in [96] which enforces the NI property of the closed-loop system.

For state feedback synthesis technique rendering the closed-loop NI, such as that employed in [20,32,65,66], not all the states are available for measurement to implement a full state feedback controller. And in cases where all the states are available for measurement, it might not be cost-effective to implement such a controller. For example, a simple 6 degree of freedom rigid body translating in space may have up to twelve different states which include linear position and velocity and angular position and velocity. Hence, measuring all these states may demand buying very expensive sensors.

On the other hand, synthesis techniques that use an ARE-based approach such as [41, 79, 80] may not be desirable as AREs are numerically challenging to solve. Furthermore, the output feedback synthesis techniques introduced in [66, 81] are complex and did not address the issue of output performance.

Motivated by the aforementioned shortcomings, the work in this chapter proposes an LMI-based procedure to design a dynamic output feedback controller applying the $\alpha-$ SNI framework that ensures robust stability against all stable, strictly proper, NI uncertainties. Regional pole placement, or pole placement in general, provides a way of achieving time domain performance such as reducing peak overshoot and settling time, increasing decay rate, etc. [73]. Furthermore, it is shown via examples that the designed controller can also satisfy a certain level of robust performance.

The main contributions of this chapter are

- Provide a definition of $\alpha-$ SNI systems and show that this class of systems are asymptotically stable system.

- Provide a dynamic output feedback synthesis technique using the $\alpha-$ SNI framework which renders the closed-loop system $\alpha-$ SNI, with a minimum decay rate for the closed-loop system dictated by the variable α. We also show that the synthesized closed-loop system will be robust to all class of NI uncertainties satisfying the DC gain condition.

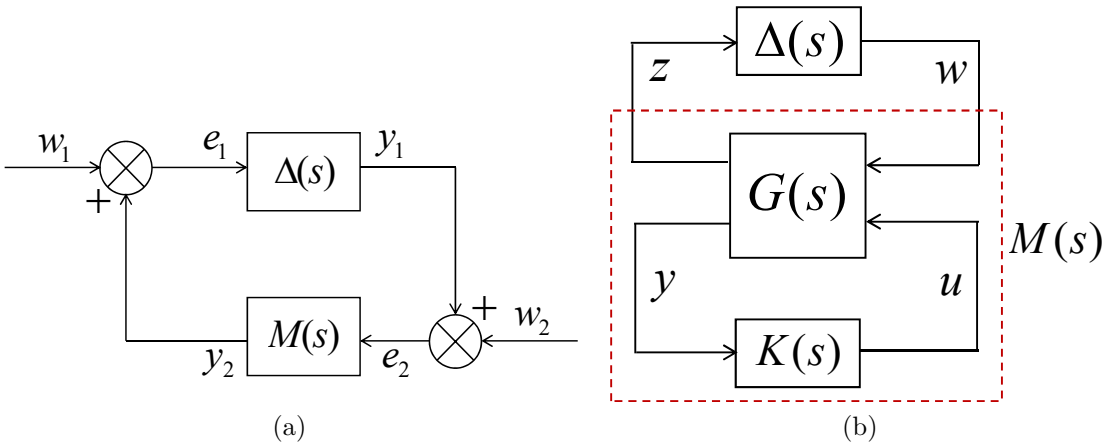

Figure 4.1: (a) Positive feedback interconnection of two NI systems; (b) $M-\Delta$ configuration for robust stability analysis.

4.2 $\alpha-$ Strictly Negative Imaginary Systems

Definition 16. *[59] Let $D = D^T$ and $\alpha > 0$. Then, $R(s) = \left[\begin{array}{c|c} A & B \\ \hline C & D \end{array}\right]$ is said to be $\alpha-$ SNI if there exists a real matrix $Y = Y^T > 0$ such that*

$$AY + YA^T + 2\alpha Y \leq 0 \quad \text{and} \quad B + AYC^T = 0. \tag{4.1}$$

We now provide some remarks which explore the properties of $\alpha-$ SNI systems and find the connections between $\alpha-$ SNI and SSNI systems properties.

Remark 1. *The $\alpha-$ SNI systems are inherently stable. This can be readily established from (4.1), which implies $AY + YA^T < 0$ for $\alpha > 0$ and $Y > 0$, which in turn ensures Hurwitzness of A applying [88, Lemma 3.19].* ■

Note that the definition of $\alpha-$ SNI systems does not require a minimal state-space realization of the underlying system. In this context, the literature [32, 79] may be

referred where it is shown that most of the analysis and synthesis results associated with NI, SNI and SSNI systems theory remain applicable in case of non-minimal system realization.

Remark 2. *From Definition 16, one may think that the set of the $\alpha-$ SNI systems is a subset of the SSNI class having poles in $\Re[s] \leq -\alpha$. But, unlike SSNI systems [21], $\alpha-$ SNI system property does not impose any restrictions on the state-space realization. It can be concluded that the set of $\alpha-$ SNI systems, say $R(s)$, with a completely observable state-space realization and $R(s) - R(-s)^T$ having full normal rank belongs to the SSNI class.* ■

Note that in case of $\alpha-$ SNI systems the full normal rank constraint on $R(s) - R(-s)^T$ is implied by (4.1) when the B matrix has full column rank. It is proved in the following lemma. The same conclusion applies to Lemma 8 as well.

Lemma 9. *[59] Let $R(s) = \left[\begin{array}{c|c} A & B \\ \hline C & D \end{array}\right]$ be an $(m \times m)$ $\alpha-$ SNI system with* rank$[B] = m$. *Then, $R(s) - R(-s)^T$ has full normal rank.*

Proof. [59] For a given $\alpha > 0$ and $Y > 0$, (4.1) implies $AY + YA^T < 0$. Then there exists a square and non-singular matrix L such that $AY + YA^T = -L^TL$. For these L and Y, the transfer function matrix $N(s) = \left[\begin{array}{c|c} A & B \\ \hline LY^{-1}A^{-1} & 0 \end{array}\right]$ acquires full column rank at $s = j\omega$ for all $\omega \in \mathbb{R}$ since A is Hurwitz and rank$[B] = m$ via assumption and rank$[LY^{-1}A^{-1}] = n$. It implies from [25, Corollary 1]

$$j\omega[R(j\omega) - R(j\omega)^*] = \omega^2 N(j\omega)^* N(j\omega) > 0 \tag{4.2}$$

for all $\omega \in \mathbb{R}\backslash\{0\}$ and $R(0) - R(0)^T = 0$ since $R(0) = CYC^T + D = R(0)^T$. This implies that there does not exist any continuum interval of $\omega \in \mathbb{R}$ for which $\det[R(j\omega) - R(j\omega)^*]$ remains zero. This in turn ensures that $R(s) - R(-s)^T$ must have full normal rank. Note minimality is not required.

4.3 Output Feedback Controller Synthesis using $\alpha-$ SNI Framework

4.3.1 Problem Formulation

Consider an LTI generalized plant $G(s)$ described by the following state-space equations

$$G(s): \begin{cases} \dot{x} = Ax + B_1 w + B_2 u, \\ z = C_1 x + D_{11} w + D_{12} u, \\ y = C_2 x + D_{21} w, \end{cases} \tag{4.3}$$

where $x(t) \in \mathbb{R}^n$ is the state vector of the generalized plant, $u(t) \in \mathbb{R}^{n_u}$ represents the control input , $y(t) \in \mathbb{R}^{n_y}$ is the measured output, $w(t) \in \mathbb{R}^m$ is the exogenous input and $z(t) \in \mathbb{R}^m$ is the objective signal. The matrices $A \in \mathbb{R}^{n\times n}$, $B_1 \in \mathbb{R}^{n\times m}$, $B_2 \in \mathbb{R}^{n\times n_u}$, $C_1 \in \mathbb{R}^{m\times n}$, $C_2 \in \mathbb{R}^{n_y\times n}$, D_{11} and D_{21} are all constant and known. Assume that $D_{12} = 0$, (A, B_2) is stabilizable and (A, C_2) is detectable. The aim is to synthesize a full-order dynamic output feedback controller

$$K(s): \begin{cases} \dot{x}_c = A_c x_c + B_c y, \\ u = C_c x_c + D_c y, \end{cases} \tag{4.4}$$

such that the nominal closed-loop system $M(s)$, which is given by the lower linear fractional transformation between the generalized plant $G(s)$ and the controller $K(s)$, is $\alpha-$ SNI and is robustly stable against all stable, strictly proper, NI uncertainties $\Delta(s)$ with $\Delta(0) \leq \gamma^{-1}$ for a given $\gamma > 0$. The state-space realization of the $M(s)$, as shown in Fig. 4.1b, from w to z is given by

$$M(s) = \left[\begin{array}{c|c} A_{cl} & B_{cl} \\ \hline C_{cl} & D_{cl} \end{array}\right] = \left[\begin{array}{cc|c} A + B_2 D_c C_2 & B_2 C_c & B_1 + B_2 D_c D_{21} \\ B_c C_2 & A_c & B_c D_{21} \\ \hline C_1 & 0 & D_{11} \end{array}\right]. \tag{4.5}$$

4.3.2 Controller Synthesis using $\alpha-$ SNI Framework

This subsection provides the main result of this chapter. Theorem 5 gives a set of sufficient conditions required for the existence of a dynamic output feedback controller $K(s)$ which makes the nominal closed-loop system given in (4.5) $\alpha-$ SNI with a given

$\alpha > 0$ and maintains closed-loop stability in presence of any stable, strictly proper, NI uncertainty satisfying the DC gain condition.

Theorem 5. *[59] Let a generalized plant $G(s)$ be given by (4.3) with $D_{11} = D_{11}^T$, $D_{12} = 0$, (A, B_2) stabilizable and (A, C_2) detectable. Let $\gamma > 0$, $\alpha > 0$ and $m \leq 2n$. Suppose there exist matrices $\hat{A} \in \mathbb{R}^{n\times n}$, $\hat{B} \in \mathbb{R}^{n\times n_y}$, $\hat{C} \in \mathbb{R}^{n_u\times n}$, $\hat{D} \in \mathbb{R}^{n_u\times n_y}$ and symmetric matrices $P \in \mathbb{R}^{n\times n}$ and $X \in \mathbb{R}^{n\times n}$ such that*

$$\left[\begin{array}{cc:c} \Phi_{11}+2\alpha P & \Phi_{12}+2\alpha I & PB_1+\hat{B}D_{21}+\hat{A}C_1^T \\ \star & \Phi_{22}+2\alpha X & \Phi_{23} \\ \hdashline \star & \star & 0 \end{array}\right] \leq 0, \tag{4.6}$$

$$\left[\begin{array}{cc} P & I \\ I & X \end{array}\right] > 0, \tag{4.7}$$

$$\text{and } C_1XC_1^T + D_{11} < \gamma I, \tag{4.8}$$

with the following shorthand

$$\Phi_{11} = PA + PA^T + \hat{B}C_2 + C_2^T\hat{B}^T, \tag{4.9a}$$

$$\Phi_{12} = \hat{A} + (A + B_2\hat{D}C_2)^T, \tag{4.9b}$$

$$\Phi_{22} = XA^T + AX + B_2\hat{C} + \hat{C}^TB_2^T, \tag{4.9c}$$

$$\Phi_{23} = B_1 + B_2\hat{D}D_{21} + AXC_1^T + B_2\hat{C}C_1^T, \tag{4.9d}$$

and the symbol $\star$ denotes the elements due to symmetry. Then, an internally stabilizing controller $K(s)$ is given by (4.4) where

$$D_c = \hat{D}, \tag{4.10a}$$

$$C_c = (\hat{C} - D_cC_2X)M^{-T}, \tag{4.10b}$$

$$B_c = N^{-1}(\hat{B} - PB_2D_c), \tag{4.10c}$$

$$A_c = N^{-1}(\hat{A} - PAX - NB_cC_2X - PB_2C_cM^T - PB_2D_cC_2X)M^{-T}, \tag{4.10d}$$

and M and N are square and non-singular solutions of the algebraic equation $MN^T = I - XP$. This controller $K(s)$ forms a closed-loop system $M(s)$, expressed as in (4.5), which is $\alpha-$ SNI and is robust to all stable, strictly proper, NI uncertainties $\Delta(s)$ satisfying $\lambda_{\max}[\Delta(0)] \leq \gamma^{-1}$.

Proof. [59] First note that $D_{cl} = D_{cl}^T$ in (4.5) and $m \leq 2n$. The proof will proceed via the following steps which establishes that for $M(s) = \left(\begin{array}{c|c} A_{cl} & B_{cl} \\ \hline C_{cl} & D_{cl} \end{array}\right)$ to be $\alpha-$ SNI with a given $\alpha > 0$, conditions (4.6)-(4.8) need to be satisfied.

Step 1

From Definition 16, $M(s) = \left(\begin{array}{c|c} A_{cl} & B_{cl} \\ \hline C_{cl} & D_{cl} \end{array}\right)$ is $\alpha-$ SNI with a given $\alpha > 0$ if there exists $Y = Y^T > 0$ such that

$$\begin{pmatrix} A_{cl}Y + YA_{cl}^T + 2\alpha Y & \star \\ B_{cl}^T + C_{cl}YA_{cl}^T & 0 \end{pmatrix} \leq 0. \tag{4.11}$$

Step 2

Since inequality (4.11) is not in LMI form due to presence of the terms containing products of unknown controller variables, a linearising change in controller variables [73, 96] is required to transform (4.11) into LMI form. Partition the closed-loop Lyapunov matrix Y and Y^{-1} as follows:

$$Y = \begin{pmatrix} X & M \\ M^T & \bullet \end{pmatrix} \quad \text{and} \quad Y^{-1} = \begin{pmatrix} P & N \\ N^T & \bullet \end{pmatrix}, \tag{4.12}$$

where X and P are symmetric $n \times n$ matrices and the symbol $\bullet$ represents matrices that are not explicitly used in the linearization process. Note Y^{-1} exists since $Y > 0$ via (4.7) which has been explained subsequently in step 4. Note also that X, P, M, N are not independent variables but must satisfy $XP + MN^T = I$ (see [73, 96] for details). Since, M and N are square and non-singular, the following block matrices

$$\Pi_1 = \begin{pmatrix} P & I \\ N^T & 0 \end{pmatrix} \quad \text{and} \quad \Pi_2 = \begin{pmatrix} I & X \\ 0 & M^T \end{pmatrix} \tag{4.13}$$

are non-singular. Π_1 and Π_2 are related through the expression

$$Y\Pi_1 = \Pi_2 \tag{4.14}$$

which is obtained from $YY^{-1} = I$. The change of controller variables are defined as

$$\begin{cases} \hat{A} = PAX + NB_cC_2X + PB_2C_cM^T + PB_2D_cC_2X + NA_cM^T, \\ \hat{B} = NB_c + PB_2D_c, \\ \hat{C} = D_cC_2X + C_cM^T, \quad \text{and} \\ \hat{D} = D_c. \end{cases} \tag{4.15}$$

Step 3

Applying a congruence transformation on (4.11) with the block diagonal matrix $\text{diag}\{\Pi_1, I\}$ and using (4.14), we obtain

$$\begin{bmatrix} \Pi_1^T A_{cl}\Pi_2 + \Pi_2^T A_{cl}^T\Pi_1 + 2\alpha\Pi_1^T\Pi_2 & \star \\ \left(B_{cl}^T + C_{cl}YA_{cl}^T\right)\Pi_1 & 0 \end{bmatrix} \leq 0. \tag{4.16}$$

Simplifying all the product terms and substituting into (4.16) the linearizing change of controller variables given in (4.15), we get back condition (4.6), that is,

$$\left[\begin{array}{cc:c} \Phi_{11} + 2\alpha P & \Phi_{12} + 2\alpha I & PB_1 + \hat{B}D_{21} + \hat{A}C_1^T \\ \star & \Phi_{22} + 2\alpha X & \Phi_{23} \\ \hdashline \star & \star & 0 \end{array}\right] \leq 0.$$

Step 4

Positive definiteness of the closed-loop Lyapunov matrix $Y = \begin{pmatrix} X & M \\ M^T & \bullet \end{pmatrix}$ is guaranteed by (4.7) via the congruence transformation shown below

$$\Pi_1^T Y \Pi_1 = \begin{pmatrix} P & I \\ I & X \end{pmatrix} > 0. \tag{4.17}$$

Step 5

The inequality condition (4.8) is equivalent to $M(0) < \gamma I$ since $M(0) = C_{cl}YC_{cl}^T + D_{11}$. This in turn implies $\lambda_{\max}[M(0)\Delta(0)] < 1$ via [15]. Thus, the interconnection of $M(s)$ being $\alpha-$ SNI and $\Delta(s)$ being stable NI satisfies all the assumptions of [15, Theorem 5] as well as the DC loop gain condition. Therefore, the interconnection is robustly stable. This completes the proof. □

Remark 3. *The implication of Theorem 5 is that the closed-loop system $M(s)$ will be robustly stable to all class of NI uncertainties with DC gain γ^{-1}. This means that in the case of a flexible structure system with collocated force actuator and position sensor, if we use a truncated model of the system as our generalized plant $G(s)$ for controller synthesis and consider the rest of the modes as unmodelled dynamics, then the result of Theorem 5 will ensure robust stability to this unmodelled dynamics as long as the DC gain of the unmodelled dynamics is less than or equal to γ^{-1}. This is due to the fact that* (4.6) *and* (4.8) *of Theorem 5 will ensure that the closed-loop system is $\alpha-$ SNI and has a DC gain less than γ,respectively.*

Remark 4. *In order to find square and non-singular solutions of M and N from the expression $MN^T = I - XP$, methods such as $Q-R$ factorisation, Cholesky factorisation or Eigen-decomposition can be used. But the easiest solution is to choose $M = I$ and accordingly, $N = I - PX$. This choice of M and N rules out the possibility of getting ill-conditioned solutions in Matlab due to computational issues.* ■

4.4 Numerical Examples

In this section, we will present two illustrative examples to elucidate the usefulness of the proposed synthesis technique.

4.4.1 Example 1

We reconsider the model of an uncertain flexible structure system with collocated position sensor and force actuator, as shown in Fig. 4.2, originally studied in [20, 32] followed later by [66]. We assume that the output of the system $\bar{y}$ is subjected to some disturbance d. This represents the measured output of the system y. This uncertainty $\Delta(s)$ is given by $\Delta(s) = P(s) - 1$, where $P(s)$ is the dynamics of the uncertain flexible structure. Since $P(s)$ is SNI, $\Delta(s)$ is also SNI. We also assume that $\Delta(s)$ satisfies $\Delta(\infty) \geq 0$. More information about the system can be found in [20, 32].

The generalized plant model G of the physical system is governed by the following state-space equations. The output of the system $y(t)$ is subjected to some bounded

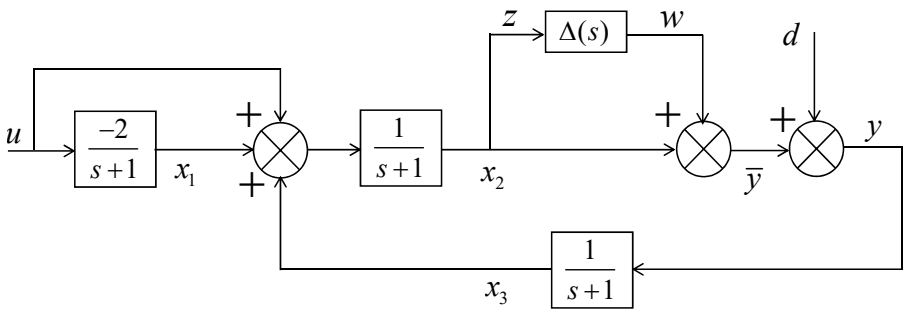

Figure 4.2: Block diagram of the simplified model of an uncertain flexible structure system taken in [32].

disturbance $d(t) \in \mathbb{R}$.

$$G : \begin{cases} \begin{bmatrix} \dot{x}_1 \\ \dot{x}_2 \\ \dot{x}_3 \end{bmatrix} = \begin{bmatrix} -1 & 0 & 0 \\ 1 & -1 & 1 \\ 0 & 1 & -1 \end{bmatrix} \begin{bmatrix} x_1 \\ x_2 \\ x_3 \end{bmatrix} + \begin{bmatrix} 0 & 0 \\ 0 & 0 \\ 1 & 1 \end{bmatrix} \begin{bmatrix} w \\ d \end{bmatrix} + \begin{bmatrix} -2 \\ 1 \\ 0 \end{bmatrix} u, \\ \begin{bmatrix} z \\ y \end{bmatrix} = \begin{bmatrix} 0 & 1 & 0 \\ 0 & 1 & 0 \end{bmatrix} \begin{bmatrix} x_1 \\ x_2 \\ x_3 \end{bmatrix} + \begin{bmatrix} 0 & 0 \\ 1 & 1 \end{bmatrix} \begin{bmatrix} w \\ d \end{bmatrix}, \end{cases}$$

and $W(s) = \Delta(s)Z(s)$, where $W(s)$ and $Z(s)$ are the Laplace transform of $w(t)$ and $z(t)$ respectively. In line with [32], $\Delta(s)$ is an SNI uncertainty with $\Delta(\infty) = 0$ and $\Delta(0) \leq 1$.

Part I. The control objective is to synthesize a dynamic output feedback controller $K(s)$ such that the nominal closed-loop system $M(s)$ becomes $\alpha-$ SNI and remains stable closed-loop in presence of any $\Delta(s)$ defined above. Choosing $\alpha = 0.8$ and applying Theorem 5, we obtain a feasible solution set of matrices

$$P = \begin{bmatrix} 126.3650 & 15.0662 & 83.8253 \\ 15.0662 & 7.8543 & 15.0240 \\ 83.8253 & 15.0240 & 126.6103 \end{bmatrix} > 0,$$

$$X = \begin{bmatrix} 33.3391 & -2.0000 & -31.8531 \\ -2.0000 & 0.5764 & 1.5764 \\ -31.8531 & 1.5764 & 30.8991 \end{bmatrix} > 0,$$

and $\hat{A}$, $\hat{B}$, $\hat{C}$, $\hat{D}$ using the CVX toolbox [95] in SDP mode with SEDUMI solver to solve the LMIs. We fix $M = I$ and hence, $N = I - PX$. The controller matrices A_c,

B_c, C_c and D_c are then uniquely reconstructed for this M and N using the relations (4.10a)-(4.10d). The controller $K(s)$ is computed as

$$K(s) = \frac{3.7491(s+1)(s+1.345)(s+6.358)}{(s+36.45)(s+1.386)(s+1.001)}$$

which constitutes the nominal closed-loop system

$$M(s) = \frac{3.749s^5 + 33.63s^4 + 97.04s^3 + 126.6s^2 + 77.97s + 18.48}{s^6 + 38.09s^5 + 174.3s^4 + 336.1s^3 + 328.9s^2 + 162s + 32.06}$$

from w to z. The closed-loop poles are given by $\lambda_i(A_{cl}) = \{-33.1278, -1.1847, -0.9259 \pm j0.1564, -0.9264, -1.00\}$. It can be readily verified that $M(s)$ is an $\alpha-$ SNI transfer function with $\Re[\lambda_i[A_{cl}]] < -0.8$ for all i. The Nyquist plot of $M(s)$ given in Fig. 4.3a also reflects that $M(s)$ is an SNI transfer function. Now, we find $M(0) = 0.5764$ and hence, $M(0)\Delta(0) = 0.5764 < 1$, which ensures robust stability in closed-loop against the given set of $\Delta(s)$ having $\Delta(0) \leq 1$ via Theorem 5. In order to show the

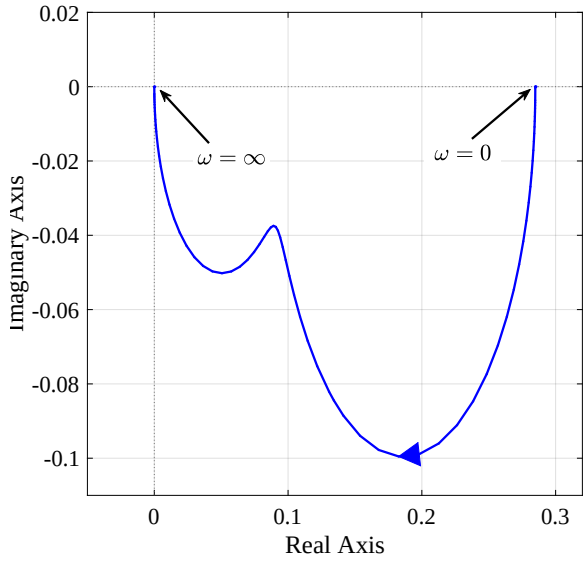

(a)

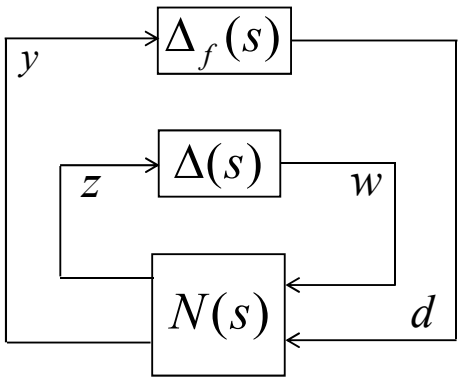

(b)

Figure 4.3: (a) Nyquist plot of the $\alpha-$ SNI transfer function $M(s)$ obtained in Example 1; (b) LFT configuration for robust performance problem by augmenting a fictitious uncertainty $\Delta_f(s)$ with the stable NI uncertainty $\Delta(s)$.

applicability of the proposed synthesis scheme, we study the disturbance-attenuation problem in presence of two arbitrarily chosen strictly proper SNI uncertainties given by $\Delta_1(s) = \frac{1}{s+2}$ and $\Delta_2 = \frac{1}{s+20}$. A pulse disturbance having amplitude 0.1 and $T_{on} = 1$s is applied to the system under all zero initial condition. Figures 4.4a-4.4e compare

the closed-loop time response corresponding to the nominal case and in presence of the uncertainties. It is observed that the designed controller $K(s)$ ensures closed-loop stability and also provides satisfactory transient performance in presence of the uncertainty. The figures reveal that the percentage deviation from nominal to perturbed condition in each of the states as well as the output $y(t)$ remains within 5% only. Moreover, despite the presence of uncertainty, the control effort $u(t)$ increases to a negligible extent with respect to nominal level.

Part II. Apart from the time domain performance analysis, we would also like to quantify and measure the robust $\mathcal{H}_\infty$ performance of the closed-loop system output (y) from the disturbance (d) achieved by the designed controller $K(s)$. Theoretically, robust $\mathcal{H}_\infty$ performance is analysed [88] by recasting the robust performance problem into a robust stability problem with respect to the augmented, two-block uncertainty $\Delta_p(s) = \begin{bmatrix} \Delta(s) & 0 \\ 0 & \Delta_f(s) \end{bmatrix}$, where $\Delta_f(s) \in \mathcal{RH}_\infty^{n_d \times n_y}$ is a fictitious uncertainty and $\Delta(s) \in \mathcal{RH}_\infty^{m \times m}$ is the physical uncertainty as depicted in Fig. 4.3b. To measure the robust $\mathcal{H}_\infty$ performance, μ-analysis technique is invoked. According to [88, Theorem 11.9], robust $\mathcal{H}_\infty$ performance with level β of the closed-loop system shown in Fig. 4.3b is guaranteed for all stable $\Delta(s)$ with $\|\Delta(s)\|_\infty < \frac{1}{\beta}$ for a given $\beta > 0$ if and only if

$$\sup_{\omega \in \mathbb{R}} \mu_{\Delta_p}(N(j\omega)) \leq \beta, \tag{4.18}$$

where $N(s)$ represents the transfer function mapping from $\begin{bmatrix} w \\ d \end{bmatrix}$ to $\begin{bmatrix} z \\ y \end{bmatrix}$. Following this approach, in the present example, we compute an upper bound to $\mu_{\Delta_p}(N(j\omega))$ using the Matlab Robust Control Toolbox for the frequency interval $\omega \in [10^{-4}, 10^4]$ and find $\sup_{\omega \in [10^{-4}, 10^4]} \mu_{\Delta_P}(N(j\omega)) \leq 2.1529$. We also calculate $\|N_{11}(s)\|_\infty = \|M(s)\|_\infty = 0.5764$. It signifies that, to satisfy robust stability alone (via Small-gain Theorem [88]), $\|\Delta(s)\|_\infty < \frac{1}{0.5764} = 1.7349$; while, to ensure the robust $\mathcal{H}_\infty$ performance with level 2.1529 via μ-analysis, $\|\Delta(s)\|_\infty < \frac{1}{2.1529} = 0.4645$ is required. However, from *Part I*, it can be seen that the synthesized controller can ensure robust performance even for $\Delta_1 = 0.5$. This is bigger set of uncertainty than that allowed by robust $\mathcal{H}_\infty$ performance.

Remark 5. *It should be noted that Part II of Example 4.4.1 is not a comparison*

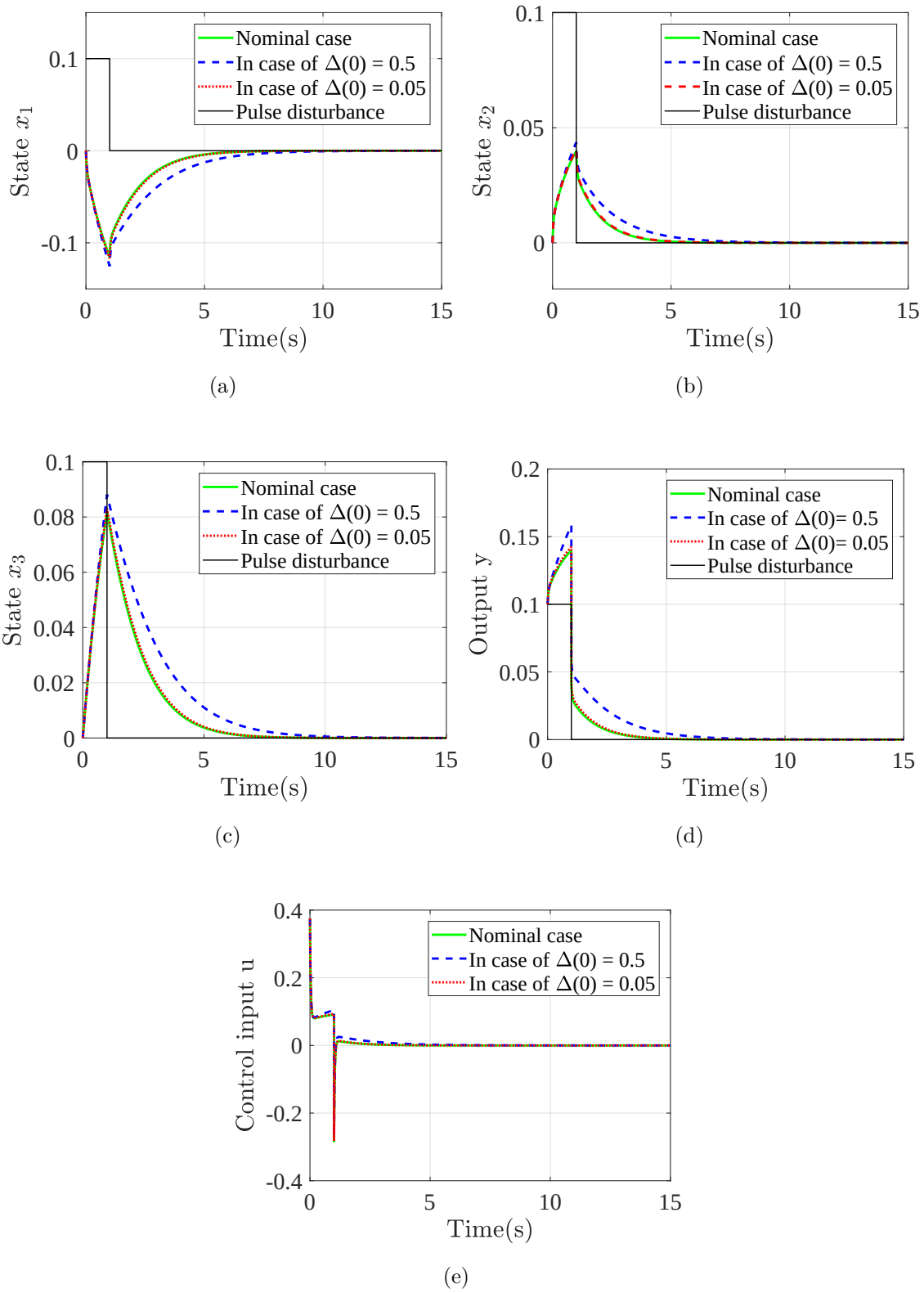

Figure 4.4: Closed-loop time responses of the designed system under the nominal as well as perturbed condition subjected to a pulse disturbance and zero initial condition: (a) State $x_1(t)$, (b) State $x_2(t)$, (c) State $x_3(t)$, (d) System output $y(t)$, (e) Control signal $u(t)$.

between robust $\mathcal{H}_\infty$ performance and robust performance of the synthesized closed-loop system in Part I. This is because more restrictions is imposed on the $\mathcal{H}_\infty$ controller for it to satisfy the robust performance, while no further restrictions is imposed on the synthesized NI closed-loop system. Hence, the $\mu-$ analysis just helps to provide a lower bound for the class of uncertainties for which robust performance can be achieved.

4.4.2 Example 2

Here, we adopt the following MIMO example from [66] being inspired by [72], where the same example was studied to show an application of a decentralized static output feedback controller. The generalized plant G is expressed via (4.3) with the following state-space matrices

$$A = \begin{bmatrix} -4 & 0 & -2 & 0 & 0 \\ 0 & -2 & 0 & 2 & 0 \\ 0 & 0 & -2 & 0 & -1 \\ 0 & -2 & 0 & -1 & 0 \\ 3 & 0 & -2 & 0 & -1 \end{bmatrix}, B_1 = \begin{bmatrix} 1 \\ 1 \\ 1 \\ 1 \\ 1 \end{bmatrix},$$

$$C_1^T = \begin{bmatrix} 0 \\ 1 \\ 0 \\ 0 \\ 0 \end{bmatrix}, B_2 = \begin{bmatrix} 1 & 0 & 0 \\ 1 & 0 & 0 \\ 0 & 0 & 0 \\ 0 & 1 & 0 \\ 0 & 0 & 1 \end{bmatrix}, C_2 = \begin{bmatrix} 1 & 0 & 0 & 0 & 0 \\ 0 & 1 & 0 & 0 & 0 \\ 0 & 0 & 0 & 0 & 1 \end{bmatrix}$$

and $D_{11} = 0$, $D_{12} = 0_{1\times 4}$, $D_{21} = 0_{3\times 1}$. The uncertainty $\Delta(s)$ is assumed to be any stable, strictly proper, NI transfer function with $\Delta(0) \leq 3.6$. Similar to Example 1, the control objective is to synthesize an output feedback controller $K(s)$ which internally stabilizes G and renders $M(s)$ from w to z $\alpha-$ SNI. Choosing $\alpha = 2$, we apply Theorem

5 on G and obtain a feasible solution set of matrices

$$X = \begin{bmatrix} 24.58 & -0.06 & -9.69 & -2.83 & -7.73 \\ -0.06 & 0.25 & 0.34 & 0.03 & 0.32 \\ -9.69 & 0.34 & 24.50 & -5.65 & 10.07 \\ -2.83 & 0.03 & -5.65 & 31.85 & -1.45 \\ -7.73 & 0.32 & 10.07 & -1.45 & 34.22 \end{bmatrix} > 0,$$

$$P = \begin{bmatrix} 21.12 & -7.37 & 1.86 & -4.69 & -7.69 \\ -7.37 & 53.42 & -10.22 & -23.68 & -7.41 \\ 1.86 & -10.22 & 11.45 & -2.81 & 1.85 \\ -4.69 & -23.68 & -2.81 & 39.11 & -4.68 \\ -7.69 & -7.41 & 1.85 & -4.68 & 21.14 \end{bmatrix} > 0,$$

and $\hat{A}$, $\hat{B}$, $\hat{C}$, $\hat{D}$. $M = I$ is taken and hence, $N = I - PX$. The controller state-space matrices are then reconstructed according to (4.10a)-(4.10d) as given below:

$$A_c = \begin{bmatrix} -10.40 & -9.92 & -13.89 & -10.27 & -9.25 \\ -5.73 & -6.89 & -5.02 & -4.09 & -4.20 \\ 1.58 & 0.80 & -1.89 & 0.82 & 1.83 \\ 9.19 & 2.87 & 3.17 & 1.89 & 6.55 \\ -3.24 & -0.09 & 6.12 & 0.08 & -6.57 \end{bmatrix},$$

$$B_c = \begin{bmatrix} 46.38 & -4.96 & -39.16 \\ -4.96 & -65.26 & -10.10 \\ 19.58 & -40.04 & 31.07 \\ 20.32 & -8.28 & 17.61 \\ -39.16 & -10.10 & -38.19 \end{bmatrix}, D_c = 0_{3\times 3},$$

$$\text{and } C_c = \begin{bmatrix} 0.27 & 0.36 & 0.31 & 0.36 & 0.28 \\ -0.04 & 0.11 & 0.06 & 0.096 & 0.026 \\ 0.39 & 0.23 & -0.24 & 0.20 & 0.38 \end{bmatrix}.$$

We compute the nominal closed-loop system

$$M(s) = \frac{(s+2.35)(s^2+4.942s+7.379)(s^2+13.89s+49.69)}{(s+2.325)(s+3.274)(s^2+4.967s+7.426)(s^2+6.174s+13.64)} \\ \frac{(s^2+6.256s+13.73)(s^2+6.423s+18.4)}{(s^2+5.95s+17.95)(s^2+11.17s+62.71)}$$

which has been verified to be SNI with $\Re[\lambda_i[A_{cl}]] < -2$. The Nyquist plot of $M(s)$ shown Fig. 4.5 confirms that it is indeed SNI. As $M(s)$ is strictly proper and $M(0)\Delta(0) = 0.2507 \times 3.6 = 0.9025 < 1$, it guarantees that the designed controller $K(s)$ ensures robust stability of the generalized plant G against any stable NI uncertainty $\Delta(s)$ satisfying $\Delta(0) \leq 3.6$ via Theorem 5.

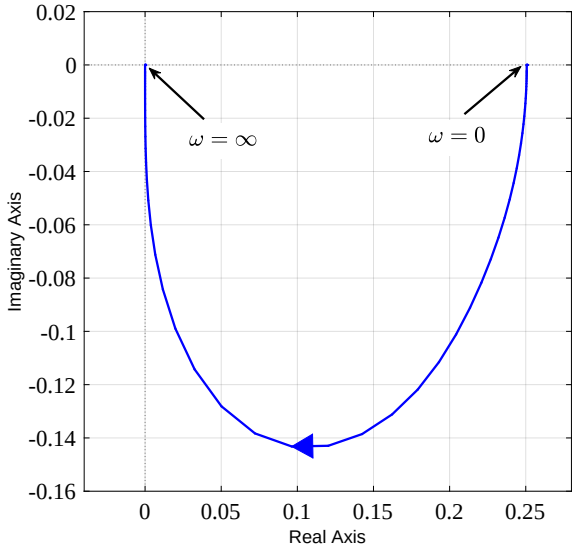

Figure 4.5: Nyquist plot of the synthesized $\alpha-$ SNI transfer function $M(s)$ obtained in Example 2.

Remark 6. *It should be noted that the choice of the variable α in both examples was an arbitrary one. It is desirable to have α as large as possible. However, choosing a very large value for α will lead to a high control action which may cause actuator saturation. Also, a very large α will mean that the class of uncertainties for which the closed-loop system is robustly stable against becomes smaller. This is to be expected because the more performance we demand from the closed-loop system, the less robust it will become. Therefore, there is always a trade-off between robustness and performance of the closed-loop system.*

4.5 Conclusions

This chapter addressed the issue of NI controller synthesis with a prescribed degree of stability. First, we provided a definition for $\alpha-$ SNI systems which are a subset of the SNI class. Subsequently, we introduced a synthesis technique that uses the

$\alpha-$ SNI framework to impose a minimum prescribed decay rate for the closed-loop synthesized system. Robust stability is ensured against any stable, strictly proper NI uncertainty satisfying the DC loop gain condition for the positive interconnection of NI-SNI systems. We presented two numerical examples that showed the usefulness of the proposed synthesis technique.

Chapter 5

Linear Time-Varying Negative Imaginary Systems

All the materials presented in this chapter were published in [60].

5.1 Introduction

There are many contributions in the NI literature that introduce different classes of NI systems and systems related to NI systems such as in [3, 8, 9, 14, 94]. However, non of these works addressed the issue of LTV NI systems. LTV NI systems may arise, for example, in real life applications such as a flexible structure with collocated force actuator and position sensor having time-varying mass or a rocket in longitudinal motion where the mass of the rocket changes as the fuel in the tank is used up. In electrical circuits, such systems may arise when the resistors, inductors or capitors are time-varying and the output of the circuit is the voltage across a capacitor connected in series with a voltage source or the current flowing through an inductor connected in parallel with a current source.

In this chapter, we introduce the notion of LTV NI systems. LTV NI systems are defined using a time domain dissipative supply rate $w(u, \dot{y})$ that depends on input to the system (u), time-derivative of the system's output ($\dot{y}$) and an index $\delta \geq 0$. For $\delta > 0$, it gives rise to a strict subclass within the LTV NI systems, termed as LTV Output SNI (OSNI) systems. For characterizing the proposed class of systems, a set of LDMI conditions are derived based on the given state-space realization. Finally,

a set of sufficient conditions are derived which ensures that the origin is a globally asymptotically stable equilibrium point of an unforced positive feedback interconnection of two uniformly asymptotically stable LTV NI systems. Subsequently, LTV NI theory is specialized to LPV cases for which, the DLMI conditions can easily be avoided by considering the rate of variation of the uncertain parameters as independent LMI variables.

The major contributions of this chapter include

- Provide a time domain definition for LTV NI systems. The definition is with respect to a supply rate $w(u, \dot{y})$, which depends on the input u and time derivative of the output $\dot{y}$.

- Provide a time domain definition for LTV OSNI systems. Similar to the LTV NI definition, the definition is with respect to the dissipative supply rate, depending on the input and time derivative of the output, in addition to a variable $\delta > 0$.

- Provide a state-space characterization of the LTV NI systems using DLMI conditions. This helps in the stability analysis and synthesis of this kind of systems.

- Provide a state-space characterization of LTV OSNI system. These conditions also use DLMI and are restricted to systems with relative degree two.

- The chapter then provides condition for the uniform global asymptotic stability of the equilibrium point of an unforced positive feedback LTV NI-OSNI interconnection.

- LPV NI and OSNI systems, which are a specialization of the LTV NI and OSNI systems respectively, are introduced. In this case, the state-space characterizations are presented using LMIs and not DLMIs as with LTV systems.

- The chapter ends by providing conditions for the global asymptotic stability of the equilibrium for an unforced positive feedback interconnection of an LPV NI-OSNI systems.

5.2 Linear Time-Varying NI Systems Theory

5.2.1 Definition and Properties

Consider a class of finite-dimensional, square, LTV dynamical systems described by the state-space equations

$$\Sigma : \begin{cases} \dot{x}(t) = A(t)x(t) + B(t)u(t), & x(0) = x_0; \\ y(t) = Cx(t), \end{cases} \tag{5.1}$$

where $x(t) \in \mathbb{R}^n$, $u(t) \in \mathbb{R}^m$ and $y(t) \in \mathbb{R}^m$ $\forall t \in \mathbb{R}_{\geq 0}$ and the matrices $A(t)$ and $B(t)$ are assumed to be continuous and bounded $\forall t \in \mathbb{R}_{\geq 0}$. Note that in this section, the admissible inputs u are considered to be in the space $\mathbb{U}^m$ along with sufficient smoothness properties such that unique solution of the state trajectory $x(t)$ exists forward in time $\forall t \in \mathbb{R}_{\geq 0}$ and also $x \in \mathcal{L}_{2e}^n$. Hence $\dot{y}(t) = C\dot{x}(t) = CA(t)x(t) + CB(t)u(t)$ also exists forward in time and $\dot{y} \in \mathcal{L}_{2e}^m$.

Definition 17. *[60] (**LTV NI systems**) Let Σ be a finite-dimensional, square, LTV system as described in* (5.1)*. Then Σ is said to be an LTV NI system if there exists a constant $\beta \in \mathbb{R}$ such that*

$$\int_0^T \dot{y}(t)^T u(t)\, \mathrm{d}t \geq \beta \tag{5.2}$$

for any admissible $u \in \mathbb{U}^m$, any initial condition $x_0 \in \mathbb{R}^n$ and all $T \in [0, \infty)$.

Remark 7. *In the SISO LTI case, the name 'negative imaginary' is motivated by the Nyquist plot of the transfer function being restricted to the third and fourth quadrants of the Nyquist plane over $\omega \in \mathbb{R}_{\geq 0}$. Since this chapter considers LTV systems of the state-space form* (5.1)*, the name 'LTV NI' is chosen for this class of systems to underpin the connection to its LTI counterpart (i.e., although the time domain definition* (5.2) *does not have a Nyquist interpretation, it specialises in the LTI case to the condition $j\omega\left[\Sigma(j\omega) - \Sigma(j\omega)^*\right] \geq 0$ $\forall \omega \in \mathbb{R}_{\geq 0}$ which recommends the name 'NI' in the LTI case [15]).*

We will now define the class of LTV OSNI systems.

Definition 18. *[60] (**LTV OSNI systems**) Let Σ be a finite-dimensional, square and stable LTV system as described in* (5.1)*. Then Σ is said to be an LTV OSNI*

system if there exist the constants $\beta \in \mathbb{R}$ *and* $\delta > 0$ *such that*

$$\int_0^T \dot{y}(t)^T u(t)\,\mathrm{d}t \geq \delta \int_0^T \dot{y}(t)^T \dot{y}(t)\,\mathrm{d}t + \beta \tag{5.3}$$

for any admissible $u \in \mathbb{U}^m$*, any initial condition* $x_0 \in \mathbb{R}^n$ *and all* $T \in [0, \infty)$*.*

Remark 8. *Definitions 17 and 18 would remain valid even when the LTV state-space system in* (5.1) *had its output equation* $y(t) = C(t)x(t)$ *with* $C(t)$ *and* $\dot{C}(t)$ *assumed to be continuous and bounded for all* $t \in \mathbb{R}_{\geq 0}$*. We do not however consider that situation in order to simplify the results that follow.*

5.2.2 State-Space Characterization of LTV NI Systems

In this subsection, state-space characterizations are provided for the LTV NI and OSNI systems which involve LDMI conditions.

Lemma 10. *[60] (**LTV NI lemma**) Let* Σ *be a finite-dimensional, square, LTV system as described in* (5.1)*. Then* Σ *is LTV NI if there exists a continuously differentiable and bounded matrix* $P(t) = P(t)^T \geq 0$ *for all* $t \in \mathbb{R}_{\geq 0}$ *such that*

$$\begin{bmatrix} \dot{P}(t) + P(t)A(t) + A(t)^T P(t) & P(t)B(t) - A(t)^T C^T \\ B(t)^T P(t) - CA(t) & -CB(t) - B(t)^T C^T \end{bmatrix} \leq 0. \tag{5.4}$$

Proof. [60] By exploiting the property of block partitioned semidefinite matrix [85], there always exist continuous and bounded matrices $L(t) \in \mathbb{R}^{m\times n}$ and $W(t) \in \mathbb{R}^{m\times m}$ for all $t \in \mathbb{R}_{\geq 0}$ such that

$$\begin{aligned} &\begin{bmatrix} \dot{P}(t) + P(t)A(t) + A(t)^T P(t) & P(t)B(t) - A(t)^T C^T \\ B(t)^T P(t) - CA(t) & -CB(t) - B(t)^T C^T \end{bmatrix} \\ &= \begin{bmatrix} -L^T(t)L(t) & -L^T(t)W(t) \\ -W^T(t)L(t) & -W^T(t)W(t) \end{bmatrix} \leq 0 \qquad \forall t \geq 0. \end{aligned} \tag{5.5}$$

Let $V(t,x) = \frac{1}{2}x^T P(t)x$ with $P(t) = P(t)^T \geq 0$ for all $t \in \mathbb{R}_{\geq 0}$ be a Lyapunov function candidate associated with the system Σ. The time derivative of $V(t,x)$ along the trajectories of Σ, given by (5.1), subjected to any admissible input $u \in \mathbb{U}^m$, is computed as $\dot{V}(t,x) = \frac{1}{2}x^T\left(\dot{P} + PA + A^T P\right)x + x^T PBu$. Integrating the last expression with respect to time t from 0 to $T \in \mathbb{R}_{\geq 0}$ and substituting $\dot{P} + PA + A^T P = -L^T L$ and $PB - A^T C^T = -L^T W$ from (5.5), we have

$$V(T, x(T)) - V(0, x(0)) = \int_0^T \left[-\frac{1}{2}x^T L^T L x + x^T (A^T C^T - L^T W)u\right]\mathrm{d}t \tag{5.6}$$

for any admissible $u \in \mathbb{U}^m$ and for all $T \in [0, \infty)$. Now using the fact that $V(T, x(T)) - V(0, x(0)) \geq -V(0, x(0))$, (5.6) implies (5.7), where $\beta = -V(0, 0) \in (-\infty, 0]$,

$$\int_0^T x^T A^T C^T u \, \mathrm{d}t \geq \int_0^T \left(\frac{1}{2} x^T L^T L x + x^T L^T W u \right) \mathrm{d}t + \beta. \tag{5.7}$$

Since CB is a square matrix, it can be expressed as $CB = \frac{1}{2}\left(CB + B^T C^T\right) + \frac{1}{2}\left(CB - B^T C^T\right)$. Below, we derive the expression for $\dot{y}^T u$ on noting that $\dot{y} = C\dot{x} = CAx + CBu$,

$$\begin{aligned} &\dot{y}^T u = x^T A^T C^T u + \frac{1}{2} u^T \left(CB + B^T C^T\right) u + \frac{1}{2} u^T \left(CB - B^T C^T\right) u \\ &\Rightarrow \dot{y}^T u = x^T A^T C^T u + \frac{1}{2} u^T \left(CB + B^T C^T\right) u \end{aligned} \tag{5.8}$$

by exploiting the property $u^T \left(CB - B^T C^T\right) u = 0 \; \forall u \in \mathbb{R}^m$ since $\left(CB - B^T C^T\right)$ is skew-symmetric [85]. Integrating (5.8) from 0 to $T \in [0, \infty)$ and plugging (5.7) into it, we find

$$\begin{aligned} &\int_0^T \dot{y}^T u \, \mathrm{d}t \geq \int_0^T \left(\frac{1}{2} x^T L^T L x + x^T L^T W u + \frac{1}{2} u^T W^T W u \right) \mathrm{d}t + \beta \\ &\Rightarrow \int_0^T \dot{y}^T u \, \mathrm{d}t \geq \beta \qquad \text{[via the completion of squares]} \end{aligned}$$

for any admissible $u \in \mathbb{U}^m$ and for all $T \in [0, \infty)$. Hence it is proved that Σ is an LTV NI system via Definition 17. ■

We will now provide the state-space characterization for LTV OSNI systems.

Lemma 11. *[60] (**LTV OSNI lemma**) Let Σ be a finite-dimensional, square, LTV system as described in* (5.1)*. Also let $CB(t) \equiv 0$ and $CA(t) \not\equiv 0$ for all $t \in \mathbb{R}_{\geq 0}$. Then Σ is LTV OSNI if there exists a continuously differentiable and bounded matrix $P(t) = P(t)^T > 0$ for all $t \in \mathbb{R}_{\geq 0}$ such that*

$$\dot{P}(t) + P(t)A(t) + A(t)^T P(t) < 0 \text{ and } P(t)B(t) = A(t)^T C^T. \tag{5.9}$$

Proof. [60] Let there exist a real-valued, continuous and bounded matrix $Q(t) = Q(t) > 0$ for all $t \in \mathbb{R}_{\geq 0}$ such that

$$\dot{P}(t) + P(t)A(t) + A(t)^T P(t) = -Q(t) < 0 \quad \forall t \in \mathbb{R}_{\geq 0}. \tag{5.10}$$

Inequality (5.10) implies uniform asymptotic stability of the OSNI system Σ. Let $V(t, x) = \frac{1}{2} x^T P(t) x$ with $P(t) = P(t)^T > 0$ be a Lyapunov function candidate for

Σ. Now, utilising (5.6) from the proof of Lemma 10 and substituting $\dot{V}(t,x) = \frac{1}{2}x^T\left(\dot{P}+PA+A^TP\right)x + x^TPBu$, we obtain

$$V(T,x(T)) - V(0,x(0)) = \int_0^T \left(-\frac{1}{2}x^TQx + x^TA^TC^Tu\right)\mathrm{d}t \tag{5.11}$$

for any admissible $u \in \mathbb{U}^m$ and for all $T \in [0,\infty)$. From (5.8), we have $\int_0^T \dot{y}^Tu\ \mathrm{d}t = \int_0^T x^TA^TC^Tu\ \mathrm{d}t$ since $CB(t) = 0\ \forall t \in \mathbb{R}_{\geq 0}$ via supposition. Utilizing this result, (5.11) implies

$$\int_0^T \dot{y}^Tu\ \mathrm{d}t = \int_0^T x^TA^TC^Tu\ \mathrm{d}t \geq \frac{1}{2}\int_0^T x^TQx\ \mathrm{d}t + \beta. \tag{5.12}$$

We also have $\dot{y}^T\dot{y} = x^TA^TC^TCAx$ for all $t \in \mathbb{R}_{\geq 0}$ since $CB = 0$ via supposition. Now exploiting the property $\lambda_{\min}[P]||x|| \leq x^TPx \leq \lambda_{\max}[P]||x||$ when $P = P^T \geq 0$ [85], we obtain $\dot{y}^T\dot{y} = x^TA^TC^TCAx \leq \bar{c}x^Tx$ and $x^TQx \geq \underline{q}x^Tx$ for all $t \in \mathbb{R}_{\geq 0}$ denoting $\bar{c} = \sup\limits_{\forall t\geq 0}\lambda_{\max}[A^TC^TCA] > 0$ and $\underline{q} = \inf\limits_{\forall t\geq 0}\lambda_{\min}[Q] > 0$. The last two expressions together imply $x^TQx \geq \frac{\underline{q}}{\bar{c}}\dot{y}^T\dot{y}\ \forall t \in \mathbb{R}_{\geq 0}$. This, in turn, implies from (5.12) that $\int_0^T \dot{y}^Tu\ \mathrm{d}t \geq \delta\int_0^T \dot{y}^T\dot{y}\ \mathrm{d}t + \beta$ for any admissible $u \in \mathbb{U}^m$, for all $T \in [0,\infty)$ and denoting $\delta = \frac{\underline{q}}{2\bar{c}} > 0$. Hence, Σ is an LTV OSNI system according to Definition 18. ■

Remark 9. *The LTV NI lemma specialises to the well-established NI lemma (i.e. in the LTI setting) [15, 57]. Whereas, the LTV OSNI lemma partly captures the LTI OSNI lemma [5, 6] since the latter does not impose the constraint $CB = 0$. Hence, the LTV OSNI result cannot be considered as a generalised version of its LTI counterpart. Moreover, LTV NI and OSNI theory is completely independent of the conventional frequency-domain characterization of the existing NI and OSNI systems.*

Remark 10. *In contrast to the conventional NI and OSNI theory (i.e. in the LTI setting), the proposed LTV results do not impose the minimality constraint since the LTV NI and OSNI lemma conditions are sufficient-type results. Minimality condition is mainly required to establish the necessity part [7]. The proposed lemmas can be rendered necessary and sufficient if uniform controllability and observability constraints are imposed. However, for LTV systems, it is numerically very difficult to test these properties a priori and hence, the results becomes less appealing to the readers.*

5.3 Closed-Loop Stability Analysis of LTV NI and OSNI Systems

This section studies an unforced positive feedback closed-loop system shown in Fig. 5.1 containing two uniformly asymptotically stable LTV NI systems of which, one is LTV OSNI. We show that the closed-loop system has a single globally asymptotically stable equilibrium point which is the origin given by $\begin{bmatrix} x_1 \\ x_2 \end{bmatrix} = \begin{bmatrix} 0 \\ 0 \end{bmatrix}$.

Theorem 6. *[60] Let Σ_1 and Σ_2 be two finite-dimensional, square and uniformly asymptotically stable LTV systems. Also let $B_2(t)$ has full column rank, $C_2B_2(t) \equiv 0$ and $C_2A_2(t) \not\equiv 0$ for all $t \in \mathbb{R}_{\geq 0}$. Suppose Σ_1 is uniformly zero-state detectable and there exist continuously differentiable and bounded matrices $P_1(t) = P_1(t)^T > 0$ and $P_2(t) = P_2(t)^T > 0$ for all $t \in \mathbb{R}_{\geq 0}$ such that Σ_1 satisfies (5.4) and Σ_2 satisfies (5.9). Then the origin is a globally uniformly asymptotically stable equilibrium point of the unforced positive feedback interconnection of Σ_1 and Σ_2 shown in 5.1 if*

$$\begin{bmatrix} P_1(t) & -C_1^TC_2 \\ -C_2^TC_1 & P_2(t) \end{bmatrix} > 0 \quad \forall t \in \mathbb{R}_{\geq 0}. \tag{5.13}$$

Proof. [60] Let there exist continuous and bounded matrices $L(t) \in \mathbb{R}^{m\times n}$, $W(t) \in \mathbb{R}^{m\times m}$ and $Q(t) = Q(t)^T > 0$ such that Σ_1 satisfies (5.5) and Σ_2 satisfies (5.10) for all $t \in \mathbb{R}_{\geq 0}$. We designate $V_1(t, x_1) = \frac{1}{2}x_1^TP_1(t)x_1$ and $V_2(t, x_2) = \frac{1}{2}x_2^TP_2(t)x_2$ be the Lyapunov function candidates associated with Σ_1 and Σ_2 respectively. Let the combined Lyapunov function candidate for the closed-loop system be $V(t, x) = V_1(t, x_1) + V_2(t, x_2) - y_1^Ty_2$ where $x = \begin{bmatrix} x_1^T & x_2^T \end{bmatrix}^T$. It is apparent that

$$\begin{aligned} V(t,x) &= \frac{1}{2}x_1^TP_1(t)x_1 + \frac{1}{2}x_2^TP_2(t)x_2 - x_1^TC_1^TC_2x_2 \\ &= \frac{1}{2}\begin{bmatrix} x_1 \\ x_2 \end{bmatrix}^T \begin{bmatrix} P_1(t) & -C_1^TC_2 \\ -C_2^TC_1 & P_2(t) \end{bmatrix} \begin{bmatrix} x_1 \\ x_2 \end{bmatrix} > 0 \end{aligned}$$

via (5.13) and $V(t_0, 0) = 0$ for any $t_0 \in \mathbb{R}_{\geq 0}$. Owing to the continuously differentiable property and boundedness of $P_1(t)$ and $P_2(t)$ $\forall t \in \mathbb{R}_{\geq 0}$, $V(t, x)$ can be characterized as $0 < \alpha_1(||x||) \leq V(t, x) \leq \alpha_2(||x||) < \infty$ $\forall x \in \mathbb{R}^{n_1+n_2}$ where $\alpha_1(\cdot)$ and $\alpha_2(\cdot)$ are class-$\mathcal{K}$ functions with α_1 being radially unbounded in x. Moreover, $V(t, x)$ is a continuously differentiable function since $\dot{V}(t, x)$ remains uniformly continuous in $t \geq 0$ (shown

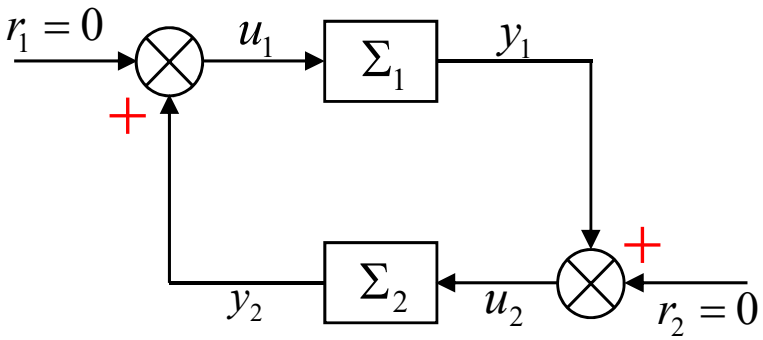

Figure 5.1: Positive feedback interconnection of LTV NI systems.

later in the ongoing proof). Now, the time-derivative of $V(t,x)$ is derived as follows:

$$\begin{aligned}
\dot{V}(t,x) &= \dot{V}_1(t,x_1) + \dot{V}_2(t,x_2) - \dot{y}_1^T y_2 - y_1^T \dot{y}_2 \\
&= \frac{1}{2} x_1^T \left(\dot{P}_1 + P_1 A_1 + A_1^T P_1\right) x_1 + x_1^T P_1 B_1 u_1 + \frac{1}{2} x_2^T (\dot{P}_2 + \\
&\quad P_2 A_2 + A_2^T P_2) x_2 + x_2^T P_2 B_2 u_2 - \dot{y}_1^T y_2 - y_1^T \dot{y}_2 \\
&= -\frac{1}{2} x_2^T Q x_2 + \dot{y}_2^T u_2 - \frac{1}{2} x_1^T \left(L^T L\right) x_1 - \frac{1}{2} u_1^T \left(W^T W\right) u_1 \\
&\quad - x_1^T L^T W u_1 + \dot{y}_1^T u_1 - \dot{y}_1^T y_2 - y_1^T \dot{y}_2 \quad \text{[using (5.5), (5.10)]} \\
&= -\frac{1}{2} x_2^T Q x_2 + \dot{y}_2^T y_1 - \frac{1}{2} \left(L x_1 + W u_1\right)^T \left(L x_1 + W u_1\right) + \\
&\quad \dot{y}_1^T y_2 - \dot{y}_1^T y_2 - y_1^T \dot{y}_2 \quad \text{[using } u_1 = y_2 \text{ and } u_2 = y_1\text{]} \\
&= -\frac{1}{2} x_2^T Q x_2 - \frac{1}{2} \left(L x_1 + W u_1\right)^T \left(L x_1 + W u_1\right) \qquad (5.14) \\
&\leq -\frac{1}{2} x_2^T Q x_2 \leq -q_{\min}\, \chi(||x_2||) \leq 0 \qquad (5.15)
\end{aligned}$$

where $q_{\min} = \inf_{\forall t \geq 0} \lambda_{\min}[Q(t)] > 0$ and $\chi(\cdot)$ is a class-$\mathcal{K}$ function. Now, [45, Theorem 8.4] and [86, Theorem 4.1] guarantee that both $x_1(t)$ and $x_2(t)$ will remain uniformly bounded for all $t \geq 0$. Then, to show uniform asymptotic stability of the states, we will seek to apply Barbalat's lemma [86]. It can be verified that $\ddot{V}(t,x)$ remains bounded $\forall t \geq 0$ since (i) x_1 and x_2 are already proved to be bounded $\forall t \geq 0$ (and hence, $y_1 = C_1 x_1$ and $y_2 = C_2 x_2$ are also uniformly bounded), (ii) the matrices $A_i(t)$ and $B_i(t)$ for $i \in \{1,2\}$ are assumed to be bounded $\forall t \geq 0$, and (iii) the input-derivative terms $\dot{u}_1 = \dot{y}_2 = C_2 \dot{x}_2 = C_2 A_2 x_2 + C_2 B_2 y_1$ and $\dot{u}_2 = \dot{y}_1 = C_1 A_1 x_1 + C_1 B_1 y_2$ are also bounded $\forall t \geq 0$. Therefore, $\dot{V}(t,x)$ is uniformly continuous for all $t \geq 0$ which ultimately implies $\dot{V}(t,x) \to 0$ as $t \to \infty$ by exploiting Barbalat's lemma. Finally, [86, Lemma 4.3] ensures that $\lim_{t\to\infty} x_2(t) = 0$ for any bounded $x_{2,0} \in \mathbb{R}^{n_2}$. This hence implies $\lim_{t\to\infty} y_2(t) = \lim_{t\to\infty} u_1(t) = 0$ as C_2 is constant and $u_1 = y_2$. Furthermore, as $t \to \infty$, the state-space equation of Σ_2, that is, $\dot{x}_2 = A_2(t) x_2(t) + B_2(t) y_1(t)$ implies

$\lim_{t\to\infty} y_1(t) = 0$ since $u_2 = y_1$, $B_2(t)$ has full column rank and due to uniform asymptotic convergence of $x_2(t)$. Now, exploiting uniform zero-state detectability (ZSD) [1] and uniform asymptotic stability of Σ_1, $u_1 \equiv 0$ and $y_1 \equiv 0$ imply $\lim_{t\to\infty} x_1(t) = 0$ for any bounded $x_{1,0} \in \mathbb{R}^{n_1}$. Combining the aforementioned arguments, it can be asserted that the positive feedback closed-loop system of Σ_1 and Σ_2 is globally uniformly asymptotically stable. ■

Remark 11. *When Σ_1 and Σ_2 are LTI NI systems, then condition* (5.13) *of Theorem 6 is equivalent to the DC gain condition of Theorem 4. This can easily be seen since $Y_1 = Y_1^T = P_1^{-1}$, $Y_2 = Y_2^T = P_2^{-1}$, both exist as $P_1 > 0$, $P_2 > 0$ and $\Sigma_1(0) = C_1 Y_1 C_1^T$, $\Sigma_2(0) = C_2 Y_2 C_2^T$ are the DC gains of Σ_1 and Σ_2 respectively. Then condition* (5.13) *can be written as*

$$\begin{bmatrix} Y_1^{-1} & -C_1^T C_2 \\ -C_2^T C_1 & Y_2^{-1} \end{bmatrix} > 0.$$

Then taking the Schur's complement with respect to Y_2^{-1}, the above condition becomes $Y_1^{-1} - C_1^T C_2 Y_2 C_2^T C_1 > 0$. But $C_2 Y_2 C_2^T = \Sigma_2(0)$. So $Y_1^{-1} - C_1^T \Sigma_2(0) T C_1 > 0$, which can then be expressed as

$$\begin{bmatrix} Y_1^{-1} & C_1^T \\ C_1 & \Sigma_2^{-1}(0) \end{bmatrix} > 0.$$

Also, taking the Schur's complement with respect to Y_1^{-1}, we have

$$\begin{aligned} &\Leftrightarrow \Sigma_2^{-1}(0) - C_1 Y_1 C_1^T > 0, \\ &\Leftrightarrow \Sigma_2^{-1}(0) - \Sigma_1(0) > 0, \\ &\Leftrightarrow \Sigma_1(0)\Sigma_2(0) < 1, \end{aligned}$$

which clearly shows that condition (5.13) *of Theorem 6 does indeed becomes the DC gain condition of Theorem 4 for the LTI case.*

5.4 Linear Parameter-Varying NI Systems

As the LTI NI and OSNI lemmas involve LDMI conditions, it may give rise to computational issues while solving the LDMIs using the SDP solver packages. To bypass

[1] The notion of uniform ZSD is defined for non-autonomous systems [10], analogous to the concept of ZSD applied to autonomous systems [45].

the LDMIs, in this section, we have specialized the previous results to LPV NI and OSNI systems considering bounded variation of the uncertain system parameters. Now, consider a class of finite-dimensional, square, LPV dynamical systems described by

$$\Sigma_{LPV}: \begin{cases} \dot{x}(t) = A(\rho)x(t) + B(\rho)u(t) & x(0) = x_0, \\ y(t) = Cx(t) \end{cases} \tag{5.16}$$

where $A(\rho)$, $B(\rho)$ depend affinely on the uncertain (possibly time-varying) parameter vector $\rho = [\rho_1, \rho_2, \cdots, \rho_K] \in \mathbb{R}^K$, that is, $A(\rho) = A_0 + \rho_1 A_1 + \cdots + \rho_K A_K$ and $B(\rho) = B_0 + \rho_1 B_1 + \cdots + \rho_K B_K$. Below, we mention two technical assumptions that must be satisfied by the LPV NI systems studied here:

A1. Each parameter ρ_i varies in the known interval $[\rho_{i,\min}, \rho_{i,\max}]$ for all $i \in \{1, 2, \cdots, K\}$. This implies that the parameter vector $\rho \in \mathbb{R}^K$ is valued in a hyper-rectangle with the set of vertices $\mathcal{V} = \{(v_1, \cdots, v_K) : v_i \in \{\rho_{i,\min}, \rho_{i,\max}\}\ \forall i\}$.

A2. The rate of variation $\dot{\rho}_i$ is well defined for all $t \in \mathbb{R}_{\geq 0}$ and $\dot{\rho}_i \in [\gamma_{i,\min}, \gamma_{i,\max}]$ where the range $\gamma_{i,\min} \leq 0 \leq \gamma_{i,\max}$ is known for all $i \in \{1, \cdots, K\}$. This implies that the vector $\dot{\rho} \in \mathbb{R}^K$ varies within a hyper-rectangle having the set of vertices $\mathcal{C} = \{(e_1, \cdots, e_k) : e_i \in \{\gamma_{i,\min}, \gamma_{i,\max}\}\ \forall i\}$.

We introduce the following notation $\rho_{\text{mean}} = \left[\frac{\rho_{1,\min}+\rho_{1,\max}}{2}, \frac{\rho_{2,\min}+\rho_{2,\max}}{2}, \cdots, \frac{\rho_{K,\min}+\rho_{K,\max}}{2}\right]$ to be used subsequently in Lemmas 12 and 13. Lemma 12 gives a set of sufficient conditions for LPV NI systems and is a specialized result of the LTV NI lemma derived in the previous section.

Lemma 12. *[60] (**LPV NI lemma**) Consider a finite-dimensional, square, LPV system Σ_{LPV}, as described in* (5.16)*, that satisfies assumptions A1 and A2. Suppose $A(\rho_{mean})$ does not have any pole in the open right-half plane and there exist $K+1$ real, symmetric matrices $P_0, P_1, \cdots, P_K$ with $P(\rho) = P_0 + \rho_1 P_1 + \cdots + \rho_K P_K$, then the following statements are the same*

(a). Σ_{LPV} is LPV NI

(b). There exist a continuous bounded matrix $P(\rho) = P(\rho)^T > 0$ such that

$$\begin{bmatrix} \dot{P}(\rho) + A(\rho)^T P(\rho) + P(\rho)A(\rho) & P(\rho)B(\rho) - A(\rho)^T C^T \\ (P(\rho)B(\rho) - A(\rho)^T C^T)^T & -CB(\rho) - B(\rho)^T C^T \end{bmatrix} \leq 0. \tag{5.17}$$

(c). There exist a continuous, bounded matrix $P_i = P_i^T > 0$ *such that*

$$\begin{bmatrix} P(v)A(v) + A(v)^T P(v) + P(e) - P_0 & P(v)B(v) - A(v)^T C^T \\ \left(P(v)B(v) - A(v)^T C^T\right)^T & -CB(v) - B(v)^T C^T \end{bmatrix} \leq 0 \quad (5.18a)$$

$$\text{and} \quad \begin{bmatrix} P_i A_i + A_i^T P_i & P_i B_i \\ B_i^T P_i & 0 \end{bmatrix} \geq 0 \quad (5.18b)$$

$\forall (v, e) \in \mathcal{V} \times \mathcal{C}$ *and* $\forall i \in \{1, \ldots, K\}$.

Proof. [60]

The equivalence between (a) and (b) can be established by realizing that if Σ_{LPV} is LPV NI then there exist a Lyapunov function $V(x, \rho) = \frac{1}{2} x^T P(\rho) x$ such that $\frac{1}{2}\dot{V}(x, \rho) - \dot{y}^T u \leq 0$ holds. This can then be expressed as

$$\frac{1}{2} x^T \left(\dot{P}(\rho) + P(\rho)A(\rho) + A(\rho)^T P(\rho)\right) x + x^T P(\rho)B(\rho)u - x^T A(\rho)^T C^T - u^T B(\rho)^T C^T u,$$

which can also be written as

$$\frac{1}{2} \begin{bmatrix} x \\ u \end{bmatrix}^T \begin{bmatrix} \dot{P}(\rho) + A(\rho)^T P(\rho) + P(\rho)A(\rho) & P(\rho)B(\rho) - A(\rho)^T C^T \\ (P(\rho)B(\rho) - A(\rho)^T C^T)^T & -CB(\rho) - B(\rho)^T C^T \end{bmatrix} \begin{bmatrix} x \\ u \end{bmatrix} \leq 0.$$

Hence, $\begin{bmatrix} \dot{P}(\rho) + A(\rho)^T P(\rho) + P(\rho)A(\rho) & P(\rho)B(\rho) - A(\rho)^T C^T \\ (P(\rho)B(\rho) - A(\rho)^T C^T)^T & -CB(\rho) - B(\rho)^T C^T \end{bmatrix} \leq 0$ since the above is a quadratic function, which shows the equivalence of (a) and (b). Finally, the equivalence between (b) and (c) can easily be established by using Theorem 3. ■

We will now present the LPV OSNI lemma which is a specialized result of LTV OSNI lemma derived in Section 5.2.

Lemma 13. *[60] (**LPV OSNI lemma**) Consider a finite-dimensional, square LPV system* Σ_{LPV}*, as described in* (5.16)*, that satisfies assumptions A1 and A2. Suppose* $CB(\rho) \equiv 0$ *and* $CA(\rho) \not\equiv 0$ *for all admissible* ρ*. Suppose further* $A(\rho_{mean})$ *is Hurwitz. If there exist* $K + 1$ *symmetric matrices* $P_0, P_1, P_2, \cdots, P_K$ *such that* $P(\rho) = P_0 + \rho_1 P_1 + \cdots + \rho_K P_K$ *then the following statements are equivalent*

1. Σ_{LPV} *is LPV OSNI*

2. *$CB(\delta) = 0$ and there exist continuous, bounded matrices $P(\delta) = P(\delta)^T > 0$ and $Q(\delta) = Q(\delta)^T > 0$ such that*

$$\dot{P}(\rho) + A(\rho)^T P(\rho) + P(\rho)A(\rho) < -Q(\rho) < 0 \tag{5.19}$$

$$P(\rho)B(\rho) = A(\rho)^T C^T \tag{5.20}$$

3.

$$P(v)A(v) + A(v)^T P(v) + P(e) - P_0 < 0 \tag{5.21a}$$

$$P(v)B(v) = A(v)^T C^T \qquad \text{and} \tag{5.21b}$$

$$\begin{bmatrix} P_i A_i + A_i^T P_i & P_i B_i \\ B_i^T P_i & 0 \end{bmatrix} \geq 0 \tag{5.21c}$$

$\forall (v, e) \in \mathcal{V} \times \mathcal{C}$ and $\forall i \in \{1, \ldots, K\}$.

Proof. [60] The proof can be done in the same spirit of the proof of Lemma 12 and by following also Lemma 11 subjected to the additional assumptions imposed for LPV OSNI systems. ■

Remark 12. *In terms of numerical implementation of Lemmas 12 and 13, there may be some feasibility issue when enforcing the multiconvexity constraint $P_i A_i + A_i^T P_i \geq 0$. This is due to the fact that in most cases, the parameter ρ_i often appears in $A(\rho)$ sparingly which may lead to an A_i matrix with low rank. Hence, the feasibility set of the $P_0, \cdots, P_K$ matrices might be a null space because $P_i A_i + A_i^T P_i \geq 0$ is not a strict condition.*

However, there is a simple trick to overcome this problem. This can be done by replacing $P_i A_i + A_i^T P_i \geq 0$ with $P_i A_i + A_i^T P_i + \epsilon I \geq 0$ and $P(v)A(v) + A(v)^T P(v) + P(e) - P_0 \leq 0$ with $P(v)A(v) + A(v)^T P(v) + P(e)(\sum_i \epsilon_i v_i^2) I < P_0$, $\forall (v, e) \in \mathcal{V} \times \mathcal{C}$ and some small enough $\epsilon_i > 0$ [11]. The resulting LMIs can now be solved by commercially available SDP solvers without feasibility problem.

Finally, we derive a sufficient condition for ensuring global asymptotic stability of the positive feedback interconnection (Fig. 5.1) comprised of a stable LPV NI system Σ_1 and an LPV OSNI system Σ_2 having minimal state-space realizations $(A_1(\rho_1), B_1(\rho_1), C_1)$ and $(A_2(\rho_2), B_2(\rho_2), C_2)$, respectively, for all $\rho_j = [\rho_{j,1}, \rho_{j,2}, \cdots, \rho_{j,K}] \in \mathbb{R}^K$ with $j \in \{1, 2\}$ where $\rho_{j,i} \in \left[\rho_{(j,i)_{\min}}, \rho_{(j,i)_{\max}}\right]$ and $\dot{\rho}_{j,i} \in \left[\gamma_{(j,i)_{\min}}, \gamma_{(j,i)_{\max}}\right]$ are

known $\forall i \in \{1, 2, \cdots, K\}$. We also define sets of vertices $\mathcal{V}_j = \{(v_{j,1}, v_{j,2}, \cdots, v_{j,K}) : v_{j,i} \in \{\rho_{(j,i)_{\min}}, \rho_{(j,i)_{\max}}\}\ \forall i\}$ with $j \in \{1, 2\}$ corresponding to ρ_1 and ρ_2 and $\mathcal{C}_j = \{(e_{j,1}, e_{j,2}, \cdots, e_{j,K}) : e_{j,i} \in \{\gamma_{(j,i)_{\min}}, \gamma_{(j,i)_{\max}}\}\ \forall i\}$ with $j \in \{1, 2\}$ corresponding to $\dot{\rho}_1$ and $\dot{\rho}_2$.

Theorem 7. *[60] Consider Σ_1 and Σ_2 be two finite-dimensional, square, stable LPV systems, as described in* (5.16)*, that satisfy the assumptions A1 and A2. Let Σ_1 be observable for all admissible ρ_1 and $A_1(\rho_{1_{mean}})$, $A_2(\rho_{2_{mean}})$ be both Hurwitz. Also let $B_2(\rho_2)$ has full column rank, $C_2B_2(\rho_2) \equiv 0$ and $C_2A_2(\rho_2) \not\equiv 0$ for all admissible ρ_2. Assume there exist real, symmetric matrices $P_{1,0}, P_{1,1}, P_{1,2}, \cdots, P_{1,K}$ such that Σ_1 satisfies* (5.18a)–(5.18b) *$\forall (v_1, e_1) \in \mathcal{V}_1 \times \mathcal{C}_1$ and $P_{2,0}, P_{2,1}, P_{2,2}, \cdots, P_{2,K}$ such that Σ_2 satisfies* (5.21a)–(5.21c) *$\forall (v_2, e_2) \in \mathcal{V}_2 \times \mathcal{C}_2$. Then the origin is a globally asymptotically stable equilibrium point of the unforced positive feedback interconnection of Σ_1 and Σ_2 shown in Fig. 5.1 if* $\begin{bmatrix} P_1(v_1) & -C_1^TC_2 \\ -C_2^TC_1 & P_2(v_2) \end{bmatrix} > 0\ \ \forall (v_1, v_2) \in \mathcal{V}_1 \times \mathcal{V}_2$.

Proof. [60] This theorem can be readily established by specializing the proof of Theorem 6 to the interconnection of a stable LPV NI and an LPV OSNI systems upon applying Lemmas 12 and 13 instead of Lemmas 10 and 11. ■

5.5 Case Study

Here, we consider a potential problem of controlling the rectilinear motion of a body with time-varying mass (which prototypes the fuel dynamics of a rocket) being motivated by a similar example taken in [13]. The time-varying mass is expressed by the relation $m(t) = m_0 + m_f\, e^{-\alpha t}$ where $m(t)$ is the total mass of the body, m_f is the initial mass, m_0 is the rest mass and $\alpha > 0$. The equation of motion is given by

$$\Sigma_m : \{m(t)\ddot{q}(t) + (\dot{m}(t) + c + k_2)\,\dot{q}(t) + k_1 q(t) = u(t) \tag{5.22}$$

where the terms $k_1q(t)$ and $c\dot{q}(t)$ are additionally embedded within the system, to be compatible with the LTV NI framework. The parameter $c > 0$ represents the static drag of the body and $k_2 > 0$ is chosen such that $k_2 > \max\limits_{t \geq 0} \left(\frac{1}{2}\alpha m_f e^{-\alpha t} - c\right)$. Now choosing position $q(t) = x_1$ and velocity $\dot{q}(t) = x_2$, the augmented dynamics (5.22) can be represented in the state-space form $\dot{x}(t) = A_1(t)x(t) + B_1(t)u(t)$ and $y(t) = C_1x(t)$

where $A_1(t) = \begin{bmatrix} 0 & 1 \\ \frac{-k_1}{m(t)} & \frac{-(\dot{m}(t)+c+k_2)}{m(t)} \end{bmatrix}$, $B_1(t) = \begin{bmatrix} 0 \\ \frac{1}{m(t)} \end{bmatrix}$, $C_1 = \begin{bmatrix} 1 & 0 \end{bmatrix}$ and $x = [x_1\ x_2]^T$. First, we will show that the augmented dynamics (5.22) satisfies the LTV OSNI property. Consider the Hamiltonian function $H(t,x) = \frac{1}{2}k_1x_1(t)^2 + \frac{1}{2}m(t)x_2(t)^2$ associated with Σ_m. It can be verified that $H(t,x) > 0\ \forall t \in \mathbb{R}_{\geq 0}$ and $H(t_0,0) = 0$ for any $t_0 \geq 0$. The time derivate of $H(t,x)$ is computed as $\dot{H}(t,x) = u(t)x_2 - \frac{1}{2}\dot{m}(t)x_2^2 - cx_2^2 - k_2x_2^2 - k_1x_1x_2 + k_1x_1x_2$. Integrating this with respect to t from 0 to $T \in [0,\infty)$, we have $\int_0^T \left(u(t)x_2 - \frac{1}{2}\dot{m}(t)x_2^2 - cx_2^2 - k_2x_2^2\right) \mathrm{d}t = H(T,x(T)) - H(0,x(0)) \geq \beta\ \forall T \in [0,\infty)$ denoting $\beta = -H(0,x(0)) \in (-\infty, 0]$ and since $H(T,x(T)) \geq 0\ \forall T$. The above expression can be rearranged into

$$\int_0^T y^T u(t)\ \mathrm{d}t \geq \int_0^T \left[\frac{1}{2}\dot{m}(t) + c + k_2\right] \dot{y}(t)^2\ \mathrm{d}t + \beta \tag{5.23}$$

which implies LTV OSNI property via Definition 18 with $\delta = \min_{t\geq 0}\{\frac{1}{2}\dot{m}(t) + c + k_2\} > 0$. Next, we will show that there exists a differentiable and bounded matrix $P_1(t) = P_1(t)^T > 0\ \forall t \in \mathbb{R}_{\geq 0}$ such that Σ_m satisfies Lemma 11. We select $P_1(t) = \begin{bmatrix} P_{11}(t) & P_{12}(t) \\ P_{21}(t) & P_{22}(t) \end{bmatrix} = \begin{bmatrix} k_1 + e^{-t}\frac{1}{\frac{t}{\eta}+a_0} & 0 \\ 0 & m(t) \end{bmatrix}$ where $k_1 \geq 1$, $a_0 > 0$ and $\eta = 2\delta$. It is evident that $P_1(t) = P_1(t)^T > 0$ and $P_1(t)B_1(t) = A_1(t)^TC_1^T$ $\forall t \in \mathbb{R}_{\geq 0}$ since $P_1(t)B_1(t) = \begin{bmatrix} P_{11}(t) & P_{12}(t) \\ P_{12}(t) & P_{22}(t) \end{bmatrix}\begin{bmatrix} 0 \\ \frac{1}{m(t)} \end{bmatrix} = \begin{bmatrix} 0 \\ 1 \end{bmatrix}$ and $A_1(t)^TC_1^T = \begin{bmatrix} 0 & 1 \\ \frac{-k_1}{m(t)} & \frac{-(\dot{m}(t)+c+k_2)}{m(t)} \end{bmatrix}^T \begin{bmatrix} 1 \\ 0 \end{bmatrix} = \begin{bmatrix} 0 \\ 1 \end{bmatrix}$. We then simplify the expression

$$\dot{P}_1(t) + P_1(t)A_1(t) + A_1(t)^TP_1(t) = \begin{bmatrix} \dot{P}_{11}(t) & 0 \\ 0 & \dot{m}(t) \end{bmatrix} + \begin{bmatrix} P_{11}(t) & 0 \\ 0 & m(t) \end{bmatrix}\begin{bmatrix} 0 & 1 \\ \frac{-k_1}{m(t)} & \frac{-(\dot{m}(t)+c+k_2)}{m(t)} \end{bmatrix} + \begin{bmatrix} 0 & 1 \\ \frac{-k_1}{m(t)} & \frac{-(\dot{m}(t)+c+k_2)}{m(t)} \end{bmatrix}^T \begin{bmatrix} P_{11}(t) & 0 \\ 0 & m(t) \end{bmatrix}$$
$$= \begin{bmatrix} \dot{P}_{11}(t) & P_{11}(t) - k_1 \\ P_{11}(t) - k_1 & -\dot{m}(t) - 2(c+k_2) \end{bmatrix}. \tag{5.24}$$

Now on taking Schur complement with respect to the term $-[\dot{m}(t)+2(c+k_2)]$ of (5.24), which remains negative $\forall t \in \mathbb{R}_{\geq 0}$ via choice of k_2, we find that $\dot{P}_{11}(t) + \frac{(P_{11}(t)-k_1)^2}{\dot{m}(t)+2(c+k_2)} = -\frac{e^{-t}}{\frac{t}{\eta}+a_0} - \frac{1}{\eta\left(\frac{t}{\eta}+a_0\right)^2}\left[e^{-t} - e^{-2t}\right] < 0\ \forall t \in \mathbb{R}_{\geq 0}$ since $k_1 \geq 1$, $\eta = 2\delta > 0$, $a_0 > 0$ and

$e^{-t}-e^{-2t} \geq 0\ \forall t \in \mathbb{R}_{\geq 0}$. Therefore, via Schur Complement Lemma, (5.24) is guaranteed to be negative definite $\forall t \in \mathbb{R}_{\geq 0}$ and hence, the augmented dynamics Σ_m is an LTV OSNI system via Lemma 11.

Finally, in order to ensure robust stability of Σ_m, we choose a simple LTI OSNI controller $K(s) = \dfrac{1}{s+1}$ with a minimal state-space realisation $(A_2, B_2, C_2, D_2) = (-1, 1, 1, 0)$. $K(s)$ satisfies Lemma 11 with $P_2 = 1$. We will now check whether Theorem 6 holds in this case or not. Inequality (5.13) holds $\forall t \in \mathbb{R}_{\geq 0}$ since, via Schur Complement Lemma, $P_2 = 1$ and $P_1(t) - C_1^T C_2 P_2^{-1} C_2^T C_1 = \begin{bmatrix} k_1 + \frac{e^{-t}}{\frac{t}{\eta}+a_0} & 0 \\ 0 & m(t) \end{bmatrix} - \begin{bmatrix} 1 & 0 \\ 0 & 0 \end{bmatrix} > 0\ \forall t \in \mathbb{R}_{\geq 0}$ on noting that $m(t) > 0$ and $k_1 + \frac{e^{-t}}{\frac{t}{\eta}+a_0} > 1$ as $k_1 \geq 1$ via design.

Matlab Simulation Results

We choose $m_0 = 1.5$kg, $m_f = 1$kg, $\alpha = 0.1$, $c = 10^{-2}$Ns/m, $k_2 = 0.1$Ns/m and $k_1 = 5$N/m. Fig. 5.3a and Fig. 5.3b show a comparative study of the step response (position and velocity) of the closed-loop dynamics (5.22) in presence of the LTI OSNI controller $K(s) = \frac{1}{s+1}$ [indicated by the Blue curves] and with only unity positive feedback [indicated by the Red curves]. The figures suggest that due to the influence of the controller, the dynamic response has improved to a significant extent compared to that obtained by using only unity feedback (used as an arbitrary baseline for comparison). Fig. 5.2a and Fig. 5.2b depict respectively the phase portraits (x_2 vs. x_1) of the closed-loop dynamics (5.22) in presence of the controller $K(s)$ and with only unity feedback. In Fig. 5.2a, the rate of convergence of the phase trajectory is much faster than shown in Fig. 5.2b. Apart from the phase portrait analysis, we have also analysed the rate of decay of a standard cost function $J = x_1^2 + x_2^2$ evaluated along the closed-loop dynamics (5.22). From Fig. 5.2c and Fig. 5.2d, it is evident that the rate of decay of cost function J in presence of the LTI OSNI controller is much faster than that with only unity positive feedback.

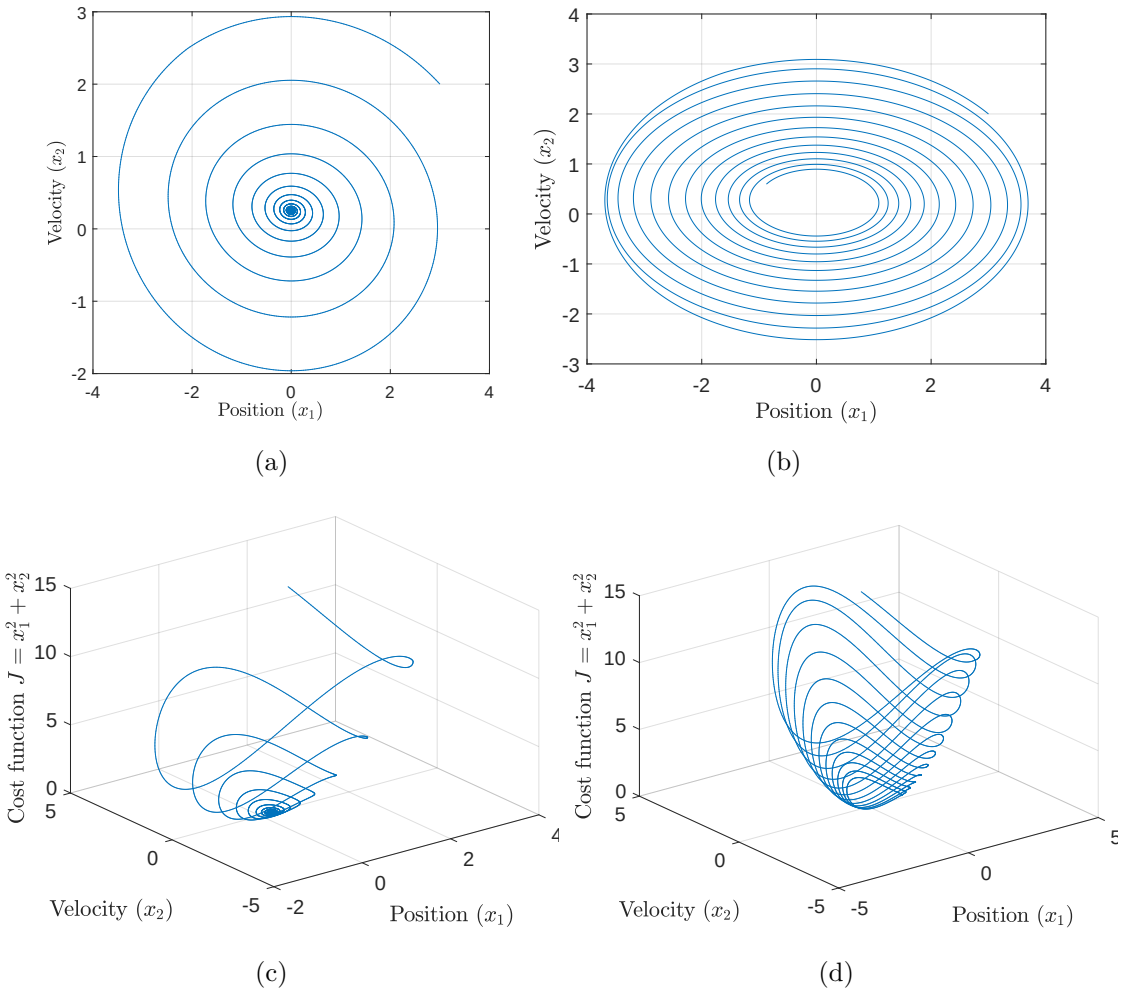

Figure 5.2: Phase portrait (x_2 vs. x_1) of the closed-loop dynamics in presence of (a) the LTI OSNI controller and (b) with only unity feedback. Level curves of the cost function $J = x_1^2 + x_2^2$ evaluated in presence of (c) the LTI OSNI controller and (d) with only unity feedback.

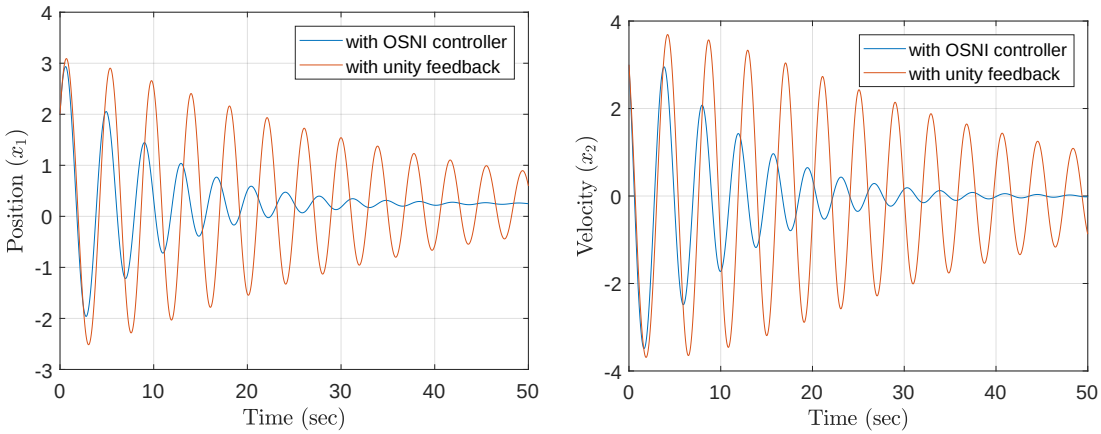

(a) (b)

Figure 5.3: Closed-loop step responses of the body with time-varying mass: (a) Position ($x_1 = q$) and (b) Velocity ($x_2 = \dot{q}$).

5.6 Conclusions

In this chapter, we extended the NI theory to LTV systems. The chapter started with the time domain definition of LTV NI and OSNI systems. These definitions were given with respect to a supply rate using the input and the derivative of the output. The LTV OSNI systems presented are similar to the LTI OSNI systems introduced in [5, 6]. The chapter then addressed the issue of state-space characterization of LTV NI and OSNI systems, which provide DLMI conditions for testing these properties and conditions for global uniform asymptotic stability of LTV NI-OSNI positive feedback interconnection were also presented. Furthermore, the LTV results were specialized to LPV systems, where the state-space characterizations were given in terms of LMIs rather than DLMIs as the former can easily be solved using commercial SDP solver packages. Finally, we considered a numeric example to show the efficacy of the presented results.

Chapter 6

Dynamic Output Feedback Controller Synthesis for Negative Imaginary Systems Using Internal Model Control Principle

All the materials presented in this chapter were submitted for publication in [61].

6.1 Introduction

In this chapter, we focus on the NI synthesis problem where the aim is to synthesis a controller that possess the NI (respectively SNI) property such that it robustly stabilizes an SNI (respectively NI) plant.

For a nominal, stable, minimum phase plants, the IMC design principle provides a simple method for designing robust controller by simply ensuring the Youla parameter is also stable. But this nice property does not extend to uncertain dynamical systems. However, almost all practical systems are uncertain and therefore, this design principle cannot be applied to such systems.

In the literature, it was shown that IRC was an SNI type of controller in [20], without providing a method for obtaining the parameters of the controller. However, in [55], a nonlinear optimization procedure was provided for obtaining the controller

parameters. However, nonlinear optimization is difficult to solve, which makes this design procedure non-appealing.

Due to the aforementioned limitations of the existing NI controller synthesis techniques, this chapter utilises the classical IMC [62, 63] framework to design an appropriate controller for the class of stable and minimum phase NI plants. The IMC scheme shown in Fig. 6.1 has the primary control objective to design a stable $Q(s)$, known as the Youla parameter, such that good nominal performance is achieved and closed-loop stability is maintained even in the presence of a model mismatch [i.e. when $G_m(s) \neq G(s)$]. This chapter proposes a positive feedback IMC scheme (refer to the equivalent block diagram in Fig. 6.3) where the controller $C(s) = Q(s)\Big[I + G_m(s)Q(s)\Big]^{-1}$ is designed to be either a stable NI/SNI/SSNI system depending on the degree of strictness of the NI plant. By combining IMC design principle and the NI theory, we extend the nice robustness property of the IMC design to uncertain, stable and minimum phase NI systems.

A frequency domain approach and a numerically tractable LMI-based technique will be presented for designing the IMC controller. The frequency domain approach seeks to solve a constrained least-square problem, while the LMI-based technique requires choosing a stable polynomial $d(s)$ such that $\frac{1}{d(s)}G_m(s)^{-1}$ becomes strictly proper. We also provide detailed guidelines on how to choose the required polynomial. The LMI-based design technique facilitates easy implementation of the scheme via the Matlab-based SDP solver packages (e.g. CVX, SeDumi, Yalmip) [95]. An in-depth simulation case study (in Section 6.3) on the vibration control problem of a lightweight cantilever beam (inspired by a real-world control problem of a vibration suppressor, as shown in Fig. 6.2) is considered in this chapter to show the usefulness of the NI-based IMC scheme.

Therefore, the major contributions of this chapter can be summarized as follows.

- Provide frequency domain based NI/SNI controller synthesis technique for stable and minimum phase NI systems using the IMC principle by solving a constrained least-square problem.

- Provide an LMI-based SSNI controller synthesis technique for stable and minimum phase NI systems using the IMC principle.

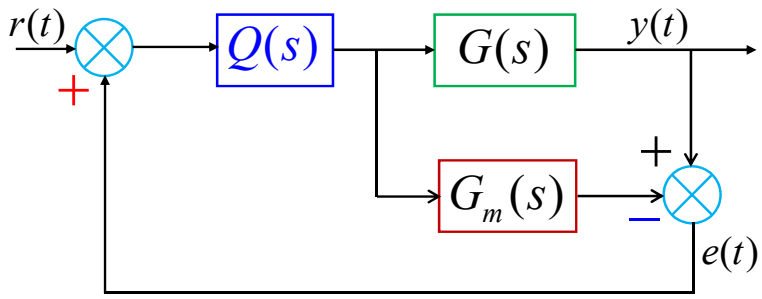

Figure 6.1: Block diagram of the classical IMC scheme.

- Provide guidelines for choosing $d(s)$, which is used as a tuning variable in the LMI synthesis technique to improve the nominal performance.
- Provide a controller synthesis technique that ensures nominal set-pointing tracking in addition to robust stability using the NI framework.

6.1.1 IMC Principle in Brief

The classical IMC scheme has been adopted in this chapter from [62] and is shown in Fig. 6.1. An IMC problem seeks to design a stable $Q(s)$, known as the *Youla parameter* [62], such that the closed-loop scheme shown in Fig. 6.1 has good nominal performance and remains closed-loop stable when $G(s) \neq G_m(s)$. Conventionally, an IMC scheme works with negative feedback. However, in this chapter, we have considered a positive feedback IMC scheme to fit into the NI framework. The performance of an IMC scheme highly relies on the accuracy of the model $G_m(s)$ of the plant $G(s)$ to be controlled. Fig. 6.1 can equivalently be drawn as in Fig. 6.3 where the red-dotted block plays the role of the internal model controller $C(s) = Q(s)\left[I + G_m(s)Q(s)\right]^{-1}$.

The Youla parameter is often designed as $Q(s) = G_m(s)^{-1}F(s)$, where $F(s)$ behaves as a low-pass filter to be determined. The filter dynamics significantly affects shaping the set-pointing tracking or regulatory response of an IMC scheme.

6.1.2 Problem Formulation

Given a stable and minimum phase NI (or SNI) plant $G(s)$ and a reasonably accurate mathematical (or identified) plant model $G_m(s)$ that closely replicates the plant behaviour, design an NI/SNI/SSNI controller $C(s)$ such that the positive feedback IMC

Figure 6.2: A custom-made vibration suppressor developed in the CDR Lab, Control Systems Centre, University of Manchester, for testing the NI controller synthesis algorithms.

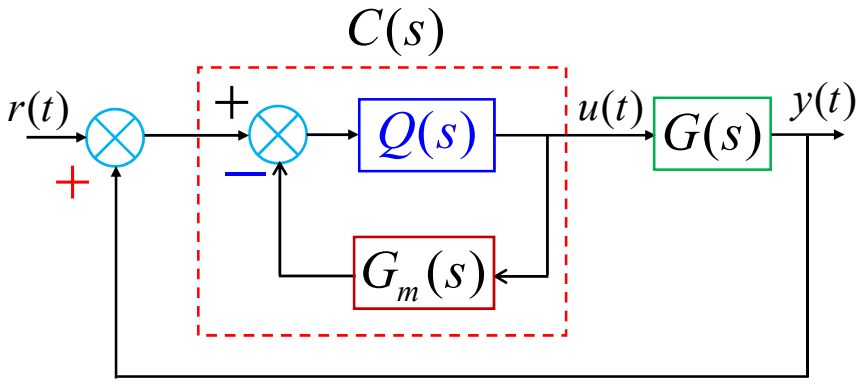

Figure 6.3: Equivalent block diagram of the classical IMC scheme shown in Fig. 6.1.

scheme shown in Fig. 6.3 [which is equivalent to Fig. 6.1] remains robustly stable and facilitates perfect nominal constant reference input tracking.

In the next section, we will present a frequency domain and an LMI-based design methodology for constructing the NI-based IMC controller $C(s)$, as shown in Fig. 6.3, for any stable and minimum phase NI plant $G(s)$ with a known $G(0)$ and having an identified stable NI plant model $G_m(s)$ satisfying $G_m(0) \geq G(0)$.

6.2 Controller Design Methodologies for Stable NI or SNI Systems using the IMC Principle

Our objective is to develop an IMC scheme for SNI or stable NI systems (both SISO and MIMO) utilising the NI property and the closed-loop stability result of an NI-SNI interconnection (Theorem 4). The proposed idea builds on the classical IMC framework

shown in Fig. 6.3 and offers a frequency domain and an LMI-based design methodology to synthesize a stable NI/SNI/SSNI controller $C(s)$ such that the positive feedback closed-loop interconnection of $G(s)$ and $C(s)$ in Fig. 6.3 remains asymptotically stable.

6.2.1 A Frequency Domain Approach for the NI-Based IMC Design

Before we present the frequency domain design technique for synthesizing the controller, we want to recall the standard polynomial factorisation principle in terms of its even and odd terms. A frequency domain polynomial $P(s)$ can be factored as

$$P(s) = \underbrace{P_0 + P_2 s^2 + \dots}_{P_{\text{even}}(s^2)} + s\underbrace{(P_1 + P_3 s^2 + \dots)}_{P_{\text{odd}}(s^2)}$$

such that if $P(j\omega) = P_r(\omega) + jP_i(\omega)$, then $P_r(\omega) = P_{\text{even}}(-\omega^2)$ and $P_i(\omega) = \omega P_{\text{odd}}(-\omega^2)$ for all $\omega \in \mathbb{R}$. Using this factorization, the plant model $G_m(s)$ can be decomposed as $G_m(j\omega) = \dfrac{N_m(j\omega)}{D_m(j\omega)} = \dfrac{N_{mr}(\omega) + jN_{mi}(\omega)}{D_{mr}(\omega) + jD_{mi}(\omega)}$.

The following lemma offers a sufficient-type frequency domain condition involving a scalar parameter $k > 0$ for designing the controller $C(s)$ via the positive feedback IMC scheme shown in Fig. 6.3. It suggests that an SNI (stable NI) controller $C(s) = \dfrac{kD_m(s)}{(s+2k)N_m(s)}$ can stabilise a SISO, minimum phase, stable NI (or SNI) plant $G(s)$ having relative degree 0 or 1. It also facilitates perfect steady state tracking when $G_m(0) = G(0)$, as discussed in Remark 13.

Lemma 14. *[61] Let $G(s)$ be a SISO, minimum phase, stable NI (or SNI) plant with a known $G(0)$ and $G_m(s)$ be a stable NI (or SNI) model of the plant having relative degree 0 or 1 with $G_m(0) > 0$. Let $F(s) = \dfrac{k}{s+k}$, with $k > 0$, be the desired nominal closed-loop transfer function. Then, the controller $C(s) = \dfrac{kD_m(s)}{(s+2k)N_m(s)}$ is SNI (or stable NI) and the positive feedback interconnection between $C(s)$ and $G(s)$, shown in Fig. 6.3, is closed-loop stable if $G_m(0) \geq G(0)$ and*

$$k\omega\Big[D_{mr}(\omega)N_{mr}(\omega) + D_{mi}(\omega)N_{mi}(\omega)\Big] + 2k^2\Big[D_{mr}(\omega) N_{mi}(\omega) - D_{mi}(\omega)N_{mr}(\omega)\Big] > 0 \ \ (\geq 0) \quad \forall \omega \in (0, \infty)\,. \tag{6.1}$$

Furthermore, when $r(\infty)$ exists, $y(\infty) = \dfrac{\left(\frac{G(0)}{G_m(0)}\right)}{2-\left(\frac{G(0)}{G_m(0)}\right)} r(\infty)$, where $y(t)$ and $r(t)$ are the output and reference signals as shown in Fig. 6.3.

Proof. [61] We begin the proof on noting that $G_m(j\omega) = \dfrac{N_m(j\omega)}{D_m(j\omega)} = \dfrac{N_{mr}(\omega) + jN_{mi}(\omega)}{D_{mr}(\omega) + jD_{mi}(\omega)}$. Utilising this decomposition, the proposed controller transfer function $C(s)$ can be expanded as:

$$C(j\omega) = \frac{k\left(D_{mr}(\omega) + jD_{mi}(\omega)\right)}{(j\omega + 2k)\left(N_{mr}(\omega) + jN_{mi}(\omega)\right)}. \tag{6.2}$$

In order to establish the SNI (or stable NI) property of the controller $C(s)$, we expand its imaginary-Hermitian part as follows:

$$\begin{aligned}
&j\left[C(j\omega) - C(j\omega)^*\right] \\
&= j\left[\frac{k\left(D_{mr}(\omega) + jD_{mi}(\omega)\right)}{(j\omega + 2k)(N_{mr}(\omega) + jN_{mi}(\omega))} - \frac{k(D_{mr}(\omega) - jD_{mi}(\omega))}{(-j\omega + 2k)(N_{mr}(\omega) - jN_{mi}(\omega))}\right] \\
&= \frac{\alpha(\omega)}{\beta(\omega)} > 0 \ \ (\geq 0) \quad \forall \omega \in (0, \infty),
\end{aligned}$$

where $\alpha(\omega) = 2k\omega D_{mr}(\omega)N_{mr}(\omega) + 4k^2 D_{mr}(\omega)N_{mi}(\omega) + 2k\omega D_{mi}(\omega)N_m i(\omega) - 4k^2 D_{mi}(\omega)N_{mr}(\omega)$ and $\beta(\omega) = \omega^2 N_{mr}^2(\omega) + \omega^2 N_{mi}^2(\omega) + 4k^2 N_{mr}^2(\omega) + 4k^2 N_{mi}^2(\omega)$.

Now, $\beta(\omega) > 0 \ \ \omega \in (0, \infty)$ since it has all squared terms with positive signs and $\alpha(\omega)$ is restricted to positive (or non-negative) values for all $\omega \in (0, \infty)$ via (6.1). Hence, $C(s)$ is SNI (or stable NI) by construction. Furthermore, since $G_m(0) > 0$, it follows that $C(0) > 0$. Moreover, the proposed controller stabilises the stable NI (or SNI) plant $G(s)$ in a positive feedback loop as the DC loop gain condition is satisfied: $C(0)G(0) \leq C(0)G_m(0) = \frac{kD_m(0)}{2kN_m(0)} \times \frac{N_m(0)}{D_m(0)} = \frac{1}{2} < 1$. In addition, we can easily show that $y(\infty) = \frac{\left(\frac{G(0)}{G_m(0)}\right)}{2 - \left(\frac{G(0)}{G_m(0)}\right)} r(\infty)$ when $r(\infty)$ exists. This completes the proof. ■

The following lemma offers another sufficient-type frequency domain condition involving two scalar parameters k, $b > 0$ for the IMC controller design. Lemma 15 puts forward an SNI (or stable NI) controller having a particular stricture $C(s) = \dfrac{kD_m(s)}{N_m(s)(s^2 + bs + 2k)}$ that can stabilise a SISO, minimum phase, stable NI (or SNI) plant $G(s)$ having relative degree 2. Similar to Lemma 14, it also depends on the identified plant model $G_m(s)$ and facilitates perfect steady state tracking when $G_m(0) = G(0)$ [see Remark 13]. However, to ensure robust stability, it also requires $G_m(0) \geq G(0)$.

Lemma 15. *[61] Let $G(s)$ be a SISO, minimum phase stable NI (or SNI) plant with a known $G(0)$ and $G_m(s)$ be a SISO, stable NI (or SNI) model of the plant having relative degree 2 with $G_m(0) > 0$. Let $F(s) = \dfrac{k}{s^2 + bs + k}$, with k, $b > 0$, be the desired*

closed-loop transfer function. Then, the controller $C(s) = \dfrac{kD_m(s)}{N_m(s)(s^2+bs+2k)}$ *is SNI (or stable NI) and the positive feedback interconnection between* $C(s)$ *and* $G(s)$*, as shown in Fig. 6.3, is closed-loop stable if* $G_m(0) \geq G(0)$ *and*

$$2k^2\Big[D_{mr}(\omega)N_{mi}(\omega) - D_{mi}(\omega)N_{mr}(\omega)\Big] + \omega kb\Big[D_{mr}(\omega)N_{mr}(\omega) + D_{mi}(\omega)N_{mi}(\omega)\Big] + \omega^2 k\Big[D_{mi}(\omega)N_{mr}(\omega) - D_{mr}(\omega)N_{mi}(\omega)\Big] > 0 \ \ (\geq 0) \qquad \forall \omega \in (0,\infty). \tag{6.3}$$

Furthermore, whenever $r(\infty)$ *exists,* $y(\infty) = \dfrac{\left(\frac{G(0)}{G_m(0)}\right)}{2-\left(\frac{G(0)}{G_m(0)}\right)} r(\infty)$*, where* $y(t)$ *and* $r(t)$ *are the output and reference signals as shown in Fig. 6.3.*

Proof. [61] Similar to the proof of Lemma 14, we begin this proof by recalling the transfer function decomposition $G_m(j\omega) = \frac{N_m(j\omega)}{D_m(j\omega)} = \frac{N_{mr}(\omega)+jN_{mi}(\omega)}{D_{mr}(\omega)+jD_{mi}(\omega)}$. The filter has been considered to be $F(s) = \dfrac{k}{s^2+bs+k}$. Then, the controller transfer function can be expressed as:

$$C(j\omega) = \frac{k(D_{mr}(\omega) + jD_{mi}(\omega))}{(N_{mr}(\omega) + jN_{mi}(\omega))(-\omega^2 + j\omega b + 2k)}. \tag{6.4}$$

To show that the proposed controller $C(s)$ satisfies the SNI (or stable NI) property, we proceed as follows:

$$j\left[C(j\omega) - C(j\omega)^*\right] = \frac{\alpha(\omega)}{\beta(\omega)}, \quad \text{where}$$

$$\alpha(\omega) = 4k^2(D_{mr}(\omega)N_{mi}(\omega) - D_{mi}(\omega)N_{mr}(\omega)) + 2\omega kb(D_{mr}(\omega)N_{mr}(\omega) + D_{mi}(\omega)N_{mi}(\omega)) + 2\omega^2 k(D_{mi}(\omega)N_{mr}(\omega) - D_{mr}(\omega)N_{mi}(\omega)) \quad \text{and}$$

$$\beta(\omega) = \omega^2 b^2 N_{mr}^2(\omega) + (\omega^2 N_{mr}(\omega) - 2kN_{mr}(\omega))^2 + \omega^2 b^2 N_{mi}^2(\omega) + (\omega^2 N_{mi}(\omega) - 2kN_{mi}(\omega))^2$$

Now, $\beta(\omega) > 0 \ \forall\, \omega \in (0,\infty)$ has all squared terms with positive signs and $\alpha(\omega)$ is restricted to be positive (or non-negative) values for all $\omega \in (0,\infty)$ via (6.3). Hence, $C(s)$ is SNI (or stable NI) via design with $C(0) > 0$ as $G_m(0) > 0$. $C(s)$ also stabilises the stable NI (or SNI) plant $G(s)$ in a positive feedback loop satisfying the DC loop gain condition $C(0)G(0) \leq C(0)G_m(0) = \frac{kD_m(0)}{2kN_m(0)} \times \frac{N_m(0)}{D_m(0)} = \frac{1}{2} < 1$. It can also be readily shown that $y(\infty) = \dfrac{\left(\frac{G(0)}{G_m(0)}\right)}{2-\left(\frac{G(0)}{G_m(0)}\right)} r(\infty)$ when $r(\infty)$ exists. This completes the proof. ■

Remark 13. *It can be readily shown that a SISO IMC controller $C(s)$ synthesized via Lemma 14 or Lemma 15 achieves perfect nominal steady state reference input tracking even in the case of a model mismatch as long as the DC gains of the plant and its model remain the same [i.e. $G(0) = G_m(0)$]. This is an advantage of the proposed scheme because in practice, it is nearly impossible to identify a perfect model of the plant, however, the DC gain of the plant can be measured with a high degree of accuracy. From Fig. 6.3, the closed-loop transfer function $T(s)$ from the reference input $R(s)$ to the output $Y(s)$ is given by $T(s) = \frac{G(s)C(s)}{1-G(s)C(s)}$, where $C(s) = \frac{Q(s)}{1+G_m(s)Q(s)}$ and $Q(s) = G_m(s)^{-1}F(s)$. Hence, $T(0) = \frac{G(0)G_m(0)^{-1}F(0)}{[1+F(0)-G(0)G_m(0)^{-1}F(0)]} = 1$ on noting that $G_m(0) = G(0)$.*

Remark 14. *The frequency domain approach offers complete freedom in choosing the filter dynamics $F(s)$ by solving a simple constrained least-square estimation problem. As the closed-loop response $y(t)$ of the IMC scheme (Fig. 6.3) subjected to $r(t)$ is mainly governed by the filter, the frequency domain approach can be conveniently used to design an IMC controller satisfying the desired transient performance criteria. However, this method may not be effective for higher-order or MIMO systems since the procedure involves a lengthy hand-driven calculation. These calculations arise in setting up the constrained least-square estimation problem which is used to ensure that $\alpha(\omega)$ is positive or non-negative $\forall\, \omega \in (0, \infty)$ depending on the controller to be synthesized.*

6.2.2 An LMI-Based Approach for the NI-Based IMC Design

Here, we present the LMI-based synthesis technique.

Theorem 8. *[61] Let $G(s) \in \mathcal{RH}_\infty^{m\times m}$ be a minimum phase NI plant and $G_m(s) \in \mathcal{RH}_\infty^{m\times m}$ be a minimum phase NI-model of the plant with $G_m(0) \geq 0$. Choose a stable polynomial $d(s)$ such that $H(s) = \frac{1}{d(s)}G_m(s)^{-1}$ is strictly proper. Let $H(s)$ have a minimal state-space realisation $\left[\begin{array}{c|c} A_H & B_H \\ \hline C_H & 0 \end{array}\right]$ with a full-rank C_H matrix. Suppose there exists real matrices $\bar{A}$, $\bar{B}$, $\bar{C}$, $\bar{D}$, $Y = Y^\top$ and $X = X^\top$ of appropriate dimensions*

such that

$$\begin{bmatrix} \Phi_{11} & \left(\bar{A}^\top + A_H\right) \\ \left(\bar{A}^\top + A_H\right)^\top & \Phi_{22} \end{bmatrix} < 0, \tag{6.5a}$$

$$\begin{bmatrix} \Phi_{13} \\ \bar{B} + \bar{A}C_H^\top \end{bmatrix} = 0, \tag{6.5b}$$

$$\begin{bmatrix} \Phi_{11} & \left(\bar{A}^\top + A_H\right) & YC_H^\top \\ \left(\bar{A}^\top + A_H\right)^\top & \Phi_{22} & C_H^\top \\ C_HY & C_H & -I_m \end{bmatrix} \leq 0, \tag{6.5c}$$

$$\begin{bmatrix} Y & I_n \\ I_n & X \end{bmatrix} > 0 \qquad \text{and} \tag{6.5d}$$

$$G_m(0)^{\frac{1}{2}}\left[C_HYC_H^\top\right]G_m(0)^{\frac{1}{2}} < I_m, \tag{6.5e}$$

where the following shorthand

$$\begin{cases} \Phi_{11} = A_HY + YA_H^\top + B_H\bar{C} + \bar{C}^\top B_H^\top, \\ \Phi_{13} = B_H\bar{D} + A_HYC_H^\top + B_H\bar{C}C_H^\top, \\ \Phi_{22} = XA_H + A_H^\top X, \end{cases} \tag{6.6}$$

has been used in (6.5a)-(6.5c).

Construct an auxiliary system $\Sigma(s)$ *as* $\Sigma(s) = D_\Sigma + C_\Sigma\left(sI - A_\Sigma\right)^{-1}B_\Sigma$ *where*

$$\begin{cases} D_\Sigma = \bar{D}, \\ C_\Sigma = \bar{C}N^{-\top}, \\ B_\Sigma = M^{-1}(\bar{B} - XB_H\bar{D}), \\ A_\Sigma = M^{-1}\left(\bar{A} - XA_HY - XB_H\bar{C}\right)N^{-\top}, \end{cases} \tag{6.7}$$

and M *and* N *are square and non-singular solutions of the algebraic equation* $NM^\top = I_n - YX$*. Then, the controller* $C(s) = H(s)\Sigma(s)$ *is SSNI and robustly stabilises* $G(s)$ *when* $G(0) \leq G_m(0)$*.*

Proof. [61] We begin the proof on noting that $C(s) = Q(s)\left[I + G_m(s)Q(s)\right]^{-1}$ in the proposed IMC scheme shown in Fig. 6.1, where the Youla parameter matrix $Q(s)$ is parametrised as $Q(s) = G_m(s)^{-1}F(s)$. $F(s)$ plays the role of a low-pass filter, which is to be determined. The proof proceeds through the following nine steps.

Step 1: We choose a stable polynomial $d(s)$ such that $\frac{1}{d(s)}G_m(s)^{-1}$ is strictly proper. Accordingly, $Q(s) = G_m(s)^{-1}F(s)$ is modified to $Q(s) = \frac{1}{d(s)}G_m(s)^{-1}\bar{F}(s)$ where $F(s) = \frac{1}{d(s)}\bar{F}(s)$. Now, $\bar{F}(s)$ is to be determined instead of $F(s)$. Denote $H(s) = \frac{1}{d(s)}G_m(s)^{-1}$ and let $H(s)$ have a minimal state-space realisation $\left[\begin{array}{c|c} A_H & B_H \\ \hline C_H & 0 \end{array}\right]$.

Step 2: We then obtain the expression of the controller $C(s) = Q(s)\Big[I+G_m(s)Q(s)\Big]^{-1} = H(s)\left(\bar{F}(s)\Big[I+F(s)\Big]^{-1}\right)$ substituting $Q(s) = H(s)\bar{F}(s)$. Denote $\Sigma(s) = \bar{F}(s)\Big[I + F(s)\Big]^{-1}$ and let $\Sigma(s)$ have a minimal state-space realisation $\left[\begin{array}{c|c} A_\Sigma & B_\Sigma \\ \hline C_\Sigma & D_\Sigma \end{array}\right]$. After that, we derive the state-space representation of the controller $C(s) = H(s)\Sigma(s)$ as

$$\left[\begin{array}{c|c} A_c & B_c \\ \hline C_c & D_c \end{array}\right] = \left[\begin{array}{cc|c} A_H & B_HC_\Sigma & B_HD_\Sigma \\ 0 & A_\Sigma & B_\Sigma \\ \hline C_H & 0 & 0 \end{array}\right].$$

Step 3: Now, $C(s) = \left[\begin{array}{c|c} A_c & B_c \\ \hline C_c & D_c \end{array}\right]$ is SSNI if (A_c, C_c) is observable and there exists $\mathcal{Y} = \mathcal{Y}^\top > 0$ such that

$$\begin{cases} A_c\mathcal{Y} + \mathcal{Y}A_c^\top < 0 & \text{and} \\ B_c + A_c\mathcal{Y}C_c^\top = 0 \end{cases} \tag{6.8}$$

via Lemma 8.

Since the conditions (6.8) are not in an LMI form due to the presence of the terms containing products of the unknown controller variables, a linearising change in the controller variables is required to transform (6.8) into an LMI form.

Step 4: We partition, as in [73], the closed-loop Lyapunov matrix $\mathcal{Y}$ and $\mathcal{Y}^{-1}$ as follow:

$$\mathcal{Y} = \begin{pmatrix} Y & N \\ N^\top & \bullet \end{pmatrix} \quad \text{and} \quad \mathcal{Y}^{-1} = \begin{pmatrix} X & M \\ M^\top & \bullet \end{pmatrix}, \tag{6.9}$$

where $Y = Y^\top \in \mathbb{R}^{n\times n}$ and $X = X^\top \in \mathbb{R}^{n\times n}$ and the symbol $\bullet$ represents the matrices that are not explicitly used in the linearisation process. Note $\mathcal{Y}^{-1}$ exists since $\mathcal{Y} > 0$ via (6.5d), which has been explained subsequently in Step 5. Note also that X, Y, M, N are not independent LMI variables but must satisfy $NM^\top = I_n - YX$ (see [73] for

details). Since M and N are square and non-singular, the following block matrices

$$\Pi_1 = \begin{pmatrix} I_n & X \\ 0 & M^\top \end{pmatrix} \quad \text{and} \quad \Pi_2 = \begin{pmatrix} Y & I_n \\ N^\top & 0 \end{pmatrix} \tag{6.10}$$

are also non-singular. Π_1 and Π_2 are related through the expression

$$\mathcal{Y}\Pi_1 = \Pi_2, \tag{6.11}$$

which has been obtained from the fundamental relationship $\mathcal{Y}\mathcal{Y}^{-1} = I$.

Step 5: The positive definiteness of the Lyapunov candidate matrix $\mathcal{Y} = \begin{pmatrix} Y & N \\ N^\top & \bullet \end{pmatrix}$ is guaranteed by (6.5d) via the congruence transformation, as shown below:

$$\Pi_1^\top \mathcal{Y} \Pi_1 = \begin{pmatrix} Y & I_n \\ I_n & X \end{pmatrix} > 0. \tag{6.12}$$

Step 6: Applying an appropriate congruence transformation on (6.8) with the help of the block diagonal matrix $\text{diag}\{\Pi_1, I\}$, we get

$$\begin{cases} \Pi_1^\top \left(A_c\mathcal{Y} + \mathcal{Y}A_c^\top \right) \Pi_1 < 0, \\ \Pi_1^\top \left(B_c + A_c\mathcal{Y}C_c^\top \right) = 0; \end{cases} \tag{6.13}$$

and then, inserting a new set of LMI variables

$$\begin{cases} \bar{A} = MA_\Sigma N^\top + XA_H Y + XB_H C_\Sigma N^\top, \\ \bar{B} = MB_\Sigma + XB_H D_\Sigma, \\ \bar{C} = C_\Sigma N^\top, \\ \bar{D} = D_\Sigma; \end{cases} \tag{6.14}$$

into (6.13), we obtain $\begin{bmatrix} \Phi_{11} & \left(\bar{A}^\top + A_H\right) \\ \left(\bar{A}^\top + A_H\right)^\top & \Phi_{22} \end{bmatrix} < 0$ and $\begin{bmatrix} \Phi_{13} \\ \bar{B} + \bar{A}C_H^\top \end{bmatrix} = 0$. These two conditions are linear in $\bar{A}$, $\bar{B}$, $\bar{C}$, $\bar{D}$, $Y > 0$, $X > 0$ and they are indeed the same as (6.5a) and (6.5b).

Step 7: The pair (A_c, C_c) is observable via (6.5c) since the associated Observability Gramian [12] condition $\mathcal{P}A_c + A_c^\top\mathcal{P} + C_c^\top C_c \leq 0 \Leftrightarrow A_c\mathcal{Y} + \mathcal{Y}A_c^\top + \mathcal{Y}C_c^\top C_c\mathcal{Y} \leq 0$, where $\mathcal{Y} = \mathcal{P}^{-1} > 0$, is equivalent to (6.5c) via a congruence transformation with respect to $\text{diag}\{\Pi_1, I_m\}$ and taking a Schur complement [12]. Note also that the

matrix $C_c = \begin{bmatrix} C_H & 0 \end{bmatrix}$ has full row-rank since rank$[C_H] = m$ via assumption. This implies from the expression $B_c + A_c \mathcal{Y} C_c^\top = 0$ that B_c has full column-rank, since $\mathcal{Y} > 0$ and A_c is Hurwitz via (6.5a). Hence, the LMI conditions (6.5a)–(6.5d) jointly ensure that $C(s)$ is SSNI (via Lemma 8).

Step 8: Reconstruct the auxiliary filter $\Sigma(s) = D_\Sigma + C_\Sigma\Big(sI - A_\Sigma\Big)^{-1} B_\Sigma$ via

$$\begin{cases} D_\Sigma = \bar{D}, \\ C_\Sigma = \bar{C} N^{-\top}, \\ B_\Sigma = M^{-1}(\bar{B} - X B_H \bar{D}), \\ A_\Sigma = M^{-1}\Big(\bar{A} - X A_H Y - X B_H \bar{C}\Big) N^{-\top}, \end{cases}$$

where M and N are square and non-singular solutions of the algebraic equation $NM^\top = I_n - YX$. From the knowledge of $\Sigma(s)$, retrieve the filter $F(s)$ relying on the relationship $F(s) = \frac{1}{d(s)}\Sigma(s)\left[I - \frac{1}{d(s)}\Sigma(s)\right]^{-1}$. Finally, we also construct the Youla parameter $Q(s) = G_m(s)^{-1} F(s)$ and the desired controller $C(s) = Q(s)\Big[I + G_m(s)Q(s)\Big]^{-1} = H(s)\Sigma(s) = \frac{1}{d(s)} G_m(s)^{-1}\Sigma(s)$.

Step 9: The inequality condition (6.5e) is equivalent to $G_m(0)^{\frac{1}{2}} C(0) G_m(0)^{\frac{1}{2}} < I$ since $C(0) = C_c \mathcal{Y} C_c^\top = C_H Y C_H^\top$. This, in turn, is equivalent to $\lambda_{\max}[C(0)G_m(0)] < 1$ via [15]. As $G_m(0) \geq G(0)$ via assumption and $C(0) \geq 0$ via construction, the preceding condition implies $\lambda_{\max}[C(0)G(0)] < 1$. Therefore, the positive feedback interconnection (in Fig. 6.3) of $C(s)$, being SSNI, and $G(s)$, being a stable and minimum phase NI system, satisfies all the assumptions of Theorem 4, as well as the DC loop gain condition. Hence, the interconnection is robustly stable. This completes the proof. ■

Remark 15. *Unlike the frequency domain approach, the LMI-based approach can efficiently handle higher-order and MIMO systems. However, in the LMI approach, the filter F(s) is not explicitly selected by the designer. It is reconstructed from the variables obtained from the solution of the LMIs. Therefore, we cannot guarantee the fulfilment of all desired closed-loop performance criteria "a priori" via this approach. In this situation, the choice of the stable polynomial $d(s)$ becomes crucial as it is the only design parameter that can be selected "a priori" to achieve a desired closed-loop response.*

Remark 16. *A necessary and sufficient condition for the stability of an IMC scheme*

where the open-loop system $G(s)$ is stable is that the Youla parameter $Q(s)$ must be stable. In the proposed NI-based IMC scheme in Fig. 6.3, $Q(s) = C(s)\left[I - G_m(s)C(s)\right]^{-1}$, which is a positive feedback interconnection between $C(s)$ and $G_m(s)$, can be readily shown to be stable. Since $G_m(s)$ is stable NI and $C(s)$ is designed to be SNI/SSNI (either via the frequency domain approach or via the LMI-based methodology) satisfying the condition $\lambda_{\max}[C(0)G_m(0)] < 1$, Theorem 8 guarantees the internal stability of the NI-based IMC scheme in Fig. 6.3, which, in turn, implies the stability of $Q(s)$.

6.2.3 Set-Pointing Tracking Performance of the LMI-Based (NI) IMC Scheme

The following lemma shows that under a reasonable and practically feasible assumption $G_m(0) = G(0)$, perfect steady state reference input tracking can be achieved by the proposed scheme if the inequality condition (6.5e) is replaced by the equality condition $G_m(0)^{\frac{1}{2}} C_H Y C_H^\top G_m(0)^{\frac{1}{2}} = \frac{1}{2} I$, keeping (6.5a)–(6.5d) intact.

Lemma 16. *[61] Let $G(s) \in \mathcal{RH}_\infty^{m\times m}$ be a minimum phase NI plant with a known $G(0)$. Suppose $G_m(0) = G(0) > 0$. Then, the NI-based IMC scheme, developed in Theorem 8, achieves perfect set-point tracking (i.e. $\lim_{t\to\infty}\Big[-r(t) + y(t)\Big] = 0$) for a constant reference signal $r(t)$ if the condition* (6.5e) *in Theorem 8 is modified to $G_m(0)^{\frac{1}{2}}\left[C_H Y C_H^\top\right] G_m(0)^{\frac{1}{2}} = \frac{1}{2} I_m$.*

Proof. [61] The closed-loop transfer function matrix from the reference input r to the output y of the IMC scheme, shown in Fig. 6.3, is given by $T(s) = G(s)C(s)\Big[I - G(s)C(s)\Big]^{-1}$. Now, substituting the expression $C(s) = G_m(s)^{-1}F(s)\Big[I + F(s)\Big]^{-1}$ and upon simplifying, we get $T(s) = G(s)G_m(s)^{-1}F(s)\Big[I + F(s) - G(s)G_m(s)^{-1}F(s)\Big]^{-1}$. This readily implies $T(0) = F(0)$ when $G_m(0) = G(0)$. Also, $G_m(0)^{\frac{1}{2}}\left[C_H Y C_H^\top\right] G_m(0)^{\frac{1}{2}} = \frac{1}{2} I_m \Leftrightarrow G_m(0)^{\frac{1}{2}} C(0)\ G_m(0)^{\frac{1}{2}} = \frac{1}{2} I_m \Leftrightarrow G_m(0)^{-1}F(0)\Big[I + F(0)\Big]^{-1} = \frac{1}{2} G_m(0)^{-1} \Rightarrow F(0) = I$. This hence ensures that $y_{ss} = \lim_{t\to\infty} y(t) = \lim_{s\to 0} sY(s) = \lim_{s\to 0} sT(s)R(s) = \lim_{s\to 0} sF(s)\ R(s) = F(0)\lim_{s\to 0} sR(s) = r_{ss}$, since $F(0) = I$ and on noting that $\lim_{s\to 0} sR(s) = r_{ss}$ is constant. ■

Remark 17. *Lemma 16 proves that the NI-based IMC scheme proposed via Theorem 8 facilitates perfect steady state reference tracking when $r(\infty)$ exists despite a model*

mismatch [i.e. when $G_m(s) = G(s)$] as long as $G_m(0) = G(0)$. This is not an overly restrictive assumption because, in practice, it is possible to measure the steady state gain (i.e. the DC gain) of a plant accurately. In that case, it is also possible to identify a reasonably accurate plant model $G_m(s)$ having the same DC gain as that of the real plant. However, the robust stability of the IMC scheme (in Fig. 6.3) remains unaffected in the presence of a model mismatch as long as $G(0) \leq G_m(0)$ since the closed-loop stability depends only the DC loop gain condition $\lambda_{\max}[C(0)G(0)] < 1$, as established in Theorem 8.

6.2.4 Guidelines on How to Choose the Polynomial $d(s)$

The choice of the stable polynomial $d(s)$ that we suggest in the proposed IMC design methodology is based on empirical analysis rather than a theoretical analysis. We have considered four different models $G_{m_1}(s)$, $G_{m_2}(s)$, $G_{m_3}(s)$ and $G_{m_4}(s)$ of a cantilever beam conforming with the practical setup shown in Fig. 6.2. The first model considered is a second-order system $G_{m_1}(s) = \frac{1}{s^2+0.2s+1}$, which has its resonant mode at $\omega = 1$ rad/s. The next model we consider is still a second-order system $G_{m_2}(s) = \frac{13}{s^2+0.1s+358}$, but it has a higher resonant frequency $\omega = 19$ rad/s. Next, we consider a fourth-order model $G_{m_3}(s) = \frac{1}{s^2+0.2s+2} + \frac{4}{s^2+0.23s+9}$ having two resonant modes at $\omega = 1.41$ rad/s and $\omega = 3$ rad/s respectively. Finally, we consider a sixth-order model $G_{m_4}(s) = \frac{1}{s^2+0.2s+2} + \frac{4}{s^2+0.23s+9} + \frac{7}{s^2+0.15s+13}$ having three resonant modes at $\omega = \{1.37,\ 2.93,\ 3.6\}$ rad/s respectively.

For each plant model, we have chosen thirty different $d(s)$ candidates as mentioned in Tables A.1–A.4 [Appendix A] and then found thirty controller transfer functions $\{C_1(s),\, C_2(s),\, \cdots, C_{30}(s)\}$ for each model $G_{m_j}(s)\ \forall j \in \{1, 2, 3, 4\}$ subject to $\{d_1(s),\, d_2(s), \cdots, d_{30}(s)\}$, using the LMI-based design algorithm. Fig. 6.4a, Fig. 6.5a, Fig. 6.6a and Fig. 6.7a show the Bode plots of the closed-loop transfer functions $\{T_1(s),\, T_2(s),\, \cdots, T_{30}(s)\}$ computed for each of the thirty $C_i(s)\ \forall i \in \{1, 2, \ldots, 30\}$ obtained for each plant model $G_{m_j}(s)$. Similarly, Fig. 6.4b, Fig. 6.5b, Fig. 6.6b and Fig. 6.7b show the impulse responses of the closed-loop systems $T_i(s)\ \forall i \in \{1, 2, \ldots, 30\}$ as mentioned before. The choice of each set of polynomials $\{d_1(s),\, d_2(s), \cdots, d_{30}(s)\}$ depends primarily on the resonant modes of the plant model and they are constructed such that some of the roots are real and slower, some of them are real and faster and

the rest are complex. This wide range of test cases and their comparative study with respect to the time domain performance criteria (e.g. peak overshoot, settling time, bandwidth, etc.) help us to suggest useful guidelines for selecting an effective $d(s)$ for a given plant model.

The following summarize our findings on the effect of $d(s)$ on the performance of the closed-loop response.

- **Bandwidth:** A leftward-shift of the negative real roots of $d(s)$ or an increase in the natural frequency of complex roots increases the bandwidth of the closed-loop system;
- **Settling time:** A leftward-shift of the roots of $d(s)$ decreases the settling time of the step (or impulse) response. However, a substantial left-shift may also increase the settling time as the closed-loop system becomes more oscillatory. On the other hand, changing the imaginary parts of the complex roots of $d(s)$ whilst keeping the real parts unchanged does not have any significant impact on the settling time;
- **Peak overshoot:** A leftward-shift of the negative real roots of $d(s)$ or an increase in the natural frequency of complex roots increases the speed of the step and impulse responses, but at the cost of an higher peak overshoot;
- **Fastest controller pole:** A leftward-shift of the real or complex roots of $d(s)$ drives the controller poles to be faster. However, this causes an increase in the control input demand.

Let the notation $\mathbb{D}\Big[G_m(s)\Big]$ be $G_m(s)^{-1}$. From the extensive simulation studies shown in Fig. 6.4a–6.7a and Fig. 6.4b–6.7b and Tables A.1–A.4, we observe that a choice of $d(s) = (s+a)\mathbb{D}\Big[G_m(s)\Big]$, where the parameter a is selected as the frequency of the first resonant mode of $G_m(s)$, offers an acceptable trade-off between the speed of response and the settling time. It also does not result in controller poles that are too fast, which inevitably demands higher control effort. However, this choice may increase the peak of the impulse response. In applications where a reduction in the peak overshoot is preferable over the other time domain performance criteria, one could choose the real root $s = -a$ of $d(s)$ at one or two decade(s) of frequency below the first resonant mode of $G_m(s)$.

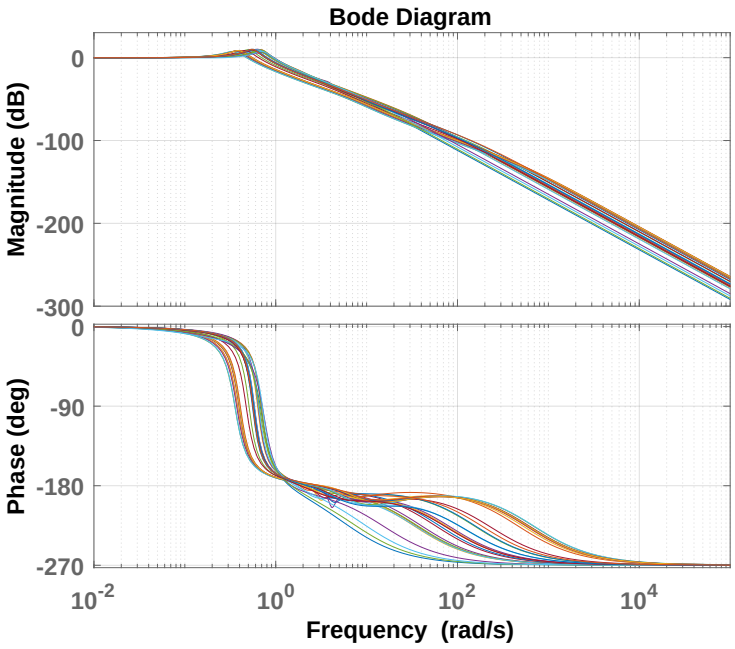

(a)

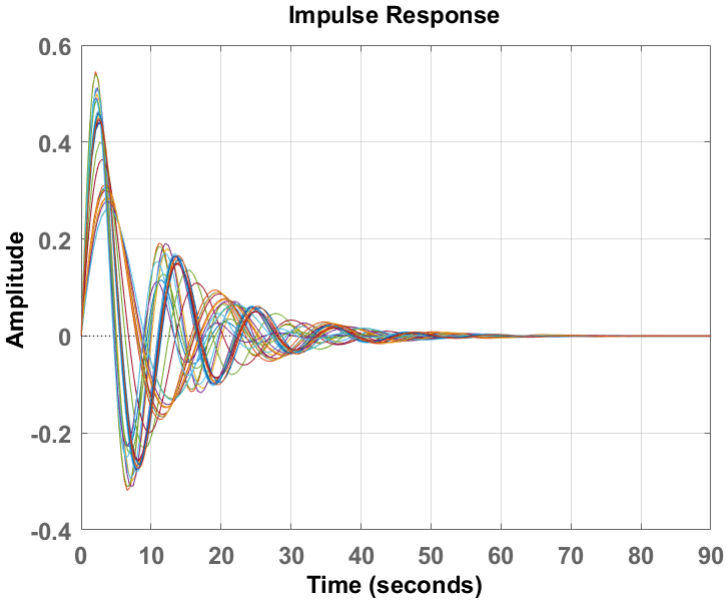

(b)

Figure 6.4: (a) Bode plots of the closed-loop transfer function $T_i(s) = \frac{G_{m_1}(s)C_i(s)}{1-G_{m_1}(s)C_i(s)}$ $\forall i \in \{1, 2, \ldots, 30\}$ corresponding to $\{d_1(s), d_2(s), \cdots, d_{30}(s)\}$ as mentioned in Table A.1; (b) Impulse responses of $T_i(s)$ for all i.

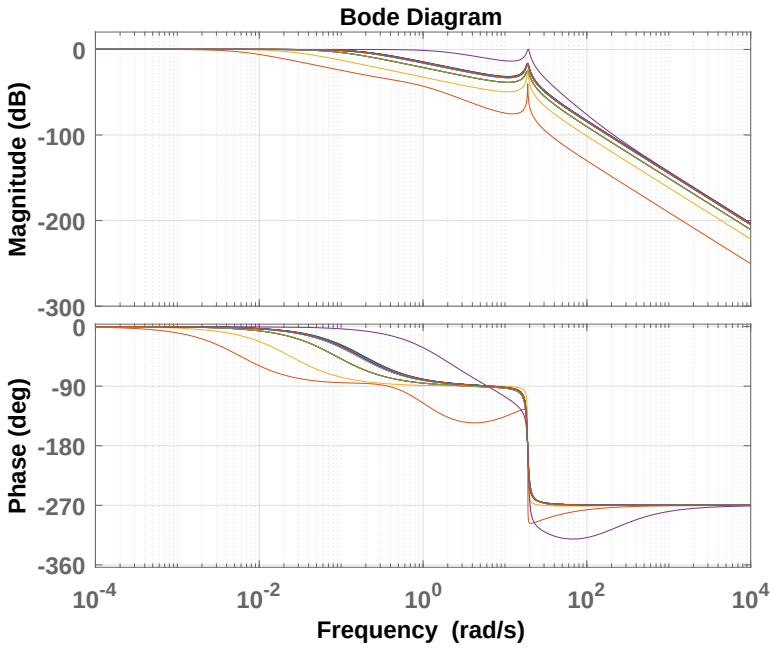

(a)

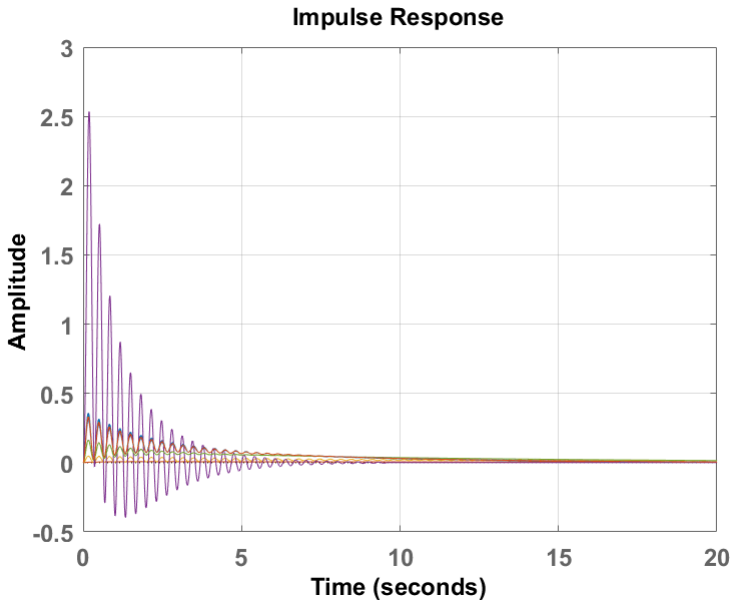

(b)

Figure 6.5: (a) Bode plots of the closed-loop transfer function $T_i(s) = \frac{G_{m_2}(s)C_i(s)}{1-G_{m_2}(s)C_i(s)}$ $\forall i \in \{1, 2, \ldots, 30\}$ corresponding to $\{d_1(s), d_2(s), \cdots, d_{30}(s)\}$ as mentioned in Table A.2; (b) Impulse responses of $T_i(s)$ for all i.

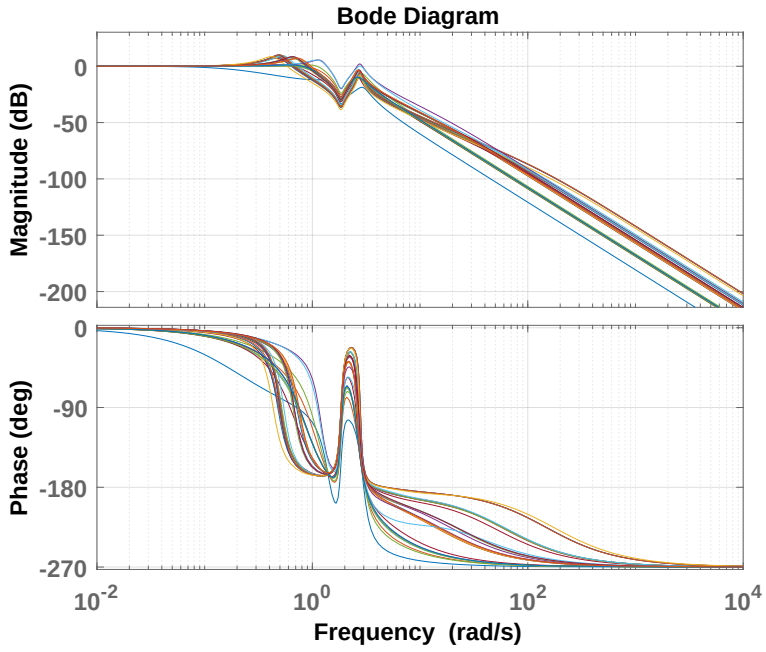

(a)

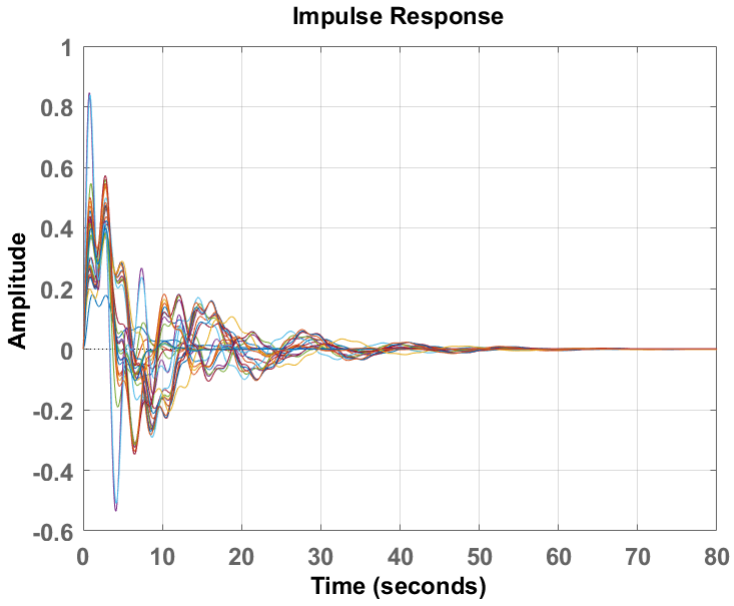

(b)

Figure 6.6: (a) Bode plots of the closed-loop transfer function $T_i(s) = \frac{G_{m_3}(s)C_i(s)}{1-G_{m_3}(s)C_i(s)}$ $\forall i \in \{1, 2, \ldots, 30\}$ corresponding to $\{d_1(s), d_2(s), \cdots, d_{30}(s)\}$ as mentioned in Table A.3; (b) Impulse responses of $T_i(s)$ for all i.

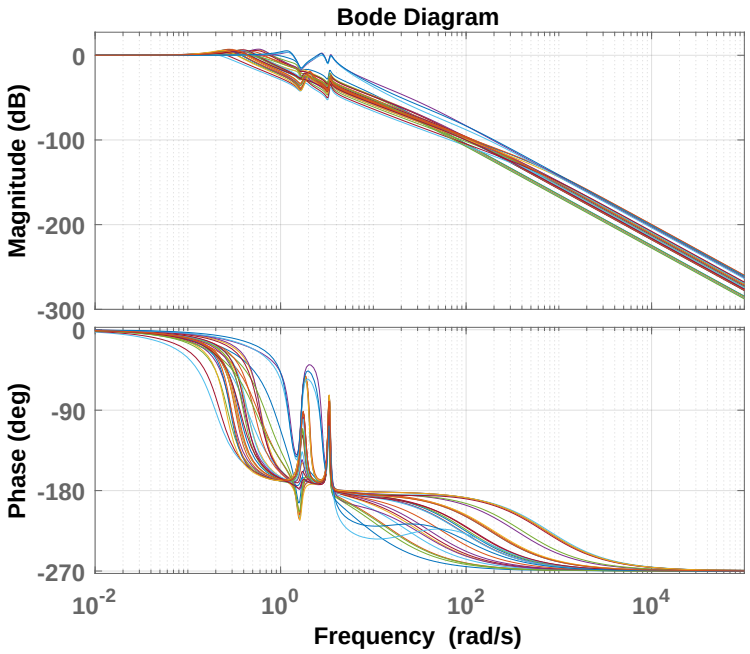

(a)

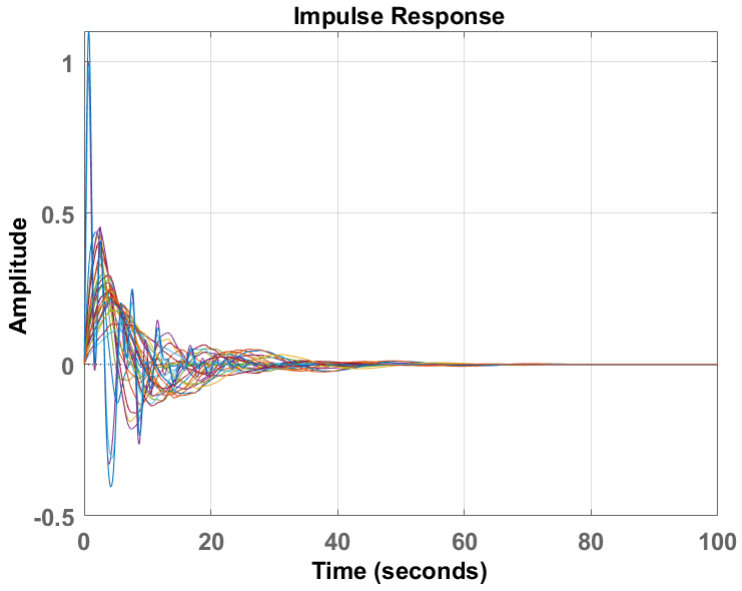

(b)

Figure 6.7: (a) Bode plots of the closed-loop transfer function $T_i(s) = \frac{G_{m_4}(s)C_i(s)}{1-G_{m_4}(s)C_i(s)}$ $\forall i \in \{1, 2, \ldots, 30\}$ corresponding to $\{d_1(s), d_2(s), \cdots, d_{30}(s)\}$ as mentioned in Table A.4; (b) Impulse responses of $T_i(s)$ for all i.

Remark 18. *The choice of* $d(s) = (s+a)\mathbb{D}\big[G_m(s)\big]$ *introduces the inverse dynamics of the model* $G_m(s)$ *into the closed-loop system. If the plant model has poorly damped zeros, we can instead choose* $d(s) = (s+a)^p$*, where the parameter* a *is selected as the frequency of the first resonant mode of* $G_m(s)$ *and* $p \geq (n-m)+1$ *such that* $\frac{1}{d(s)}G_m(s)^{-1}$ *becomes strictly proper (preferably with relative degree equals one). This choice of* $d(s)$ *results in a reduced overshoot of the closed-loop step/impulse response, but at the cost of compromising the speed.*

6.3 Simulation Case Study

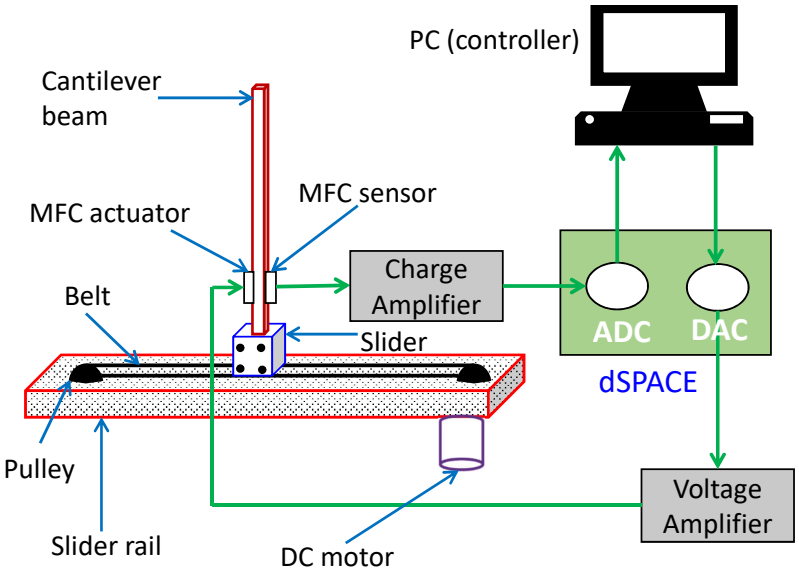

Figure 6.8: Schematic diagram of the proposed closed-loop control for the vibration suppressor using dSPACE platform.

This section will apply the proposed NI-based IMC scheme for the vibration control of a lightweight cantilever beam attached to a fixed end. The schematic diagram of the closed-loop control set-up of the vibration suppressor is shown in Fig. 6.8. The beam is equipped with a pair of collocated Macro Fiber Composite (MFC) sensor and actuator patches. This set-up prototypes the custom-made vibration suppressor shown in Fig. 6.2. A simplified, finite-dimensional, minimum phase, stable NI transfer function model of the lightweight cantilever beam in Fig. 6.2 and Fig. 7.1 is given by [refer to Subsection 7.2.2 for identification details]

$$G_m(s) = \frac{30050(s^2 + 1.996s + 7631)}{(s^2 + 1.108s + 6350)(s^2 + 28.43s + 2.21 \times 10^5)}. \tag{6.15}$$

We now test the usefulness of Lemma 14, Lemma 15 and Theorem 8 in designing an IMC scheme for stable NI/SNI plants. It can be readily verified that a minimal state-space realisation of $G_m(s)$ satisfies the NI lemma (i.e. Lemma 6) with

$$Y = \begin{bmatrix} 0.0026 & -0.0000 & -0.0039 & 0.0001 \\ -0.0000 & 0.0155 & -0.0005 & -0.0333 \\ -0.0039 & -0.0005 & 0.0334 & -0.0001 \\ 0.0001 & -0.0333 & -0.0001 & 0.0856 \end{bmatrix} > 0,$$

which indicates that $G_m(s)$ is NI. For a graphical interpretation, we have also included the Bode plot of $G_m(s)$ in Fig. 6.9, which confirms the NI property of the plant model $G_m(s)$.

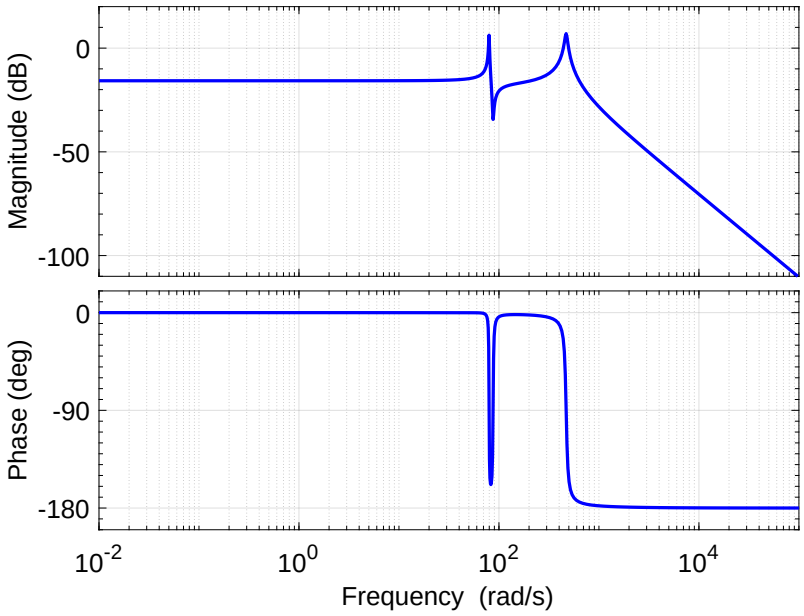

Figure 6.9: Bode plot of the plant model $G_m(s)$.

6.3.1 Frequency Domain Approach for IMC Design

Following the ideas presented in Subsection 6.2.1, we can decompose the plant model as $G_m(j\omega) = \dfrac{N_m(j\omega)}{D_m(j\omega)} = \dfrac{N_{mr}(\omega) + jN_{mi}(\omega)}{D_{mr}(\omega) + jD_{mi}(\omega)}$ where

$$D_{mr}(\omega) = \omega^4 - 2.272 \times 10^5\omega^2 + 1.41 \times 10^9,$$

$$D_{mi}(\omega) = 4.017 \times 10^5\omega - 29.75\omega^3,$$

$$N_{mr}(\omega) = 2.293 \times 10^8 - 30050\omega^2 \qquad \text{and}$$

$$N_{mi}(\omega) = 5.998 \times 10^4.$$

Since the plant model $G_m(s)$ has relative degree 2, we choose the filter $F_1(s) = \frac{k}{(s^2+bs+k)}$ and the controller $C_1(s) = \frac{kD_m(s)}{N_m(s)(s^2+bs+2k)}$ following Lemma 15. The controller parameters b, $k > 0$ need to be selected such that $C_1(s)$ becomes SNI (or stable NI). According to Lemma 15, $C_1(s)$ is SNI (or stable NI) if

$$\begin{aligned}
&2k^2(-8.34\times10^5\omega^5 + 5.27\times10^9\omega^3 - 7.5\times10^{12}\omega)+\\
&\omega kb(-30050\omega^6 + 7.06\times10^9\omega^4 - 9.45\times10^{13}\omega^2+\\
&3.23\times10^{17}) + \omega^2k(8.34\times10^5\omega^5 - 5.27\times10^9\omega^3\\
&+ 7.5\times10^{12}\omega) > 0 \ \ (\geq 0) \qquad \forall\omega\in(0,\infty).
\end{aligned}$$

The polynomial in the left-hand side of the above inequality

$$\begin{aligned}
&(8.34\times10^5k - 30050kb)\omega^7+\\
&(7.06\times10^9kb - 1.67\times10^6k^2 - 5.27\times10^9k)\omega^5+\\
&(1.05\times10^{10}k^2 - 9.45\times10^{13}kb - 7.5\times10^{12}k)\omega^3+\\
&(3.23\times10^{17}kb - 1.50\times10^{13}k^2)\omega
\end{aligned}$$

remains positive $\forall\omega \in (0,\infty)$ if the coefficients of all the ω terms take on positive values, which can be mathematically formulated as

$$\begin{bmatrix} 0 & 30050 \\ 1.67\times10^6 & -7.06\times10^9 \\ -1.05\times10^{10} & 9.45\times10^{13} \\ 1.51\times10^{13} & -3.23\times10^{17} \end{bmatrix} \begin{bmatrix} k \\ b \end{bmatrix} \leq \begin{bmatrix} 8.34\times10^5 \\ -5.27\times10^9 \\ -7.5\times10^{12} \\ 0 \end{bmatrix}.$$

This can be considered a constrained, linear, least-square problem, which can readily be solved using the commercially available SDP solver packages. We set the lower bounds for k and b as 100 and 20, respectively, so that the filter poles can be placed at $s_{1,2} = -10$. This choice of the filter poles is an arbitrary one to ensure that the closed-loop system is neither too sluggish nor too fast. Solving the least-square problem using CVX [95], we get a feasible solution $k \leq 4.2891\times10^5$ and $b \leq 20$. The filter is obtained as $F_1(s) = \frac{1}{s^2+20s+100}$ and the desired SNI controller is given by

$$C_1(s) = \frac{\alpha_1(s)}{\beta_1(s)}, \tag{6.16}$$

where $\alpha_1(s) = 3.3278\times10^{-3}(s^2+1.108s+6350)(s^2+28.43s+2.21\times10^5)$ and $\beta_1(s) = (s^2+20s+200)(s^2+1.996s+7631)$. We then verify the DC loop gain condition

$C_1(0)G_m(0) = 3.0599 \times 0.1634 = 0.4999 < 1$. Hence, the NI-based IMC scheme shown in Fig. 6.3 is guaranteed to be internally stable via Theorem 4. Figure 6.10 confirms the SNI property of the synthesized controller.

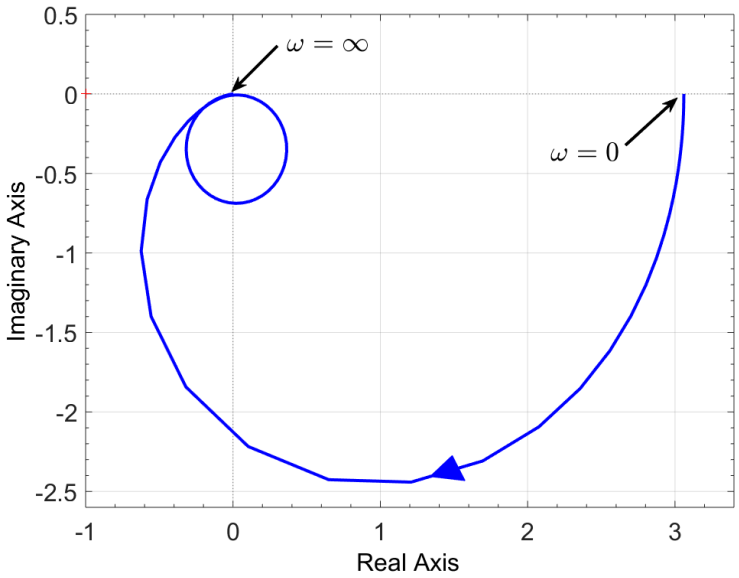

Figure 6.10: Nyquist plot of the controller $C_1(s)$ designed via the frequency domain approach.

6.3.2 LMI-Based Approach for IMC Design

To proceed with the controller design methodology according to Theorem 8, we choose the polynomial $d(s) = (s + 80)\mathbb{D}\big[G_m(s)\big]$ since the plant model $G_m(s)$ has the first resonant peak at $\omega = 80$ rad/s. Upon solving the set of LMI conditions (6.5a)–(6.5e), we obtain the desired SSNI controller

$$C_2(s) = \frac{14.383(s + 1429)}{(s + 80)(s + 83.97)} \tag{6.17}$$

and reconstruct the filter transfer function

$$F_2(s) = \frac{\alpha_2(s)}{\beta_2(s)},$$

where $\alpha_2(s) = 4.3222 \times 10^5(s + 1429)(s^2 + 1.996s + 7631)$, $\beta_2(s) = (s + 132.1)(s + 24.99)(s^2 + 4.647s + 6394)(s^2 + 31.79s + 2.234 \times 10^5)$ and $C_2(s) = G_m(s)^{-1}F_2(s)\big[I + F_2(s)\big]^{-1}$. The Nyquist plot of $C_2(s)$ in Fig. 6.11 confirms that $C_2(s)$ is SSNI since its phase angle contribution $\phi_c \in (-\pi, 0)\ \forall \omega \in (0, \infty)$ and $\lim_{\omega\to\infty} \phi_c(\omega) = -\frac{\pi}{2}$. It can be

readily verified that the DC loop gain is less than one $[C_2(0)G(0) = C_2(0)G_m(0) = 3.0599 \times 0.1634 = 0.5000 < 1]$, which guarantees the closed-loop stability of the IMC scheme shown in Fig. 6.3.

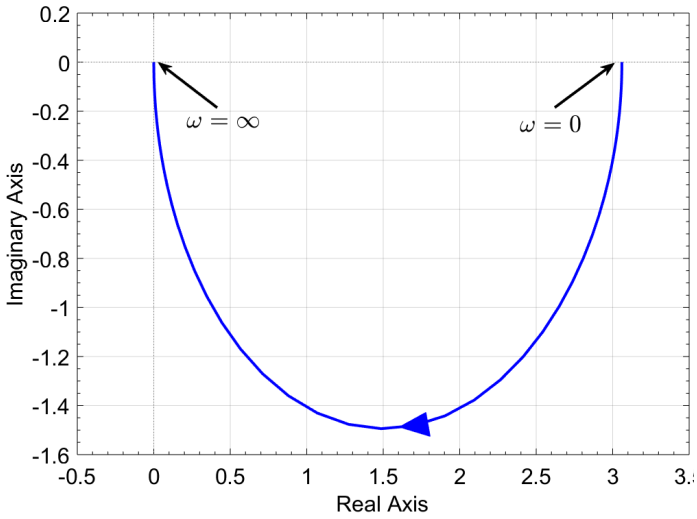

Figure 6.11: Nyquist plot of the controller $C_2(s)$ designed via the LMI-based approach for $d_1(s) = (s + 80)\mathbb{D}[G_m(s)]$.

6.3.3 Simulation Results

This subsection presents the Matlab simulation results and analyses the regulatory and tracking performances of the controllers $C_1(s)$ and $C_2(s)$ in response to a pulse input of amplitude 1 and duration of 0.1 s and to a unit step input. The responses of the open-loop system to the pulse and step inputs are shown in Fig. 6.12a and Fig. 6.12b. The open-loop pulse response has a peak value of 0.272 cm, while the open-loop step response has a steady state value of 0.1639. Fig. 6.12d shows that in the ideal case [i.e. $G(s) = G_m(s)$], both the LMI-based and the frequency domain (IMC) controllers achieve perfect steady state tracking. Also, $C_1(s)$ results in a well-damped closed-loop response with no overshoot, while the closed-loop with $C_2(s)$ exhibits some overshoot. However, the latter offers a remarkable improvement in the settling time than the former. The closed-loop with $C_2(s)$ achieves a settling time of 0.29 s, while the closed-loop with $C_1(s)$ achieves a much higher settling time of 0.58 s. To analyse the disturbance (subject to a pulse input) rejection capacity of the controllers, Fig. 6.12c shows that $C_2(s)$ achieves a settling time of 0.62 sec and a peak overshoot of 0.3537

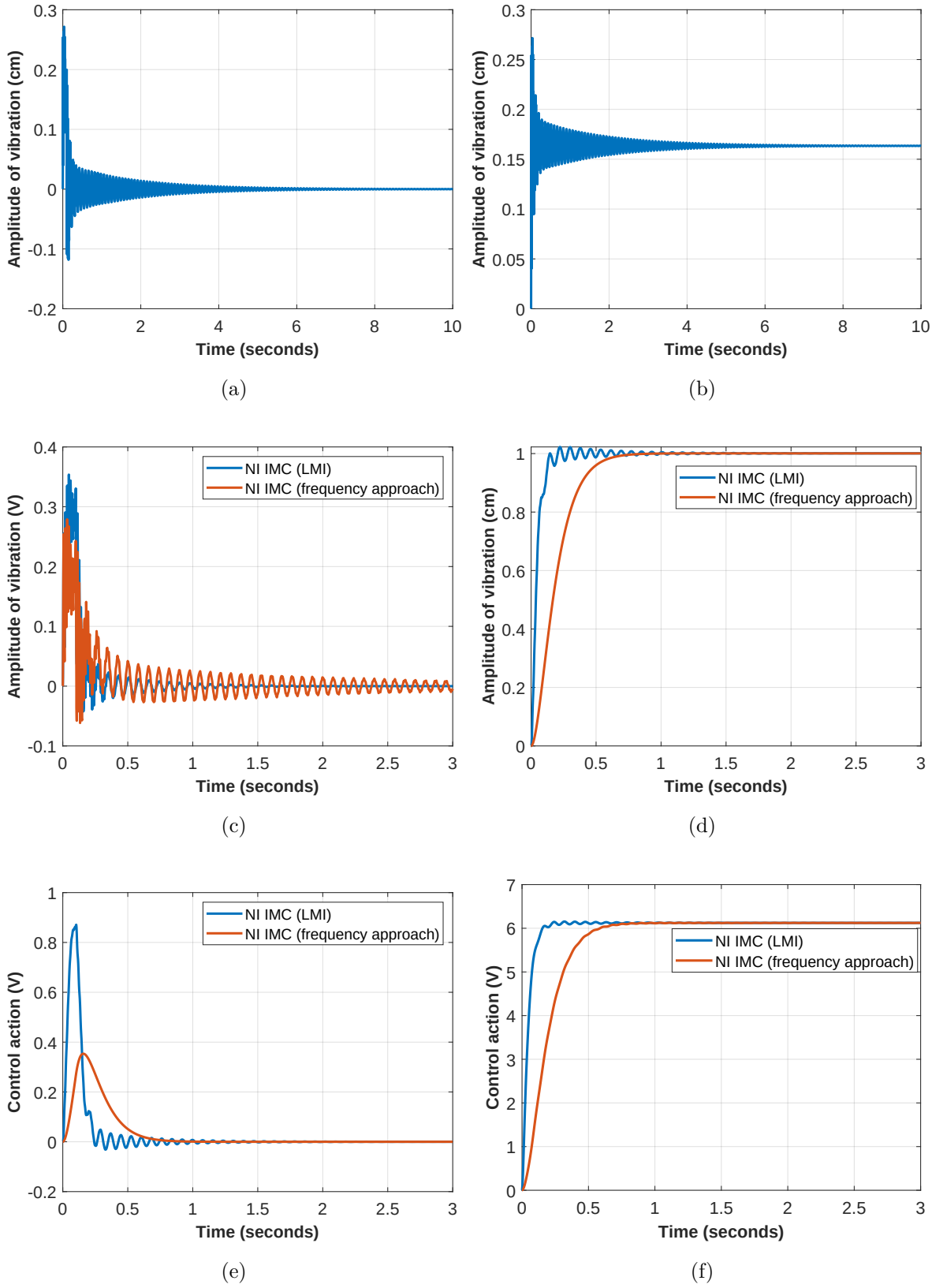

Figure 6.12: [Simulated responses considering $G_m(s) = G(s)$] (a) Open-loop response to a pulse input; (b) Open-loop response to a unit step input; (c) Closed-loop pulse response using the controllers $C_1(s)$ [via frequency domain approach] and $C_2(s)$ [via the LMI-based approach]; (d) Closed-loop unit step response achieved by $C_1(s)$ and $C_2(s)$; (e) Control effort demanded in the case of pulse response; and (f) Control effort demanded in the case of step response.

cm. Note that the peak overshoot can be reduced by choosing an appropriate $d(s)$, as outlined in Subsection 6.2.4, but at the cost of an increased settling time. On the other hand, $C_1(s)$ causes a peak overshoot of 0.2789 cm and a settling time of 2.56 sec. Hence, we can conclude that the performance achieved by the frequency domain design technique is less effective compared to the LMI-based design methodology.

6.3.4 Impact of a Model Mismatch

Now, we consider the case where the plant (i.e. the cantilever beam) $G(s)$ is different from its identified model $G_m(s)$. However, we impose a reasonable and practically feasible assumption $G(0) = G_m(0)$. Let the transfer function of the beam be chosen as:

$$G(s) = \frac{1502.5(s^2 + 1.996s + 3816)}{(s^2 + 2.108s + 1270)(s^2 + 10.43s + 2.763 \times 10^4)}. \tag{6.18}$$

In this subsection, our objective is to test the robustness of the designed controllers

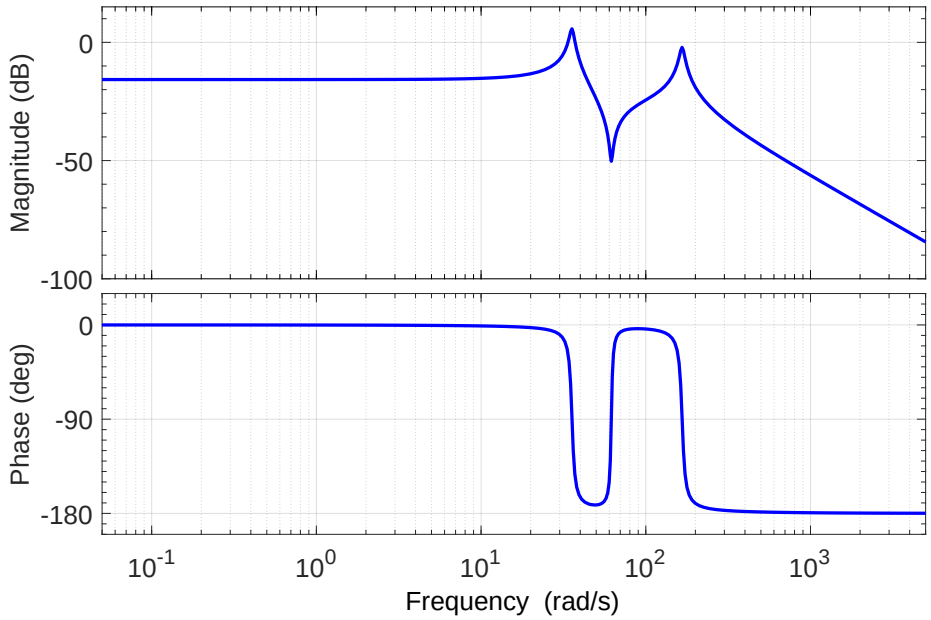

Figure 6.13: Bode plot of the cantilever beam $G(s)$ that is different from $G_m(s)$.

$C_1(s)$ and $C_2(s)$ against the model mismatch [i.e. $G(s) \neq G_m(s)$]. It can be readily verified that $G(s)$ is a stable and minimum phase SNI transfer function. Moreover, its Bode plot (in Fig. 6.13) shows that $G(s)$ satisfies also the SNI property. The closed-loop stability of the desired controllers remains preserved for both the designed controllers $C_1(s)$ and $C_2(s)$ since the DC loop gain condition holds in both the cases: $C_1(0)G(0) = 3.0599 \times 0.1634 = 0.5000 < 1$ and $C_2(0)G(0) = 3.0599 \times 0.1634 = 0.5000 < 1$.

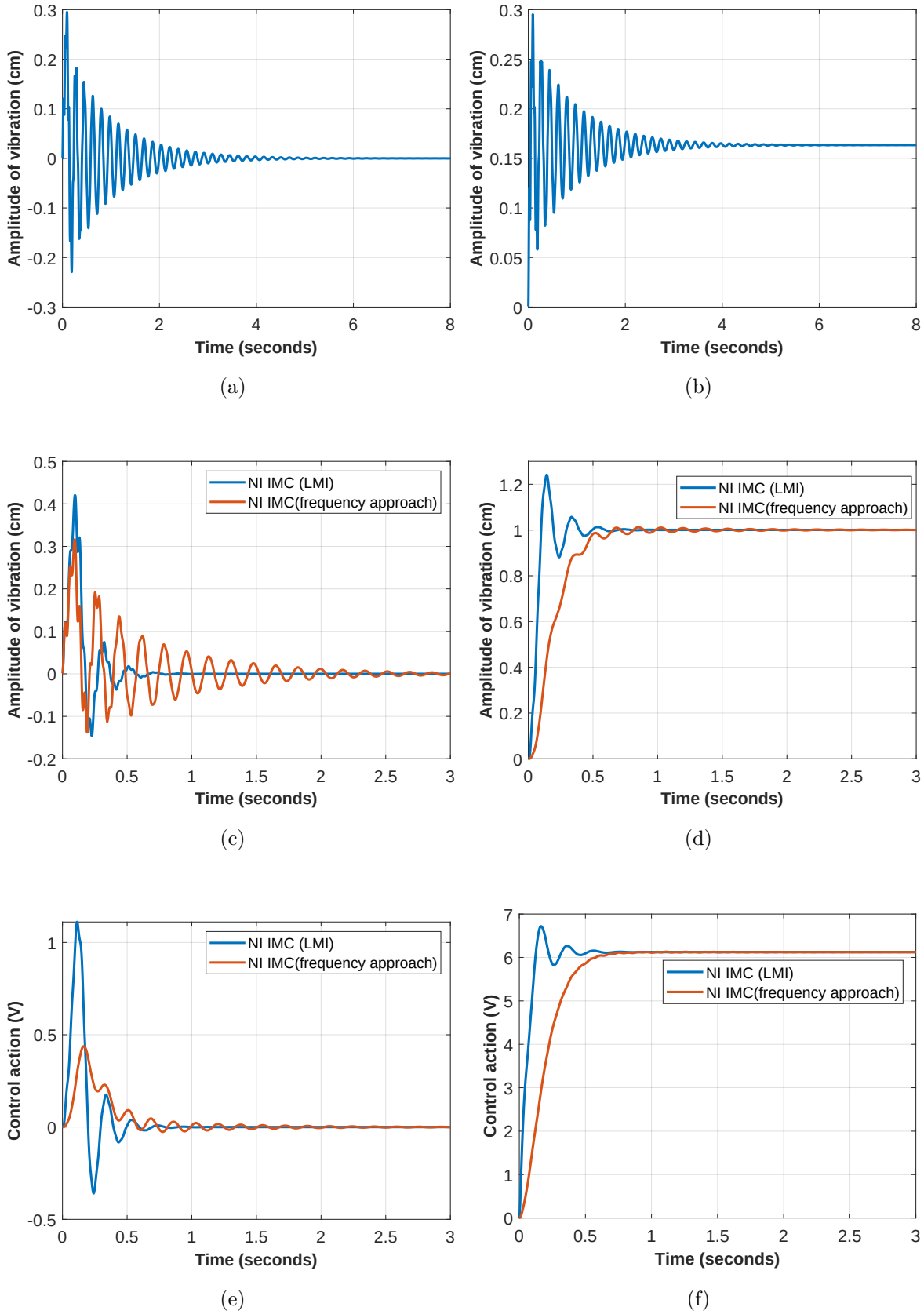

Figure 6.14: [Simulated responses considering a perturbed plant $G(s) \neq G_m(s)$] (a) Open-loop response to a pulse input; (b) Open-loop response to a unit step input; (c) Closed-loop pulse response using the controllers $C_1(s)$ [via frequency domain approach] and $C_2(s)$ [via the LMI-based approach]; (d) Closed-loop unit step response using the controllers $C_1(s)$ and $C_2(s)$; (e) Control effort for the pulse response; and (f) Control effort for the step response.

Fig. 6.14a–Fig. 6.14d show the open-loop and closed-loop responses of the perturbed plant $G(s)$ subject to the same pulse and unit step inputs considered in Fig. 6.12a–Fig. 6.12d. The time responses in Fig. 6.14c and Fig. 6.14d reveal that the controllers $C_1(s)$ and $C_2(s)$ ensure closed-loop stability despite the model mismatch [i.e. $G_m(s) \neq G(s)$]. However, the achieved transient performance in Fig. 6.14c and Fig. 6.14d is not that impressive as observed in Fig. 6.12c and Fig. 6.12d due to the model mismatch. In both Fig. 6.14a and Fig. 6.14b, the peak values of the responses are around 0.30 cm. Fig. 6.14c reveals that although the reduction in the peak value is negligible, the decay of oscillation is significant. Besides, it also reveals that $C_2(s)$ designed via the LMI-based approach performs better than $C_1(s)$ obtained via the frequency domain design approach. Fig. 6.14d indicates that both $C_1(s)$ and $C_2(s)$ achieve perfect steady state tracking although $C_2(s)$ offers a faster dynamic performance than $C_1(s)$. However, $C_2(s)$ produces almost 23% peak overshoot, while $C_1(s)$ results in a type of critically-damped response. Fig. 6.14e and Fig. 6.14f show the control effort demanded by the controllers $C_1(s)$ and $C_2(s)$ during the pulse response and the step response respectively. The figures confirm that the demanded control effort remain within the allowable range. However, in both the cases, $C_2(s)$ requires more control effort than that of $C_1(s)$. The same observation applies to Fig. 6.12e and Fig. 6.12f as well, pertaining to the case when $G_m(s) = G(s)$. Note that both $C_1(s)$ and $C_2(s)$ are able to achieve perfect steady state step input tracking despite the model mismatch (as reflected in Fig. 6.14d) only due to the fact that $G_m(0) = G(0)$. When $G_m(0) \neq G(0)$, to eliminate the inevitable steady state error, an additional feed-forward control input can be designed following the ideas given in [63] and [62].

6.4 Conclusions

In this chapter, we introduced an NI controller synthesis using the IMC framework. We introduced two different methods; the first is a frequency domain approach which involves the solution of constrained least-square problem. The second approach is an LMI-based approach that can easily be solved using commercially available SDP solvers. We also showed that the synthesized controllers can achieve nominal tracking in addition to robust stability as long as the certain DC gain conditions are satisfied. Furthermore,

the LMI-based controller can be tuned to improve the nominal performance of the closed-loop system and we provided guidelines on how to choose the particular tuning parameter. Finally, we used the model of a flexible structure to show the usefulness of the proposed synthesis technique via the simulation studies by considering the pulse and step responses of the closed-loop system.

Chapter 7

Active Vibration Suppression of a Flexible Structure

All the materials presented in this chapter were submitted for publication in [61].

7.1 Introduction

Flexible structures can be found in quite a number of important applications such as the wing of an aircraft, UAV, robotic systems, hard disk drives, space satellites, to mention but a few. The flexible structures are prone to high amplitude oscillations when subjected to slight external disturbances because they are highly resonant systems [55]. This pose a safety concern in many applications and can affect the structural integrity of the whole system. It is therefore always desirable to mitigate or outrightly eliminate the high amplitude oscillations.

When flexible structures have collocated force actuators and position sensors, the underlying transfer function has the NI property. However, flexible structures have an infinite number of lightly damped modes because their dynamics are usually described by Partial Differential Equations (PDEs) [55,56]. But the PDE model is approximated to a finite order model for control purpose. This gives rise to what is referred to as the spillover dynamics, which can degrade the performance of the closed-loop system or in some cases lead to instability.

In this problem, we use a collocated MFC for sensing and actuation. MFC has many

advantages compared to the tradionally used PZT. This include better flexibility, more durability and reliability and ease of attachment to the surface of structures [54]. An NI model of the flexible structure will first be obtained using Matlab system identification toolbox. A controller will then be designed which will guarantee robust stability using the NI theory. The controller will also improve the damping of the flexible structure.

The main contribution of this chapter is the validation of the LMI-based NI controller synthesis presented in Chapter 6. The designed controller should be able to maintain robust stability in the presence of the spillover dynamics of the flexible structure. Moreover, the designed controller should also improve the damping performance of the closed-loop system.

7.2 Experimental Validation

7.2.1 Description of the Vibration Suppressor

The designed vibration suppressor system shown in Fig. 7.1 consists of a lightweight aluminium beam, whose properties are given in Table 7.1, clamped at one end and mounted on a solid plate. The plate sits on top of a moving rail powered by a 12 V, 251 rpm metal-geared DC motor. The motor has a stalling current of 7 A and a no-load current of 350 mA. The motor is controlled by a PWM signal injected through a motor driver. In this application, we used an MD10C R3 motor driver capable of sustaining the motor input voltage up to 30 V and a maximum current of 13 A. The motor driver is powered by a WATSON POWER-MAX-65-NF power supply. The cantilever

Table 7.1: Specifications of the beam used in our experiment

Parameter	**Value**
Length	350 mm
Thickness	1.8 mm
Width	22.5 mm
Density	2.8×10^3 kg/m^3
Young Modulus	7.0×10^{10} N/m^2

beam has been equipped with a pair of collocated MFC sensor and actuator patches. We used an M0714-P2 MFC for sensing and an M2814-P1 MFC for actuation. The properties of the MFC patches are given in Table 7.2. We implemented the designed

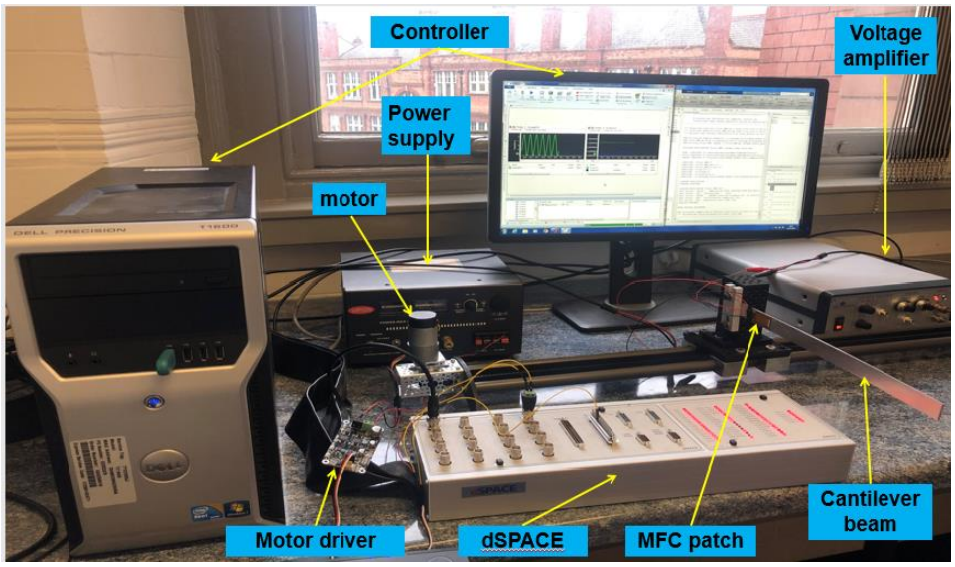

Figure 7.1: Closed-loop control set-up of the vibration suppressor using the dSPACE platform.

Table 7.2: Specifications of the MFC sensor and actuator patches

Parameter	**M0714-P2**	**M2814-P1**
Active length mm	7	28
Active width mm	14	14
Free strain ppm ±10%	−540	1160
Blocking force in N ±10%	−57	146
Allowable voltage range	−60 to 360 V	−500 to 1500 V

controller using a dSPACE board connected to a 200× HVA 1500/50-2 high voltage amplifier, as shown in Fig. 7.1. The maximum positive and negative voltages of the amplifier were +1500 V and −500 V respectively.

7.2.2 System Identification of the Vibration Suppressor

To obtain a non-parametric model of the cantilever beam, we applied a chirp signal to the MFC actuator patch for 30 s over the frequency range 0–200 Hz. We used a sampling frequency of 250 Hz for the data acquisition. The corresponding output was recorded via dSPACE using the MFC sensor patch. ControlDesk was used to store the data. For the system identification, we used the Matlab System Identification Toolbox

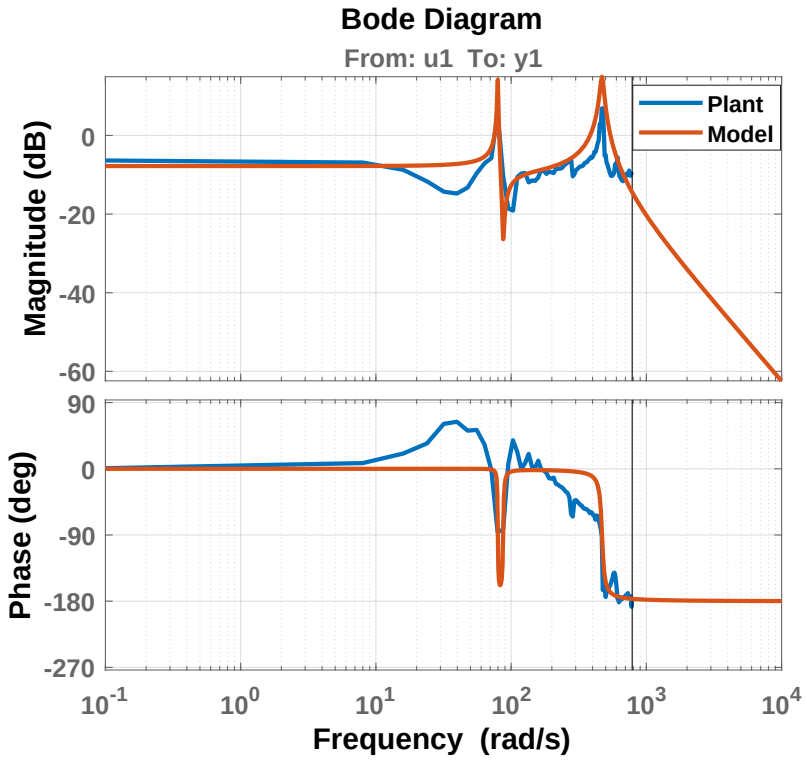

Figure 7.2: Bode plots of the physical plant $G(s)$ and its identified model $G_m(s)$.

to transform the time domain data into frequency domain and obtained a fourth-order model of the system given by

$$G_m(s) = \frac{30050(s^2 + 1.996s + 7631)}{(s^2 + 1.108s + 6350)(s^2 + 28.43s + 2.21 \times 10^5)}.$$

$G_m(s)$ is indeed a stable and minimum phase transfer function having relative degree 2. This model was used in Section 6.3, as given in (6.15), for the simulation case study. Fig. 7.2 reveals that the identified model $G_m(s)$ is indeed a good representation of the physical plant (i.e. the vibration suppressor shown in Fig. 6.2), especially at the low-frequency range. Moreover, the identified model $G_m(s)$ is stable NI, as confirmed by the red-coloured Bode plot in Fig. 7.2.

7.2.3 Experimental Validation Results

In this subsection, we will test the feasibility and performance of the NI-based IMC controller $C_2(s)$, designed by the LMI-based methodology, in response to a pulse signal applied directly at the input of the beam and a disturbance produced by the belt-pulley-motor assembly of the vibration suppressor system (Fig. 7.1). We will also test

the robustness of the designed controller $C_2(s)$ against a deliberate model mismatch.

7.2.3.1 Response of the System to a Pulse Signal

Fig. 7.3a shows the open-loop and closed-loop responses of the practical vibration suppressor system, shown in Fig. 7.1, to a pulse signal of amplitude 2 applied directly at the input of the beam for 0.5 s. The pulse input signal has a start time of 0.5 s.

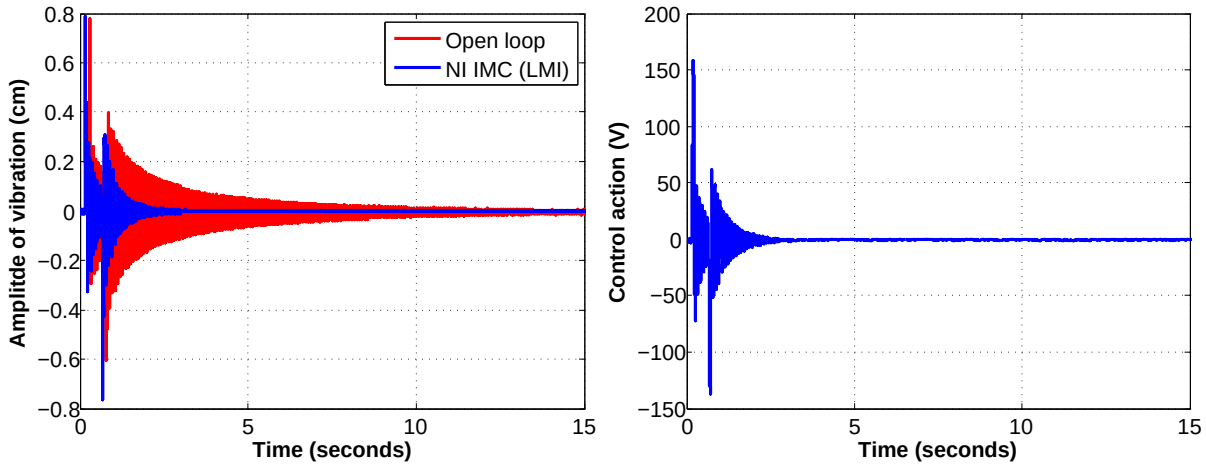

(a) (b)

Figure 7.3: [Experimental validation results] (a) Open-loop and closed-loop [achieved by $C_2(s)$] responses of the vibration suppressor subject to a pulse signal applied at the input of the beam; and (b) Demanded control effort pertaining to case (a).

We can see that the controller design scheme in this paper ensures closed-loop stability of the vibration suppressor system and significantly increases the speed of vibration attenuation as shown in Fig. 7.3a. The settling time of the closed-loop response is 1.85 s compared to 8.59 s in the case of open-loop configuration. The figure suggests that although the reduction in the amplitude of vibration is negligible, the improvement in the settling time is note worthy. The performance of the controller in this case is similar to what was observed in the simulation study. Fig. 7.3b shows that the demanded control effort by $C_2(s)$ remains within the allowable limit [which is -500 to 1500 V] of the MFC actuator patch used in our experiment.

7.2.3.2 Regulatory Response Subject to a Disturbance Produced by the Belt-Pulley-Motor Assembly

The regulatory response of the vibration suppressor system was tested by shaking the base unit (i.e. the fixed end) of the system mounted on a rail, through the belt-pulley-motor arrangement as shown in Fig. 7.1. A PWM signal was applied to the input of the motor for a duration of 0.5 s to produce a jerk causing the vibration in the beam. The PWM signal had a start time of 0.5 s. The open-loop response and the closed-loop regulatory response are depicted in Fig. 7.4a. Figure 7.4a reveals that the controller

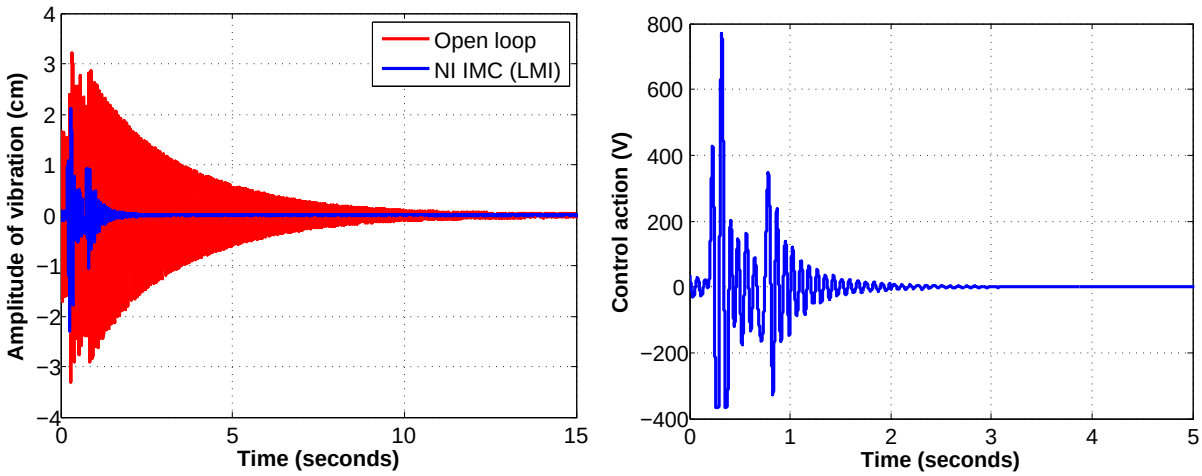

(a) (b)

Figure 7.4: [Experimental validation results] (a) Open-loop and closed-loop [achieved by $C_2(s)$] responses of the vibration suppressor subject to the disturbance produced by the belt-pulley-motor assembly; (b) Control effort demanded by $C_2(s)$ during the disturbance attenuation.

$C_2(s)$, designed via the LMI-based algorithm, has remarkably improved the vibration attenuation performance in the closed-loop in response to the disturbance produced by the belt-pulley-motor assembly. The closed-loop regulatory response has a decaying time of 2.17 s and a peak overshoot of 2.036 cm compared to the open-loop response having a decaying time of 11.50 s and a peak overshoot of 3.2190 cm.

7.2.3.3 Robustness to Model Mismatch

To test the robustness of the proposed NI controller design scheme against model mismatch, we attached an external weight of 5 g mass to the cantilever beam of the existing vibration suppressor system (shown in Fig. 7.1) to shift its resonant modes.

The beam has a mass of 30 g, making the total mass of the beam and weight 35 g. Fig. 7.5a shows the open-loop and closed-loop regulatory responses of the vibration suppressor system being burdened with the additional weight attached with the beam. Moreover, we notice a significant (almost 4 times) improvement in the settling time of the closed-loop response, which is 2.49 s compared to the open-loop response, which has a settling time of 9.14 s. This hence confirms that the designed controller is robust to this model mismatch and achieves satisfactory disturbance rejection performance despite the model mismatch due to attaching an additional weight with the beam.

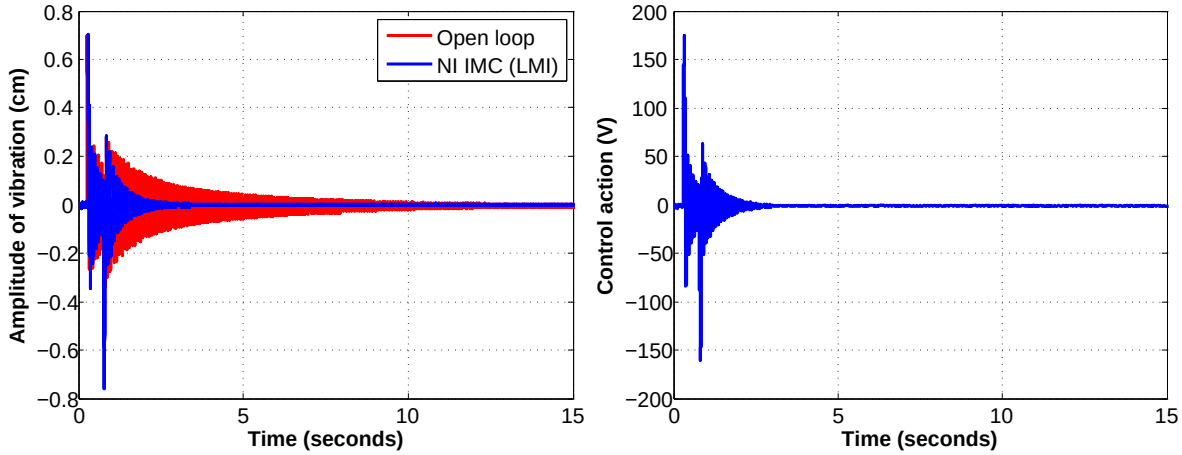

(a) (b)

Figure 7.5: [Experimental validation results] (a) Open and closed-loop response, achieved by $C_2(s)$, of the vibration suppressor [burdened with an external weight attached to the beam] subject to a pulse signal applied at the input of the beam; (b) Control action demanded by $C_2(s)$.

We also evaluate the robustness of the controller subject to external disturbance generated from the motor.

Fig. 7.6a shows the open-loop and closed-loop regulatory responses of the vibration suppressor system being burdened with an additional weight attached with the beam subject to the disturbance produced by the belt-pulley-motor assembly. It can be seen that the controller also has good performance in this case. The open-loop response has a decaying time of 12.93 s and a peak of 3.815 cm. The controller reduces the decaying time of the closed-loop response to 2.05 s and the peak to 2.4170 cm.

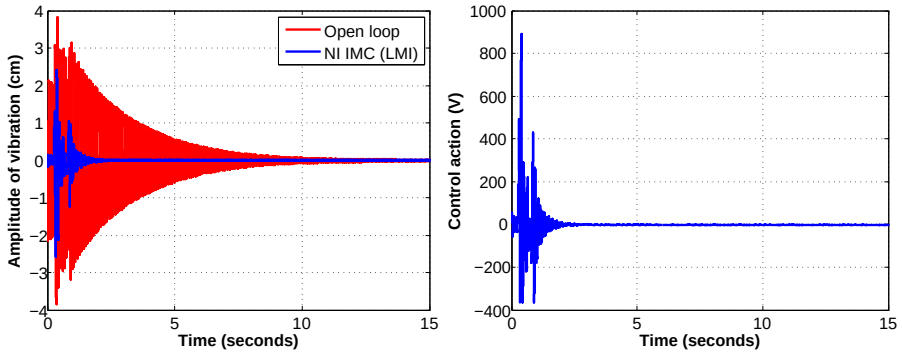

(a) (b)

Figure 7.6: [Experimental validation results] (a) Open and closed-loop response, achieved by $C_2(s)$, of the vibration suppressor [burdened with an external weight attached to the beam] subject to the disturbance produced by the belt-pulley-motor assembly; (b) Control action demanded by $C_2(s)$.

7.2.3.4 Effect of the Choice of $d(s)$ on the LMI-Based Design

In this subsection, we analyse the effect of varying the real root (i.e. at $s = -a$) of the polynomial $d(s)$ in the closed-loop performance achieved from the experimentation. We have considered two different choices $a_1 = 0.8$ and $a_2 = 8$ fixed respectively at two decades and one decade below the first resonant mode (at $\omega = 80$ rad/s) of the identified plant model $G_m(s)$. We seek to redesign the controllers $C_3(s)$ and $C_4(s)$ corresponding to the two new polynomials $d_2(s) = (s+0.8)\mathbb{D}\Big[G_m(s)\Big]$ and $d_3(s) = (s+8)\mathbb{D}\Big[G_m(s)\Big]$ via the LMI-based controller design methodology (i.e. Theorem 8). The new controllers are obtained as:

$$C_3(s) = \frac{5.9357(s + 0.8385)}{(s + 0.8)(s + 2.033)} \tag{7.1}$$

and

$$C_4(s) = \frac{10.941(s + 12.56)}{(s + 8)(s + 5.615)}. \tag{7.2}$$

The Nyquist plots of $C_3(s)$ and $C_4(s)$ shown in Fig. 7.7a and Fig. 7.7b confirm the SSNI property of the controllers. This design also relies on the same identified plant model $G_m(s)$, as mentioned in (6.15), which has its first resonant mode at $\omega = 80$ rad/s. Note that $C_3(s)$ and $C_4(s)$ contain slower poles than $C_2(s)$, which have been dictated by the factor $(s + 0.8)$ in $d_2(s)$ and $(s + 8)$ in $d_3(s)$. The internal stability of the controller scheme design is still guaranteed since both the new controllers $C_3(s)$ and $C_4(s)$ satisfy the DC loop gain condition, as verified here: $C_3(0)G_m(0) = 3.0592 \times 0.1618 = 0.4950 < 1$ and $C_4(0)G_m(0) = 3.0596 \times 0.1618 = 0.4951 < 1$. Fig. 7.8a and Fig. 7.8b portray

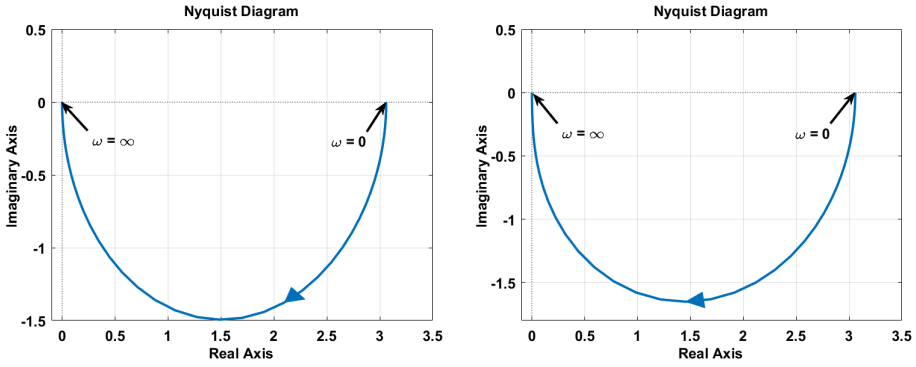

(a) (b)

Figure 7.7: (a) Nyquist plot of the controller $C_3(s)$ designed via the LMI-based approach for $d_2(s) = (s + 0.8)\mathbb{D}\Big[G_m(s)\Big]$; and (b) Nyquist plot of the controller $C_4(s)$ designed via the LMI-based approach for $d_3(s) = (s + 8)\mathbb{D}\Big[G_m(s)\Big]$.

the closed-loop regulatory responses, subjected to the disturbance generated by the belt-pulley-motor assembly, achieved by the new controllers $C_3(s)$ and $C_4(s)$. Comparing Fig. 7.8a, Fig. 7.8b and Fig. 7.4a, it can be asserted that $C_2(s)$ offers the best vibration attenuation performance. The settling time (considering a 2% tolerance band) in case of $C_2(s)$ is even less than 2 s in contrast to 8.5 s achieved by $C_3(s)$ and 4 s achieved by $C_4(s)$. Therefore, we can conjecture that as the value of the parameter $a > 0$ in the polynomial $d(s) = (s + a)\mathbb{D}\Big[G_m(s)\Big]$ increases, the speed of response improves. Regarding the amplitude reduction of the vibration, $C_4(s)$ and $C_2(s)$ reduce the open-loop peak vibration of 3.2 cm to 1.95 cm (shown in Fig. 7.8b) and 2.095 cm (shown in Fig. 7.4a) respectively. However, the degree of vibration attenuation in the case of $C_3(s)$ is much less than that achieved by $C_2(s)$ and $C_4(s)$. On the other hand, a faster controller (for instance, $C_2(s)$) requires a larger control effort than a relatively slower controller (for instance, $C_4(s)$ or $C_3(s)$), as reflected through Fig. 7.4b, Fig. 7.8d and Fig. 7.8c. It is evident that the control effort demanded by $C_2(s)$ is significantly higher than that of $C_4(s)$ and $C_3(s)$. This may be regarded as the cost of achieving more than five times improvement in the settling time with respect to the open-loop response (in Fig. 7.4a). The experimental results indicate that the real root (at $s = -a$) of $d(s)$ should not be placed more than a decade below the first resonant mode of the plant model $G_m(s)$. In practical applications, depending on the physical capacity of the actuators, a control designer needs to choose a trade-off between a high degree of

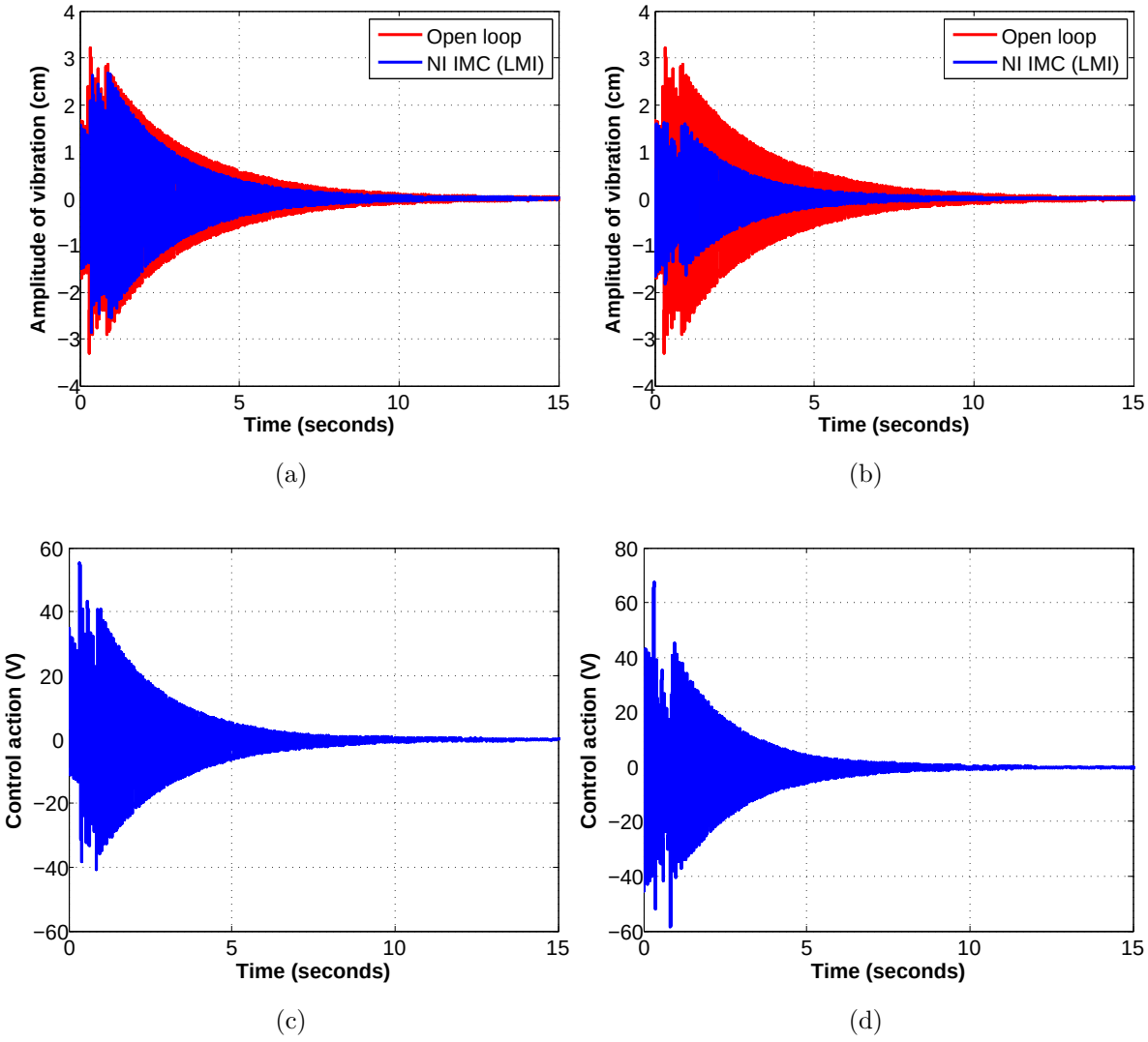

Figure 7.8: [Experimental validation results] (a) Open-loop and closed-loop [achieved by $C_3(s)$] responses of the vibration suppressor subject to the disturbance produced by the belt-pulley-motor assembly; (b) Open-loop and closed-loop [achieved by $C_4(s)$] responses of the vibration suppressor subject to the disturbance produced by the belt-pulley-motor assembly; (c) Demanded control effort pertaining to case (a); and (d) Demanded control effort pertaining to case (b).

dynamic performance and the demanded control effort.

7.3 Conclusions

In this chapter, we validated the LMI-based controller synthesized in Chapter 6 on a vibration attenuation problem of a flexible structure system. We started by obtaining an LTI finite-dimensional NI transfer function model of the flexible structure system. We then used the model to design a controller that ensures robust stability and significantly improve the damping performance of the closed-loop system. We used two different disturbance signals; one is a pulse disturbance at the input of the plant and the other one was a disturbance generated by the motor connected to the rail on which the beam is clamped. In both cases, the controller was able to achieve good nominal performance of the closed-loop system. Finally, the we finished the chapter by showing the effect of the tuning variable $d(s)$ on the performance of the closed-loop system.

Chapter 8

Conclusions and Future Work

8.1 Conclusions

In this thesis, we set out to provide a solution to the NI synthesis problem. We divided this problem into two different categories viz: synthesizing a controller such that the closed-loop system NI and is robust to an NI uncertainty. The second approach is that of synthesizing a controller that is itself NI and robustly stabilizes an uncertain NI plant. In the first approach, neither the plant nor the controller is required to be NI, but the closed-loop system and the uncertainty both have to possess the NI property.

Furthermore, it was our aim to provide synthesis methods that also improve the performance of the closed-loop system. It is worth noting that the performance we considered in this thesis is not the traditional type of performance such as $\mathcal{H}_\infty$ or $\mathcal{H}_2$ performance measures commonly considered in the NI literature. Our performance measures are time domain performance such as decay rate, settling time, damping and overshoot of the closed-loop system. Moreover, it was our that these synthesis techniques should be appealing for application to practical systems due to ease of synthesis.

In Chapter 4, we were able to address the first type of NI synthesis problem. First, we provided a definition for $\alpha-$ SNI systems and then used the $\alpha-$ SNI framework to successfully provide an LMI-based dynamic output feedback controller synthesis technique. The controller renders the closed-loop system $\alpha-$ SNI and robustly stabilizes it against a class of NI uncertainties. In this synthesis technique, we used the dacay rate of the closed-loop system, which is dictated by the parameter α, as a measure of

the closed-loop system performance.

In Chapter 6, we addressed the second type of the NI synthesis problem. In this approach, we were able to successfully combine the IMC design principle with the NI systems theory to provide a dynamic output feedback controller synthesis technique that produce an NI controller robustly stabilizes an uncertain NI system. We were able to provide two different synthesis technique for this solution to the NI synthesis problem. The first method was a frequency-based approach that allows the designer to decide the closed-loop dynamics based on the dynamics of a chosen filter dynamics. The second method was an LMI-based synthesis approach which uses a design parameter to improve the closed-loop performance. Both methods also facilitate perfect constant set-point tracking.

Hence, in these two chapters, we were able to successfully address the NI synthesis problem that improve the performance of the closed-loop system. We were also able to provide simple design technique using LMIs that can easily be solved to obtain these controllers.

As most of the works in the field of NI controller synthesis in the literature were purely theoretical, it was also our aim to validate some of the synthesis technique we provided with an experimental validation. Hence, we addressed the vibration attenuation problem of a lightly damped flexible structure. First, we successfully built a custom-made flexible structure, which is in the form of a cantilever beam mounted on a metal rail and subjected to external disturbances. We used the first two resonant modes of the cantilever beam for controller design and considered the other modes as unmodelled system dynamics. We successfully designed a robustly stabilizing controller for the beam using the LMI-based NI IMC controller synthesis technique that attenuates the vibration of the flexible structure as it is subjected to external disturbance.

Although the NI literature has seen a significant amount of contribution over the years, there were still some systems that possess the NI property which were yet to be captured in the NI literature. So, our aim was also to extend the NI literature to account for such systems. We were able to successfully do that by providing a definition of LTV and LPV NI and OSNI systems. We also provided a state-space characterisation for all the systems. Moreover, we successfully provided a stability

result for the positive feedback interconnection of LTV OSNI-NI and LPV OSNI-NI system.

Therefore, the main contributions of this thesis are as follows.

In Chapter 4, We provided a definition for a new class of systems called $\alpha-$ SNI system (Definition 16). We showed that these are asymptotically stable systems with pole location dictated by α. We also showed how those systems are different from the SSNI systems that existed in the literature. We then used that definition of $\alpha-$ SNI system to propose an LMI-based dynamic output feedback controller synthesis technique that renders the closed-loop $\alpha-$ SNI systems and remains robustly stable to a class of NI uncertainty satisfying the NI DC gain condition(Theorem 5).

In a similar theme to Chapter 4, in Chapter 6 we provided a frequency domain-based NI/SNI (Lemma 14 and Lemma 15) and an LMI-based SSNI controller synthesis technique (Theorem 8). We also showed that both techniques can facilitate constant set-point tracking and can also improve the performance of the closed-loop system. Moreover, we were able to design the controller for the vibration attenuation of a flexible structure system in Chapter 7.

In Chapter 5 where we provided a theoretical extension to the NI systems literature, we were able to propose a definition for LTV NI (Definition 17) and OSNI (Defintion 18) systems. We also provided a state-space characterization of LTV NI (Lemma 10) and OSNI (Lemma 11) systems. Stability condition for LTV OSNI-NI interconnection was also provided (Theorem 7). Finally, these results were extended to account for LPV NI systems in (Lemma 12), (Lemma 13)and (Theorem 7).

8.2 Future Work

Although the aims and objective of this project were achieved, there are more research areas in the field of NI theory yet to be explored. The following can be considered as possible research areas for future work.

- In the $\alpha-$ controller synthesis method introduced in this thesis, there is no systematic approach of choosing the α. It is therefore desirable to extend the work and provide a more established method of choosing the variable. For example, recasting the controller synthesis problem as a maximisation problem

of α subject to LMI constraints. Moreover, the synthesis technique proposed was only a sufficient condition. Therefore, the result can be strengthened to a necessary and sufficient condition.

- In the state-space characterisation of the LTV and LPV NI, only sufficient conditions were proposed. Moreover, the stability result for both the LTV and LPV feedback interconnection were also sufficient conditions. It will therefore be desirable if these results are strengthened to necessary and sufficient conditions. Also, LTV OSNI systems were restricted to systems with a relative degree of two. A possible future work is to relax that restriction to account for wider class of systems.

- Recently, the NI theory was extended to nonlinear systems. However, there are many areas yet to be explored in the nonlinear NI theory. This include controller design for nonlinear NI systems and also proposing a systematic necessary and sufficient conditions for characterizing the systems based on the state vectors of the system. The study of such systems is important as they occur in real life. For example, all Hamiltonian systems with force actuator and position sensor exhibit the nonlinear NI property.

- It is common knowledge that linear control techniques are usually used to control nonlinear systems by linearizing the nonlinear systems about an operating point. This is due to the fact that the literature of linear systems is more documented and it is easier to control linear systems compared to their nonlinear counterpart. Hence, it will be desirable to be able to establish the relationship between linear and nonlinear NI systems. For example, the linearized dynamics of a simple pendulum, where the measured output is the horizontal position has the loseless NI property though the underlying nonlinear system dynamics does not have nonlinear NI property.

Appendix A

Table with Performance Parameters for Different Choice of $d(s)$

Let $\Gamma(s, z_i) = (s + z_i)(s + \bar{z}_i)$.

Table A.1: Quantitative information of the performance parameters of the closed-loop impulse response of the plant model G_{m_1} subject to the choice of the pole polynomials $\{d_1(s),\, d_2(s),\, \cdots, d_{30}(s)\}$.

Choice of $d(s)$	**Bandwidth**	**Impulse response settling time**	**Peak of impulse response**	**Farthest controller pole**
$d_1(s) = (s + 0.5)\Gamma(s, 0.5 + j)$	1.018	26.474	0.484	-5.911
$d_2(s) = (s + 0.5)\Gamma(s, 0.5 + 2j)$	1.052	35.207	0.545	-34.710
$d_3(s) = (s + 0.5)\Gamma(s, 0.5 + 3j)$	0.964	38.718	0.499	-32.533
$d_4(s) = (s + 0.5)\Gamma(s, 0.5 + 4j)$	0.981	38.272	0.512	-39.526
$d_5(s) = (s + 1)\Gamma(s, 1 + j)$	1.051	34.994	0.538	-36.433
$d_6(s) = (s + 1)\Gamma(s, 1 + 2j)$	0.991	37.108	0.511	-34.295
$d_7(s) = (s + 1)\Gamma(s, 1 + 3j)$	0.858	43.075	0.440	-56.949
$d_8(s) = (s + 1)\Gamma(s, 1 + 4j)$	0.883	42.331	0.461	-63.009
$d_9(s) = (s + 2)\Gamma(s, 2 + j)$	0.448	42.349	0.484	-75.035
$d_{10}(s) = (s + 2)\Gamma(s, 2 + 2j)$	0.881	42.153	0.455	-77.485
$d_{11}(s) = (s + 2)\Gamma(s, 2 + 3j)$	0.891	41.910	0.463	-81.548
$d_{12}(s) = (s + 2)\Gamma(s, 2 + 4j)$	0.776	47.642	0.400	-152.346
$d_{13}(s) = (s + 3)\Gamma(s, 3 + j)$	0.888	42.220	0.463	-112.141
$d_{14}(s) = (s + 3)\Gamma(s, 3 + 2j)$	0.717	45.156	0.363	-225.809
$d_{15}(s) = (s + 3)\Gamma(s, 3 + 3j)$	0.847	44.215	0.442	-156.8465
$d_{16}(s) = (s + 3)\Gamma(s, 3 + 4j)$	0.574	48.655	0.286	-458.572
$d_{17}(s) = (s + 4)\Gamma(s, 4 + j)$	0.569	49.046	0.283	-523.863
$d_{18}(s) = (s + 4)\Gamma(s, 4 + 2j)$	0.559	49.712	0.278	-569.341
$d_{19}(s) = (s + 4)\Gamma(s, 4 + 3j)$	0.534	51.637	0.262	-683.768
$d_{20}(s) = (s + 4)\Gamma(s, 4 + 4j)$	0.535	51.756	0.263	-691.803
$d_{21}(s) = (s + 5)\Gamma(s, 5 + j)$	0.597	53.713	0.301	-617.6388
$d_{22}(s) = (s + 5)\Gamma(s, 5 + 2j)$	0.606	53.183	0.307	-597.666

Continued on the next page

Table A.1 – *Continued from previous page*

$d(s)$	**Bandwidth**	**Impulse settling time**	**Peak of impulse response**	**Farthest controller pole**
$d_{23}(s) = (s+5)\Gamma(s, 5+3j)$	0.618	52.458	0.313	-576.443
$d_{24}(s) = (s+5)\Gamma(s, 5+4j)$	0.605	53.389	0.306	-599.979
$d_{25}(s) = (s+1)\mathbb{D}\left[G_m(s)\right]$	1.054	24.714	0.491	-15.136
$d_{26}(s) = (s+1)^3$	0.997	27.596	0.486	-7.511
$d_{27}(s) = (s+0.5)^3$	1.048	29.637	0.488	-9.414
$d_{28}(s) = (s+2)^3$	0.865	42.384	0.445	-74.781
$d_{29}(s) = (s+3)^3$	0.877	42.664	0.457	-114.690
$d_{30}(s) = (s+4)^3$	0.858	43.775	0.449	-185.911

Table A.2: Quantitative information of the performance parameters of the closed-loop impulse response of the plant model G_{m_2} subject to the choice of the pole polynomials $\{d_1(s),\, d_2(s),\, \cdots,\, d_{30}(s)\}$.

Choices of $d(s)$	**Bandwidth**	**Impulse response settling time**	**Peak of impulse response**	**Farthest controller pole**
$d_1(s) = (s+15)\Gamma(s, 15+j)$	0.087	37.684	0.162	-15
$d_2(s) = (s+15)\Gamma(s, 15+2j)$	0.087	37.641	0.162	-15
$d_3(s) = (s+15)\Gamma(s, 15+3j)$	0.088	37.573	0.163	-15
$d_4(s) = (s+15)\Gamma(s, 15+4j)$	0.088	37.473	0.163	-15
$d_5(s) = (s+16)\Gamma(s, 16+j)$	0.162	20.262	0.304	-16
$d_6(s) = (s+16)\Gamma(s, 16+2j)$	0.162	20.252	0.304	-16
$d_7(s) = (s+16)\Gamma(s, 16+3j)$	0.162	20.240	0.304	-16
$d_8(s) = (s+16)\Gamma(s, 16+4j)$	0.162	20.220	0.304	-16
$d_9(s) = (s+17)\Gamma(s, 17+j)$	0.171	19.200	0.320	-17
$d_{10}(s) = (s+17)\Gamma(s, 17+2j)$	0.171	19.186	0.321	-17
$d_{11}(s) = (s+17)\Gamma(s, 17+3j)$	0.171	19.164	0.321	-17
$d_{12}(s) = (s+17)\Gamma(s, 17+4j)$	0.171	19.130	0.322	-17
$d_{13}(s) = (s+18)\Gamma(s, 18+j)$	0.181	18.114	0.340	-18
$d_{14}(s) = (s+18)\Gamma(s, 18+2j)$	0.181	18.101	0.340	-18
$d_{15}(s) = (s+18)\Gamma(s, 18+3j)$	0.181	18.077	0.340	-18
$d_{16}(s) = (s+18)\Gamma(s, 18+4j)$	0.182	18.042	0.341	-18
$d_{17}(s) = (s+19)\Gamma(s, 19+j)$	0.177	18.558	0.332	-19
$d_{18}(s) = (s+19)\Gamma(s, 19+2j)$	0.177	18.553	0.332	-19
$d_{19}(s) = (s+19)\Gamma(s, 19+3j)$	0.177	18.541	0.332	-19
$d_{20}(s) = (s+19)\Gamma(s, 19+4j)$	0.177	18.525	0.332	-19
$d_{21}(s) = (s+20)\Gamma(s, 20+j)$	0.190	17.223	0.357	-20
$d_{22}(s) = (s+20)\Gamma(s, 20+2j)$	0.190	17.224	0.357	-20
$d_{23}(s) = (s+20)\Gamma(s, 20+3j)$	0.190	17.224	0.357	-20
$d_{24}(s) = (s+20)\Gamma(s, 20+4j)$	0.190	17.223	0.357	-20
$d_{25}(s) = (s+19)\mathbb{D}\left[G_m(s)\right]$	1.671	5.585	2.372	-19
$d_{26}(s) = (s+15)^3$	0.087	37.689	0.162	-15
$d_{27}(s) = (s+16)^3$	0.162	20.261	0.304	-16
$d_{28}(s) = (s+17)^3$	0.171	19.204	0.320	-17
$d_{29}(s) = (s+18)^3$	0.181	18.119	0.340	-18
$d_{30}(s) = (s+19)^3$	0.177	18.561	0.332	-19

Table A.3: Quantitative information of the performance parameters of the closed-loop impulse response of the plant model G_{m_3} subject to the choice of the pole polynomials $\{d_1(s),\, d_2(s),\, \cdots, d_{30}(s)\}$.

Choices of $d(s)$	**Bandwidth**	**Impulse settling time**	**Peak of impulse response**	**Farthest controller pole**
$d_1(s) = (s+0.5)\Gamma(s, 0.5+j)$	0.187	21.613	0.180	-0.500
$d_2(s) = (s+0.5)\Gamma(s, 0.5+2j)$	1.113	9.935	0.438	-2.204
$d_3(s) = (s+0.5)\Gamma(s, 0.5+3j)$	0.933	10.962	0.378	-2.788
$d_4(s) = (s+0.5)\Gamma(s, 0.5+4j)$	0.994	11.247	0.399	-3.160
$d_5(s) = (s+1)\Gamma(s, 1+j)$	1.258	11.625	0.547	-2.398
$d_6(s) = (s+1)\Gamma(s, 1+2j)$	0.938	10.981	0.380	-2.875
$d_7(s) = (s+1)\Gamma(s, 1+3j)$	0.819	15.026	0.387	-4.3269
$d_8(s) = (s+1)\Gamma(s, 1+4j)$	1.013	25.767	0.535	-13.631
$d_9(s) = (s+2)\Gamma(s, 2+j)$	1.035	24.387	0.533	-14.170
$d_{10}(s) = (s+2)\Gamma(s, 2+2j)$	1.051	24.261	0.539	-14.418
$d_{11}(s) = (s+2)\Gamma(s, 2+3j)$	1.000	31.285	0.559	-19.215
$d_{12}(s) = (s+2)\Gamma(s, 2+4j)$	0.948	31.772	0.559	-21.571
$d_{13}(s) = (s+3)\Gamma(s, 3+j)$	0.971	31.574	0.572	-23.823
$d_{14}(s) = (s+3)\Gamma(s, 3+2j)$	0.711	37.441	0.412	-49.524
$d_{15}(s) = (s+3)\Gamma(s, 3+3j)$	0.703	44.379	0.424	-58.237
$d_{16}(s) = (s+3)\Gamma(s, 3+4j)$	0.720	43.426	0.438	-58.267
$d_{17}(s) = (s+4)\Gamma(s, 4+j)$	0.753	41.711	0.462	-60.540
$d_{18}(s) = (s+4)\Gamma(s, 4+2j)$	0.750	42.160	0.461	-61.670
$d_{19}(s) = (s+4)\Gamma(s, 4+3j)$	0.765	41.233	0.472	-60.913
$d_{20}(s) = (s+4)\Gamma(s, 4+4j)$	0.798	44.505	0.499	-62.081
$d_{21}(s) = (s+5)\Gamma(s, 5+j)$	0.736	49.277	0.470	-148.413
$d_{22}(s) = (s+5)\Gamma(s, 5+2j)$	0.742	48.953	0.475	-147.945
$d_{23}(s) = (s+5)\Gamma(s, 5+3j)$	0.754	47.966	0.484	-146.765
$d_{24}(s) = (s+5)\Gamma(s, 5+4j)$	0.640	49.269	0.381	-174.383
$d_{25}(s) = (s+1.41)\mathbb{D}\left[G_m(s)\right]$	1.445	20.512	0.846	-15.706
$d_{26}(s) = (s+1.41)^3$	0.955	11.146	0.384	-3.056
$d_{27}(s) = (s+3)\mathbb{D}\left[G_m(s)\right]$	1.445	16.041	0.839	-32.709
$d_{28}(s) = (s+3)^3$	0.974	31.521	0.572	-23.508
$d_{29}(s) = (s+1.41)^2(s+3)$	0.995	11.387	0.398	-3.458
$d_{30}(s) = (s+1.41)(s+3)^2$	1.062	27.553	0.547	-15.706

Table A.4: Quantitative information of the performance parameters of the closed-loop impulse response of the plant model G_{m_4} subject to the choice of the pole polynomials $\{d_1(s),\, d_2(s),\, \cdots, d_{30}(s)\}$.

Choices of $d(s)$	**Bandwidth**	**Impulse response settling time**	**Peak of impulse response**	**Farthest controller pole**
$d_1(s) = (s+0.5)\Gamma(s, 0.5+j)$	1.197	15.725	0.438	-7.769
$d_2(s) = (s+0.5)\Gamma(s, 0.5+2j)$	0.745	16.0688	0.330	-15.272
$d_3(s) = (s+0.5)\Gamma(s, 0.5+3j)$	0.899	25.163	0.427	-30.813
$d_4(s) = (s+0.5)\Gamma(s, 0.5+4j)$	0.906	30.061	0.450	-40.171
$d_5(s) = (s+1)\Gamma(s, 1+j)$	0.921	15.558	0.390	-12.305
$d_6(s) = (s+1)\Gamma(s, 1+2j)$	0.573	21.040	0.255	-23.090
$d_7(s) = (s+1)\Gamma(s, 1+3j)$	0.856	26.372	0.405	-34.181
$d_8(s) = (s+1)\Gamma(s, 1+4j)$	0.518	41.412	0.242	-97.868
$d_9(s) = (s+2)\Gamma(s, 2+j)$	0.755	24.216	0.358	-54.891
$d_{10}(s) = (s+2)\Gamma(s, 2+2j)$	0.636	28.746	0.300	-88.390
$d_{11}(s) = (s+2)\Gamma(s, 2+3j)$	0.587	36.184	0.271	-87.837

Continued on the next page

Table A.4 – *Continued from previous page*

$d(s)$	**Bandwidth**	**Impulse settling time**	**Peak of impulse response**	**Farthest controller pole**
$d_{12}(s) = (s+2)\Gamma(s, 2+4j)$	0.582	39.256	0.281	-104.549
$d_{13}(s) = (s+3)\Gamma(s, 3+j)$	0.642	34.516	0.295	-86.870
$d_{14}(s) = (s+3)\Gamma(s, 3+2j)$	0.617	42.560	0.295	-115.381
$d_{15}(s) = (s+3)\Gamma(s, 3+3j)$	0.483	45.954	0.239	-180.854
$d_{16}(s) = (s+3)\Gamma(s, 3+4j)$	0.476	47.855	0.248	-190.276
$d_{17}(s) = (s+4)\Gamma(s, 4+j)$	0.485	45.965	0.240	-199.757
$d_{18}(s) = (s+4)\Gamma(s, 4+2j)$	0.428	51.235	0.207	-347.180
$d_{19}(s) = (s+4)\Gamma(s, 4+3j)$	0.386	46.667	0.181	-404.683
$d_{20}(s) = (s+4)\Gamma(s, 4+4j)$	0.261	48.585	0.112	-779.683
$d_{21}(s) = (s+5)\Gamma(s, 5+j)$	0.306	53.346	0.134	-685.419
$d_{22}(s) = (s+5)\Gamma(s, 5+2j)$	0.424	63.030	0.217	-729.551
$d_{23}(s) = (s+5)\Gamma(s, 5+3j)$	0.437	61.940	0.226	-714.432
$d_{24}(s) = (s+5)\Gamma(s, 5+4j)$	0.377	59.740	0.183	-739.188
$d_{25}(s) = (s+1.37)\mathbb{D}\left[G_m(s)\right]$	1.418	20.982	0.998	-30.837
$d_{26}(s) = (s+1.37)^3$	0.645	15.785	0.289	-14.587
$d_{27}(s) = (s+2.93)\mathbb{D}\left[G_m(s)\right]$	1.445	16.041	0.839	-32.709
$d_{28}(s) = (s+2.93)^3$	0.523	33.702	0.238	-119.702
$d_{29}(s) = (s+3.6)\mathbb{D}\left[G_m(s)\right]$	1.430	20.048	1.101	-83.771
$d_{30}(s) = (s+3.6)^3$	0.501	44.872	0.250	-181.865

Bibliography

[1] C. J. Goh and T. K. Caughey, "On the stability problem caused by finite actuator dynamics in the collocated control of large space structures," *International Journal of Control*, vol. 41, no. 3, pp. 787-802, 1985

[2] J. L. Fanson and T. K. Caughey, "Positive position feedback control for large space structures," *AIAA Journal*, vol. 28, no. 4, pp. 717-724, 1990.

[3] A. J. van der Schaft "Positive feedback interconnection of Hamiltonian systems," in *Proceedings of the 50th IEEE Conference on Decision and European Control Conference,* Dec 2011, pp. 6510-6515.

[4] H. L. Royden, *Real analysis,* 3rd ed. Englewood Cliffs, New Jersey, USA: Prentice-Hall, Inc., 1988

[5] P. Bhowmick and A. Lanzon, "Output strictly negative imaginary systems and its connections to dissipativity theory," in *Proceedings of 58th IEEE Conference on Decision and Control,* Dec 2019, pp. 6754-6759.

[6] P. Bhowmick and S. Patra, "On LTI output strictly negative imaginary systems," *Systems & Control letters*, vol. 100, pp.32-47, 2017.

[7] B. D. O. Anderson and P.Moylan, "Synthesis of linear time-varying passive networks," *IEEE Transactions on Circuits and Systems*, vol. 21, no. 5, pp. 678-687, 1974.

[8] A. G. Ghallab, M. A. Mabrok and I. R. Petersen, "Extending Negative Imaginary Systems Theory to Nonlinear Systems," *2018 IEEE Conference on Decision and Control (CDC)*, 2018, pp. 2348-2353.

[9] M. Liu, H. Lin and X. Jing, "Necessary and sufficient conditions on the negative imaginariness for interval SISO transfer functions and their interconnection," *IEEE Transactions on Automatic Control,* pp. 1-8, 2019.

[10] B. Brogliato, R. Lozano, B. Maschke, and O. Egeland, *Dissipative Systems Analysis and Control: Theory and Applications,* 3rd ed. Berlin, Heidelberg: Springer-Verlag, 2020.

[11] P. Gahinet, P. Apkarian, and M. Chilali, "Affine parameter-dependent Lyapunov functions and real parametric uncertainty," *IEEE Transactions on Automatic Control,* vol. 41, no. 3, pp. 436-442, March 1996.

[12] S. Boyd, L. El Ghaoui, E. Feron, and V. Balakrishnan. *Linear Matrix Inequalities in System and Control Theory,* volume 15 of *Studies in Applied Mathematics.* SIAM, Philadelphia, PA, June 1994.

[13] J. R. Forbes and C. J. Damaren, "Passive linear time-varying systems: State-space realizations, stability in feedback and controller synthesis," in *Proceedings of the 2010 American Control Conference,* June 2010, pp. 1097-1104.

[14] M. R. Opmeer, "Infinite-Dimensional Negative Imaginary Systems," in *IEEE Transactions on Automatic Control,* vol. 56, no. 12, pp. 2973-2976, Dec. 2011.

[15] A. Lanzon and I. R. Petersen, “Stability robustness of a feedback interconnection of systems with negative imaginary frequency response," *IEEE Transactions on Automatic Control*, vol. 53, no. 4, pp. 1042-1046, 2008.

[16] A. Lanzon and I. R. Petersen, "A modified positive-real type stability condition," *Proceedings of the 2007 European Control Conference*,pp. 3912-3918, Kos, Greece, 2007.

[17] G. Vinnicombe, "*Uncertainty and Feedback: H_∞ loop-shaping and the μ-gap metric*" Imperial College Press, 2000.

[18] M. Green and D. J. N. Limebeer, "*Linear robust control*" Prentice Hall, Englewood Cliffs, NJ, 1995.

[19] B. D. O. Anderson and S. Vongpanitlerd "*Network analysis and synthesis: A modern systems theory approach*" Dover Publications Inc., 2006.

[20] I. R. Petersen and A. Lanzon, “Feedback control of negative imaginary systems," *IEEE Control Systems Magazine*, vol. 30, no. 5, pp. 54-72, 2010.

[21] A. Lanzon, Z. Song, S. Patra, and I. R. Petersen, “A strongly strict negative-imaginary lemma for non-minimal linear systems," *Communications in Information and Systems,* vol. 11, no. 2, pp. 139-152, 2011.

[22] J. Xiong, I. R. Petersen and A. Lanzon, "On lossless negative imaginary systems," in *2009 7th Asian Control Conference,* 2009, pp. 824-829.

[23] J. Xiong, I. R. Petersen and A. Lanzon, "Finite frequency negative imaginary systems," in *Proceedings of the 2010 American Control Conference,* 2010, pp. 323-328.

[24] J. Xiong, I. R. Petersen and A. Lanzon, "Finite frequency negative imaginary systems," *IEEE Transactions on Automatic Control,* vol. 57, no. 11, pp. 2917-2922, 2012.

[25] J. Xiong, I. R. Petersen and A. Lanzon, “A negative imaginary lemma and the stability of interconnections of linear negative imaginary systems," *IEEE Transactions on Automatic Control*, vol. 55, no. 10, pp. 2342-2347, 2010.

[26] C. Cai and G. Hagen, “Stability analysis for a string of couple stable subsystems with negative imaginary frequency response," *IEEE Transactions on Automatic Control*, vol. 55, no. 8, pp. 1958-1963, 2010.

[27] S. Engelken, S. Patra, A. Lanzon and I. R. Petersen, “Stability analysis of negative imaginary systems with real parametric uncertainty - the SISO case," *IET Control Theory and Applications*, vol. 4, no. 11, pp. 2631-2638, 2010.

[28] S. Patra and A. Lanzon, “Stability analysis of interconnected systems with ‘mixed’ negative imaginary and small-gain properties," *IEEE Transactions on Automatic Control*, vol. 56, no. 6, pp. 1395-1400, 2011.

[29] M. A. Mabrok, A. G. Kallapur, I. R. Petersen and A. Lanzon, "A new stability result for the feedback interconnection of negative-imaginary systems with a pole at the origin," in *Proceedings of IEEE Conference on Decision and Control and European Control Conference*, pp. 3753-3757, Orlando, FL, USA, 2011.

[30] Z. Song, A. Lanzon, S. Patra and I. R. Petersen, "Robust performance analysis for uncertain negative imaginary systems," *International Journal of Robust and Nonlinear Control*, vol. 22, no. 3, pp. 262-281, 2012.

[31] A. Lanzon, Z. Song and I. R. Petersen, "Reformulating negative imaginary frequency response systems to bounded-real systems," in *Proceedings of the IEEE Conference on Decision and Control,* pp. 322-326, 2008.

[32] Z. Song, A. Lanzon, S. Patra and I. R. Petersen, "A negative imaginary lemma without minimality assumptions and robust state-feedback synthesis for uncertain negative imaginary systems," *System & Control Letters*, vol. 61, no. 12, pp. 1269-1276, 2012.

[33] Z. Song, A. Lanzon, S. Patra and I. R. Petersen, "Towards controller synthesis for systems with negative imaginary frequency response," *IEEE Transactions on Automatic Control,* vol. 55, no. 6, pp. 1506-1511, 2010.

[34] J. Xiong, I. R. Petersen and A. Lanzon, "On lossless negative imaginary systems," *Automatica*, vol. 48, no. 6, pp. 1213-1217, 2012.

[35] A. Ferrante and L. Ntogramatzidis, "Some new results in the theory of negative-imaginary systems with symmetric transfer matrix function," *Automatica*, vol. 49, no. 7, pp. 2138-2144, 2013.

[36] A. S. Saad and M. A. Mabrok, "Retrofitting of bridge superstructures using negative imaginary control theory," *International Journal of Control,* pp. 1-9, 2021.

[37] A. Ferrante, A. Lanzon and L. Ntogramatzidis, "Discrete-time negative imaginary systems," *Automatica,* vol. 79, pp. 1-10, 2017.

[38] B. Cheekati and B. Bhikkaji, "A negative imaginary approach to the actuation of a guitar string," *Mechatronics,* vol. 23, no. 8, pp. 997-1004, 2013.

[39] M. A. Mabrok, A. G. Kallapur, I. R. Petersen and A. Lanzon, “Generalizing negative-imaginary systems theory to include free body dynamics: Control of highly resonant structures with free body motion," *IEEE Transactions on Automatic Control*, vol. 59, no. 10, pp. 2692-2707, 2014.

[40] M. A. Mabrok, A. G. Kallapur, I. R. Petersen and A. Lanzon, “Spectral conditions for negative imaginary systems with applications to nanopositioning," *IEEE/ASME Transactions on Mechatronics,* vol. 19, no. 3, pp. 895-903, 2014.

[41] M. Mabrok, A. G. Kallapur, I. R. Petersen, and A. Lanzon, “A generalized negative imaginary lemma and Riccati-based static state feedback negative imaginary synthesis," Systems & Control Letters, vol. 77, pp. 63–68, 2015.

[42] M. Mabrok, A. Kallapur, I. R. Petersen, D. Schutte, T. Boyson and A. Lanzon, "Locking a three-mirror optical cavity: A negative imaginary systems approach," *2nd Australian Control Conference,* vol. 8, pp. 476-480, 2012.

[43] S. K. Das, H. R. Pota and I. R. Petersen, “Damping Controller Design for Nanopositioners: A Mixed Passivity, Negative-Imaginary and Small-Gain Approach," *IEEE/ASME Transactions on Mechatronics,* vol. 20, no. 1, pp. 416-426, 2015.

[44] S. K. Das, H. R. Pota, and I. R. Petersen, "Resonant controller design for a piezoelectric tube scanner: A mixed negative imaginary and small gain approach," *IEEE Transactions on Control Systems Technology,* vol. 22, no. 5, pp. 1899-1906, 2014.

[45] H.K. Khalil, "*Nonlinear Systems*", 3rd Edition, Upper Saddle River, NJ, USA: Prentice Hall, Inc., 2002.

[46] S. Z. Khong, I. R. Petersen, and A. Rantzer, "Robust feedback stability of negative imaginary systems: An integral quadratic constraint approach," in *Proceedings of European Control Conference,* pp. 1998-2002, Austria, July, 2015.

[47] A. Ferrante, A. Lanzon and L. Ntogramatzidis, “Foundations of not necessarily rational negative-imaginary systems theory: Relations between classes of negative-imaginary and positive-real systems," *IEEE Transactions on Automatic Control*, vol. 61, no. 10, pp. 3052-3057, 2016.

[48] J. Wang, A. Lanzon, and I. R. Petersen, “Robust cooperative control of multiple heterogeneous negative imaginary systems," *Automatica*, vol. 61, pp. 64–72, 2015.

[49] J. Wang, A. Lanzon, and I. R. Petersen, “Robust output feedback consensus for networked negative imaginary systems," *IEEE Transactions on Automatic Control*, vol. 60, no. 9, pp. 2547–2552, 2015.

[50] V. P. Tran, M. Garratt, and I. R. Petersen, “Formation control of multi-UAVs using negative-imaginary systems theory," in *Proceedings of 11th Asian Control Conference,* pp. 2031–2036, Gold Coast, Australia, Dec 2017.

[51] V. P. Tran, M. A. Garratt, and I. R. Petersen, "Switching time-invariant formation control of a collaborative multi-agent system using negative imaginary systems theory," *Control Engineering Practice,* vol. 95, pp. 1-16, 2020.

[52] V. P. Tran, M. A. Garratt, and I. R. Petersen, "Multi-vehicle formation control and obstacle avoidance using negative imaginary systems theory," *IFAC Journal of Systems and Control,* vol. 15, pp. 1-23, March 2021.

[53] O. Skeik and A. Lanzon, "Robust output consensus of homogeneous multi-agent systems with negative imaginary dynamics," *Automatica,* vol. 113, pp. 1-9, March 2020.

[54] W. K. Miao, M. L. Xu and C. S. Wu, "Active vibration control of cantilever beam using MFC sensor and actuator," *Recent Advances in Structural Integrity Analysis - Proceedings of the International Congress (APCF/SIF),* pp. 447-452, 2014.

[55] B. Bhikkaji and S. O. R. Moheimani, "A negative imaginary approach to modeling and control of a collocated structure," *IEEE/ASME Transactions on Mechatronics,* vol. 17, no. 4, pp. 717-727, 2012.

[56] S. O. R. Moheimani, D. Halim and A. J. Fleming, "Spatial control of vibration: Theory and experiments." Singapore: World Scientific, 2003.

[57] A. Lanzon and H. J. Chen, “Feedback stability of negative imaginary systems," *IEEE Transactions on Automatic Control,* vol. 62, no. 11, pp. 5620-5633, 2017.

[58] P. Bhowmick and S. Patra, "Solution to negative imaginary control problem for uncertain LMI systems with multi-objective performance," *Automatica,* vol. 112, pp. 1-9, 2020.

[59] S. Kurawa, P. Bhowmick and A. Lanzon, "Dynamic output feedback controller synthesis using an LMI-based $\alpha-$strictly negative imaginary framework," In *Proceedings of 27th Mediterranean Conference on Control and Automation,* pp. 81-86, July 2019.

[60] S. Kurawa, P. Bhowmick and A. Lanzon, "Negative imaginary theory for a class of linear time-varying systems," *Systems & Control Letters,* vol. 5, no. 3, pp. 1001-1006, July 2021.

[61] S. Kurawa, P. Bhowmick and A. Lanzon, "A dynamic controller synthesis methodology for negative imaginary systems using th internal model control principle," submitted to *Automatica,* July 2021.

[62] M. Morari and E. Zafiriou. *Robust Process Control,* Prentice Hall, Englewood Cliffs, New Jersey, USA, 1st edition, 1989.

[63] C. E. Garcia and M. Morari, "Internal model control: A unifying review and some new results," *Industrial and Engineering Chemistry Process Design and Development,* vol. 21, no. 2, pp. 308-323, April, 1982.

[64] K. Z. Liu, M. Ono, X. Li and M. Wu, "Robust performance synthesis for systems with positive-real uncertainty and an extension to the negative-imaginary case," *Automatica,* vol. 82, pp. 194-201, 2017.

[65] M. Lie and J. Xiong, "On α- and $\mathcal{D}$- negative-imaginary systems," *International Journal of Control,* vol. 88, no. 10, pp. 1933-1941, 2015.

[66] J. Xiong, J. Lam and I. R. Petersen, "Output feedback negative imaginary synthesis under structural constraints," *Automatica,* vol. 71, pp. 222-228, 2016.

[67] M. Liu, J. Lam, B. Zhu, and K-W. Kwok, "On positive realness, negative imaginariness, and $\mathcal{H}_\infty$ control of state-space symmetric systems," *Automatica,* vol. 101, pp. 190-196, 2019.

[68] A. Dey, S. Patra, and S. Sen, "Integral control of stable negative imaginary systems preceded by hysteresis nonlinearity," *IEEE Transactions on Automatic Control,* vol. 65, no. 3, pp. 1333-1339, 2020.

[69] A. Dey, S. Patra, and S. Sen, "Stability analysis and controller design for Luré systems with hysteresis nonlinearities: A negative imaginary theory based approach," *International Journal of Control,* vol. 92, no. 8, pp. 1903-1913, 2019.

[70] J. Dannatt, I. R. Petersen and A. Lanzon, "Strictly negative imaginary state feedback control with a prescribed degree of stability," *Automatica,* vol. 119, 2020.

[71] J. Xiong, A. Lanzon and I. R. Petersen, "Negative imaginary lemmas for descriptor systems," *IEEE Transactions on Automatic Control,* vol. 61, no. 2, pp. 491-496, 2016.

[72] J. Rubió-Massegú, J. M. Rossell, H. R. Karimi, and F. Palacios-Quiñonero, "Static output-feedback control under information structure constraints," *Automatica,* vol. 49, no. 1, pp. 313-316, 2013.

[73] C. Scherer, P. Gahinet and M. Chilali, "Multi objective output-feedback control via LMI optimization," *IEEE Transactions on Automatic Control,* vol. 42, no. 7, pp. 896-911, 1997.

[74] M. A. Mabrok, A. G. Kallapur, I. R. Petersen, and A. Lanzon,"Generalized negative imaginary lemma for descriptor systems," *Journal of Mechanics Engineering and Automation,* vol. 2, no. 1, pp. 17-21, 2012.

[75] M. A. Mabrok, A. G. Kallapur, I. R. Petersen, and A. Lanzon, "Stabilization of conditional uncertain negative-imaginary systems using Riccati equation approach," in *Proceedings of the 20th International Symposium on Mathematical Theory of Networks and Systems,* pp. 1–6, 2012.

[76] M. Liu and J. Xiong, "On non-proper negative imaginary systems," *Systems & Control Letters,* vol. 88, pp. 47–53, 2016.

[77] M. Liu and J. Xiong, "Properties and stability analysis of discrete-time negative imaginary systems," *Automatica*, vol. 83, pp. 58-64, 2017.

[78] M. Liu and J. Xiong, "Bilinear transformation for discrete-time positive real and negative imaginary systems," *IEEE Transactions on Automatic Control,* vol. 63, no. 12, pp. 4264-4269, Dec 2018.

[79] G. Salcan-Reyes and A. Lanzon, “On negative imaginary synthesis via solutions to Riccati equations," in *Proceedings of European Control Conference,* pp. 870-875, Cyprus, June, 2018.

[80] G. Salcan-Reyes and A. Lanzon, "Negative imaginary synthesis via dynamic output feedback and static state feedback: A Riccati approach," *Automatica,* vol. 104, pp. 220-227, 2019.

[81] G. Salcan-Reyes, A. Lanzon, and I. R. Petersen, “Controller synthesis to render a closed loop transfer function strongly strictly negative imaginary," in *Proceedings of 57th IEEE Conference on Decision and Control,* pp. 2988-2993, Miami, USA, Dec. 2018.

[82] K. Lee and J. R. Forbes, "Synthesis of strictly negative imaginary controllers using a $\mathcal{H}_\infty$ performance index," in *Proceedings of American Control Conference,* pp. 497-502, Philadelphia, USA, July 2019.

[83] S. Z. Khong, I. R. Petersen, and A. Rantzer, "Robust stability conditions for feedback interconnections of distributed-parameter negative imaginary systems," *Automatica,* vol.90, pp. 310-316, 2018.

[84] J. Doyle, A. Packard, and K. Zhou, "Reviews of LFTs, LMIs and Mu," in *Proceedings of the 30th IEEE Conference on Decision and Control,* pp. 1227-1232, Brighton, UK, Dec. 1991.

[85] R. A. Horn and C. R. Johnson, *“Matrix Analysis,"* Cambridge University Press, USA, 1990.

[86] J. J. E. Slotine and W. Li *Applied Nonlinear Control.* Englewood Cliffs, New Jersey, USA: Prentice-Hall, Inc. 1991.

[87] K. S. Tsakalis and P.A. Ioannou *Linear Time-Varying Systems: Control and Adaptation.* Englewood Cliffs, New Jersey, USA: Prentice-Hall, Inc. 1993.

[88] K. Zhou, J. C. Doyle and K. Glover, "*Robust and Optimal Control,*" Prentice Hall, Englewood Cliffs, NJ, 1996.

[89] A. Laub, *"Matrix Analysis for Scientist and Engineers,"* Society for Industrial and Applied Mathematics, PA, 2005.

[90] S. Skogestad and I. Postlethwaite, *"Multivariable feedback control: Analysis and design,"* 1st Edition, Wiley, New York, 1996.

[91] J. Gallier, "The Schur complement and symmetric positive semidefinite (and definite) matrices", Dec., 2010.

[92] D. S. Bernstein, "*Matrix Mathematics: Theory, Facts and Formulas,*" 2nd Edition, Princeton University Press, 2009.

[93] P. Bhowmick and A. Lanzon Time-domain output negative imaginary systems and its connection to dynamic dissipativity. In *Proceedings of 59th IEEE Conference on Decision and Control,* pp. 5167-5172, Dec 2020.

[94] D. Angeli, Systems with counterclockwise input-output dynamics, *IEEE Transactions on Automatic Control,* vol. 51, no. 7, pp. 1130-1143, July 2006.

[95] M. Grant and S. Boyd, CVX: Matlab software for disciplined convex programming, version 2.1, http://cvxr. com/cvx, March 2014.

[96] M. Chilali and P. Gahinet, "$\mathcal{H}_\infty$ design with pole placement constraints: An LMI approach," *IEEE Transactions on Automatic Control,* vol. 41, no. 3, pp. 358-367, 1996.

[97] B. DeSchutter, "Minimal State-Space Realization in Linear System Theory: An Overview," *Journal of Computational and Applied Mathematics,* vol. 121, no.1, pp. 331-354, 2000.